416

REPORT NO. 1317

NP-10699

[redacted]

MASTER

SUPPLEMENTARY ANALYSIS OF THE POWER-LIMITING SYSTEM for the ENRICO FERMI ATOMIC POWER PLANT

Bendix
AVIATION CORPORATION
RESEARCH LABORATORIES DIVISION
DETROIT, MICHIGAN

NP-10699

PROJECT 2191-020

Report No. 1317
Copy 416

SUPPLEMENTARY ANALYSIS OF THE POWER-LIMITING SYSTEM for the ENRICO FERMI ATOMIC POWER PLANT

30 SEPTEMBER 1959

Submitted to
Atomic Power Development Associates, Inc.
1911 First Street, Detroit 26, Mich.

By

Bendix Aviation Corporation
Research Laboratories Division
P.O. Box 5115, Detroit 35, Michigan

Approved by: C. M. Edwards
C. M. Edwards, Associate Director, Technical

157 01

TABLE OF CONTENTS

157 06

LIST OF ILLUSTRATIONS

LIST OF TABLES

FORWORD

The Research Laboratories Division of Bendix Aviation Corporation is actively engaged in analog computer studies of the Enrico Fermi Atomic Power Plant. Since early 1955, several simulation programs have been conducted at the Division's analog computer facility. These programs have included simulations of the core coolant flow during a scram, frequency response of a reactor to sinusoidal excitations, investigations of start-up accidents, power failures, and temperature transient responses.

In November 1958, the Research Laboratories Division submitted a report to Atomic Power Development Associates entitled Analysis of the Power-Limiting System for the Enrico Fermi Atomic Power Plant. That report presented a discussion of some anticipated emergency conditions, the ways in which the power-limiting system would respond to each emergency, and the signals used to initiate the responses. The present report is a supplement to the above analysis which considers the effects of some reactor plant design changes on the design of the power-limiting system.

The authors are pleased to aknowledge the assistance of the engineering staff of Atomic Power Development Associates in providing information and for helpful discussions. In particular we wish to thank Mr. W. J. McCarthy and Mr. E. L. Alexanderson for their constructive criticism of the manuscript, Mr. R. G. Olson for instructive discussions and engineering data, Mr. J. D. Herb for a discussion of statistical hot-channel factors, and Mr. R. B. Nicholson for information on the effect of sodium boiling in a core channel. We are also indebted to The Holley Carburetor Company for the results of their simulation study, which were transmitted to us by Atomic Power Development Associates.

This report has been prepared by:

J. H. Talboy, Jr.
E. H. Lemon
W. H. Baur

This report has been approved by:

A. B. VanRennes

SECTION 1

INTRODUCTION

1.0 GENERAL

On November 1, 1958, the Research Laboratories Division of Bendix Aviation Corporation completed an analysis of the power-limiting system for the Enrico Fermi Atomic Power Plant. The results of this study were submitted to Atomic Power Development Associates, Inc., (APDA) as Bendix Report No. 1052. Since that study was finished, changes in design and operating philosophy by APDA have made it necessary to re-examine the study. The results of the re-examination are presented in this report.

1.1 DESCRIPTION OF THE ATOMIC POWER PLANT

The Enrico Fermi Atomic Power Plant is a fast-breeder nuclear reactor power plant, now under construction by the Power Reactor Development Company at Lagoona Beach, Michigan.

Figure 1.1 is a schematic diagram of the flow paths for the heat transfer fluid through the power plant. The heat transfer fluid, or coolant, is liquid sodium. Heat is transferred from the reactor core to intermediate heat exchangers by three parallel liquid sodium loops having the reactor in common. The secondary heat transfer fluid is also liquid sodium. Each secondary loop includes a steam generator which produces steam for a common turbo-generator.

The reactor has two control systems. One system regulates the small fluctuations of reactor power which occur during normal operation, and keeps the reactor at the desired power level. In this report, this system is known as the regulating system. The regulating system controls the reactor by means of two regulating rods. These rods have a total reactivity worth of 92 cents. The regulating rods are never completely withdrawn from the core under normal operating conditions. Furthermore, the motion of the regulating rods is so limited that positive reactivity can neither be inserted nor removed at a rate greater than one cent per second. When the study that was described in Bendix Report 1052 was made, the design of

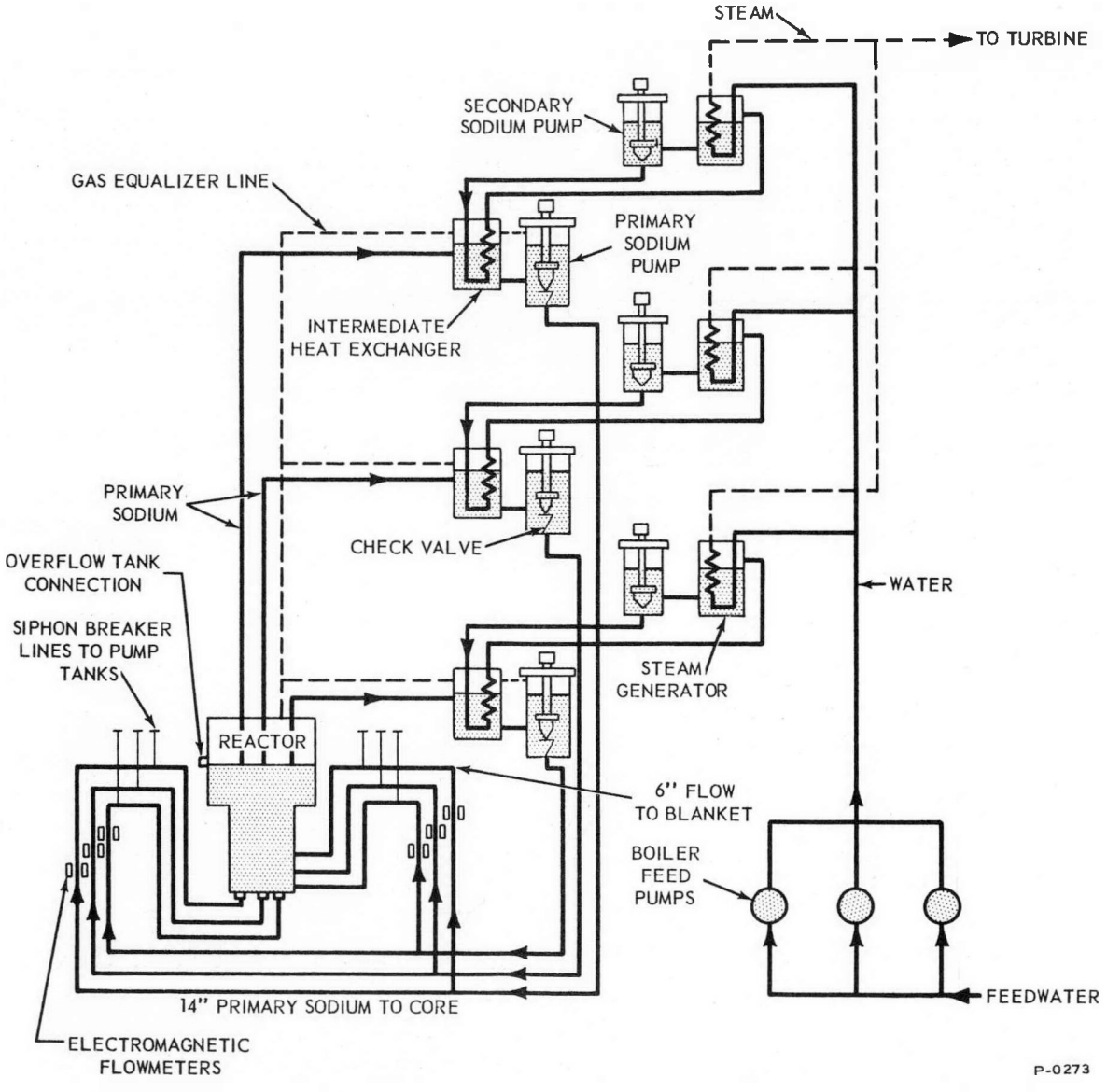

Figure 1.1 - Flow Diagram of the Atomic Power Plant

the regulating system was such that the total worth of the regulating rods could be changed at the nominal rate of one cent per second. When the computer runs reported here were made the design had not been changed. However, the design of the regulating system has now been modified so that only one rod can move fast enough to change reactivity at the rate of one cent per second. The other of the two regulating rods has its speed so limited that it can only change reactivity at the average rate of one cent per minute. Thus, it is to be noted that all of the excursions, caused by reactivity insertions, that are discussed in this report are much more severe than any that can be caused by the regulating system as it is presently designed. With the present design, only 46 cents worth of reactivity can be inserted at the nominal rate of one cent per second, instead of the 92 cent total which was used in computing the curves presented here. In principle, it is possible to estimate the effect of stopping the reactivity insertion at 46 cents for the cases where the excursion does not begin in the subpower region. However, it must be remembered that for a constant rod speed, the reactivity inserted is not a linear function of time; especially at the ends of the rod.

The second of the two reactor-control systems is designed to control large fluctuations in power whose magnitude and rate fall outside of the preset limits of operation of the regulating system. This latter system is called, the power-limiting system in this report. It is the conceptual design of the latter system that is analyzed here, and in Bendix Report 1052. In the reference design, the power-limiting system scrams the reactor by means of eight safety rods. Each safety rod has a reactivity worth of approximately one dollar. During operation, the safety rods are completely withdrawn from the core and from the upper axial blanket. The speed of inward motion of the safety rods is only limited, in the scram mode, by the force available to accelerate them. In the reference design, these rods pass through the upper axial blanket and seat in the core within 0.6 second after being released. For the purposes of this simulation, the scram rods are assumed to pass instantaneously through the upper axial blanket. The outward motion of the safety rods is so limited, that when moving together, they can only insert positive reactivity at the maximum total rate of one cent per second.

1.2 THE STUDY

When designing a power-limiting system for a nuclear-reactor power plant, information about the transients that it will have to

control is essential. Also, studies must be made of the best responses of the apparatus. Finally, the methods, of and the levels for, tripping the responses must be selected. This report presents the results of such an analysis. In some cases, the arguments are based on mathematical details developed in Bendix Report 1052. The details are not repeated here, but appropriate references to that report are made as needed.

The Research Laboratories Division of Bendix Aviation Corporation undertook the study, which resulted in Bendix Report 1052, during the Fall of 1957. The present analysis was begun in December 1958. The simulations were done at the analog computer facility of the Division. Both studies only consider the transients resulting from failures in the electrical and mechanical equipment associated with the reactor.

For the purposes of this study, as for the preceeding one, the rated full output of the reactor plant has been taken to be 300 thermal negawatts. This limitation is imposed by the design of the first core. A later core is expected to have an output of 430 thermal megawatts. Since the characteristics of the later core are not yet known, this study was based on the first core, whose parameters are known.

It is recognized that failures in the various pieces of apparatus associated with the reactor can lead to undesired reactivity insertions and flow changes. These in turn induce temperature changes that can result in coolant boiling and fuel melting. These conditions will be discussed in more detail in the paragraphs that follow.

In considering damaging events, knowledge of what conditions cause undesirable effects is necessary. With guidance from APDA, the following temperatures have been selected as those which can cause fuel melting:

Coolant boiling	1620°F
Uranium melting	2070°F

Because of the sodium head above the core, the sodium will actually boil at a slightly higher temperature than 1620°F.

A basic assumption used during these studies has been that the reactor will never be loaded with more than 92 cents worth of excess

reactivity. A larger excess reactivity will give more severe temperature transients from low power operation than those considered. However, the addition of reactivity at the rate of one cent per second will not cause the reactor to increase power with a growth factor greater than one neper per second; even if more than one dollar's worth of reactivity can be inserted.

Some of the computer runs predict that fuel melting will not take place. Those predictions depend upon certain assumptions and approximations, and must be considered as being only qualitative

1.2.1 High Temperature Damage

If sodium boiling occurs in a coolant channel of the Enrico Fermi Reactor core at a time when the power is greater than five to ten percent of the full value, it is believed that the boiling in a subassembly will cause flashing of the coolant in the subassembly and that effective cooling will therefore be lost The results to the fuel of such a loss of cooling could be quite serious, possibly causing local or general melting; depending strongly on the details of the situation. The power-limiting system must therefore, be designed to prevent sodium boiling

While, in general, the fuel will be at a higher temperature than the coolant and will melt, at the hottest point, before the coolant boils, cases can also be found where the coolant will boil first Therefore, the power-limiting equipment must be so designed as to prevent the damaging event which would take place first.

1.2.2 Thermal Shock

In the first study, the power-limiting system was designed in such a manner as to minimize thermal shocks The parts of the reactor and structure that were considered most sensitive to thermal shocks were: the inlet and outlet nozzles, and the hold-down plate over the core To minimize these shocks the power-limiting system was designed to have three modes of response: setback, sequential scram, and scram. The setback made use of a reversal of regulating-rod motion to bring the reactor to some safe power level in case of a slow positive excursion. The sequential scram was a response that would introduce negative reactivity in such a manner as to keep the reactor outlet temperature from undergoing rapid fluctuations in the event of a complete primary flow failure.

The scram of course, was a last resort. The thermal shocks, accompanying the scram, were severe and would not be alleviated.

Since the first study was finished, APDA has acquired data which show that the sequential scram mode can be eliminated because the various parts of the reactor and structure are protected by thermal baffles, and can withstand the thermal shocks from repeated scrams. Thus, one reason for a re-examination of the original analysis, was the need to redesign the power-limiting system using only a scram to arrest serious transients.

1.2.3 Temperature Coefficients of Reactivity

The analysis performed previously was based on the best data available at that time for the values of the temperature coefficients of reactivity. Since uncertainty about the actual values of temperature coefficients of reactivity always exists until a reactor is operated, it was considered advisable to examine the transients for a band of temperature coefficient values. Also, redesign of the core has effectively eliminated the temperature coefficients of reactivity due to expansion of the upper and lower grid plates, and has introduced one due to the expansion of the core center. These considerations, provided another reason for a re-examination of the previous study.

The calculated temperature coefficients of reactivity used are listed in Appendix A of this report. They are based on the best information available at the time that the present study was begun. The relationship of these coefficients to power and temperature are discussed in the report: Enrico Fermi Atomic Power Plant, APDA-124, January, 1959. APDA now has information, from critical assembly studies, that shows that the actual coefficients will have values near one-and-one-half times the calculated value.

1.3 SIMULATION

1.3.1 Primary Coolant Loop

To analyze the power-limiting system a large analog computer was used to observe the behavior of the reactor under a variety of conditions. Figure 1.2 shows a simplified schematic diagram of the reactor and primary coolant loop, indicating the temperatures that were simulated to serve the purposes of the study. In the

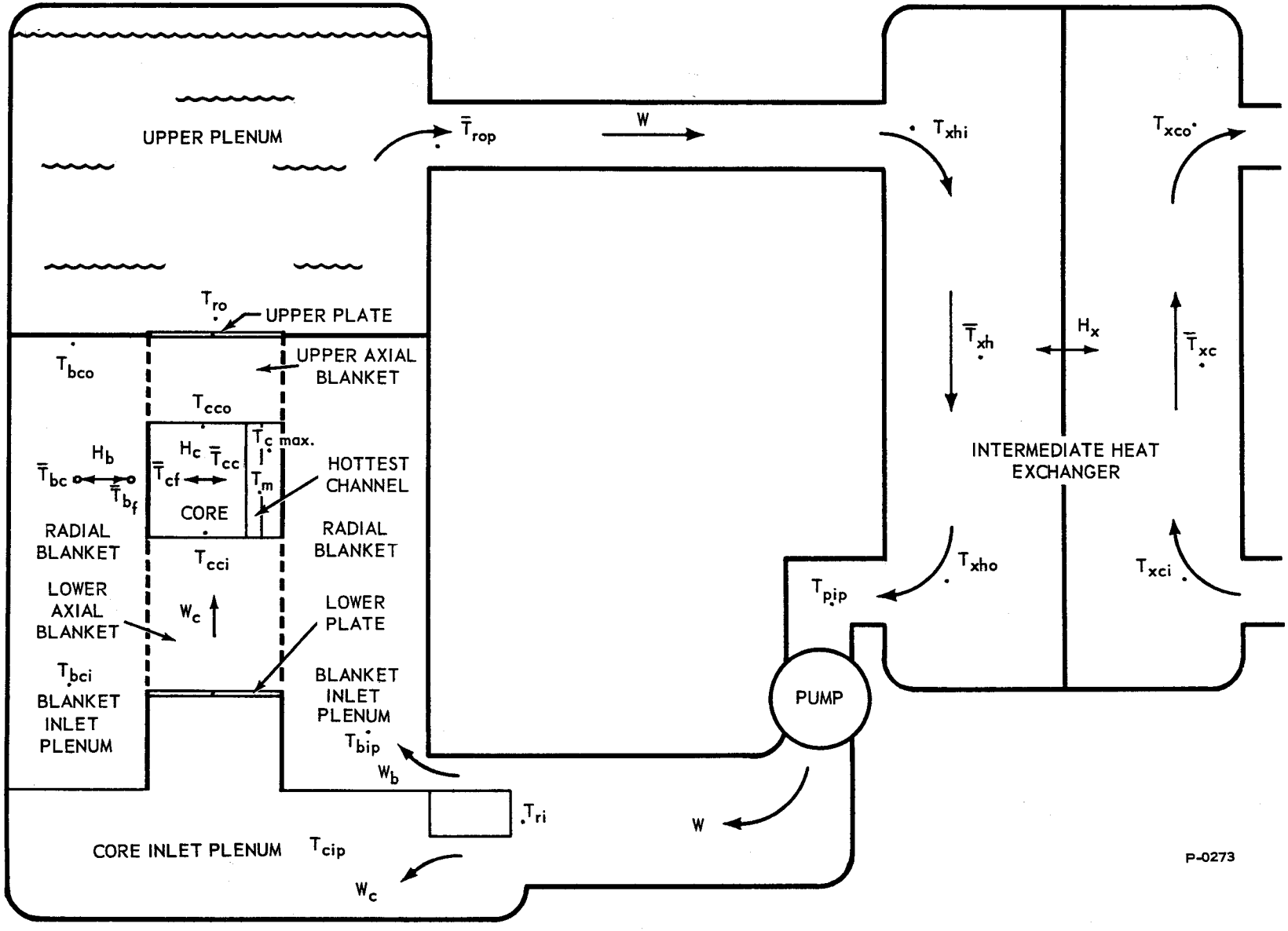

Figure 1.2 - A Simplified Schematic Diagram of a Primary Coolant Loop

reactor core and blanket, these temperatures include: The mean temperature of an effective blanket fuel element ($\bar{T}_{bf}$), the mean temperature of an average core fuel element ($\bar{T}_{cf}$), the mean temperature of the blanket coolant ($\bar{T}_{bc}$), the mean temperature of the core coolant ($\bar{T}_{cc}$), the maximum temperature of the hottest fuel element (T_m), and the maximum temperature of the coolant in the hottest channel (T_{cm}). When the core coolant, at an outlet temperature of (T_{cco}), mixes with the blanket coolant, at an outlet temperature (T_{bco}), the temperature of the reactor outlet coolant (T_{ro}) is established. Additional quantities pertaining to the core and blanket, indicated in Figure 1.2, are: the heat transfer coefficients for the core and blanket; (H_c) and (H_b), respectively, the total weight flow of the coolant (W), the weight flow of the coolant through the core (W_c), and the weight flow of the coolant through the blanket (W_b).

The mean temperature of the reactor outlet plenum ($\bar{T}_{rop}$) follows the temperature of the reactor outlet coolant; after a mixing delay in the plenum. The temperature of the coolant in the inlet plenum of the hot side of the intermediate heat exchanger is (T_{xhi}); and follows the temperature of the reactor outlet plenum with a delay due to the transport time in the pipes. Some mixing also takes place in the intermediate-heat-exchanger inlet plenum. The mean temperature of the hot, or primary, side of the intermediate heat exchanger ($\bar{T}_{xh}$), and the outlet temperature (T_{xho}) are then obtained. From the outlet plenum of the hot side of the intermediate heat exchanger, the coolant flows to the pump inlet plenum with a temperature (T_{pip}) where, again, mixing occurs. After a transport time delay from the pump to the reactor, the coolant arrives at the reactor inlet with a temperature (T_{ri}). After mixing, the temperatures of the coolant arriving at the core and blanket inlet plenums are (T_{cip}) and (T_{bip}) respectively. Additional transport time delay is present between the reactor inlet and the blanket inlet plenum. The temperatures of the core inlet coolant (T_{cci}) and the blanket inlet coolant (T_{bci}) are the same as the temperatures of the coolant in the corresponding inlet plenums.

The temperatures of the secondary coolant at the intermediate heat exchanger shown in Figure 1.2 are: the temperature of the inlet coolant (T_{xci}), and the temperature of the outlet coolant (T_{xco}). The heat transfer coefficient of the intermediate heat exchanger is (H_x).

A complete list of defined symbols is given in Appendix A.

1.3.2 Effect of Core Design Changes

When the analysis presented in Bendix Report 1052 was performed, the reference design was such that the expansion of the upper and lower core grid plates influenced the effective reactivity. For this reason temperature coefficients of reactivity for the upper and lower plates were included in that simulation, and the mean temperatures of the upper plate (T_{up}), and of the lower plate ($T_{\ell p}$) were computed. Since the latter study was completed, the design of the core has changed. It is now rigidly fixed at the center, and the expansion of the upper and lower plates has a negligible effect on the reactivity. In the present analysis a temperature coefficient of reactivity depending on the expansion of the core center is introduced. This reactivity effect is due to the expansion of the fuel subassembly can walls, and of the spacer-pads. The temperature coefficients of reactivity pertaining to the upper and lower plate expansions are no longer used, and so T_{up} and $T_{\ell p}$ are not computed.

1.3.3 Changes in Temperature Coefficients of Reactivity

At the beginning of this study, APDA had obtained information which led to changes in the calculated temperature coefficients of reactivity from the values used in the earlier analysis. These calculated values were based on the best information available at that time. Since the coefficients are not completely known before the actual reactor is operated, a set of three coefficients has been used here. This set was obtained by multiplying the calculated coefficient, ρo, by one half and by one-and-one-half. The coefficients used were then, $\rho o/2$, ρo, and $3\rho o/2$. A complete list of the constants used in this study is given in Appendix A. APDA now has information which places the presently estimated value of the temperature coefficient of reactivity near $3\rho o/2$.

1.3.4 Shut-Down Temperature Change

In the analysis performed previously, it was assumed that the reactor would be kept at a temperature of 600 degrees F when it was not operating. The shut-down temperature has been changed to 550 degrees F; the value used in the analysis reported here. This change only affects the excursion from low power, and the start-up excursion because more reactivity is available for insertion at low power. This change increases the rate-of-change of power during the transients, but not the maximum power obtainable.

If the shut-down temperature is decreased still further the rate will increase still more, but the maximum power will not be affected.

1.3.5 Hot Channel Considerations

1.3.5.1 Average Hot Channel

In this study, as in the previous one, the maximum fuel and coolant temperatures were obtained by considering the average hot channel. The equations used in Bendix Report 1052 were empirically derived from curves given in APDA-115, Enrico Fermi Fast Breeder Reactor-Plant, November 1, 1956, p 32. The derivation is explained in detail in Appendix B, Section 4, of Bendix Report 1052, p. 132. Since the latter report was finished, APDA has recalculated the temperature distribution to be expected in the hottest channel, and this has led to a revision of the equations used in the simulation. The equations used when performing the calculations for this report are derived in detail in Appendix B, Section B 4. The curves upon which the derivation is based are given in APDA-124, Enrico Fermi Atomic Power Plant, Jan. 1959, p. 44. The re-evaluation of the hot channel factors given in APDA-124 Enrico Fermi Atomic Power Plant, has led to changes in the maximum fuel and coolant temperatures that are expected at full-power operation. In the previous study the maximum fuel temperature was 1320 degrees, and the maximum coolant temperature was 1020 degrees F. Now, the maximum fuel temperature is 1134 degrees and the maximum coolant temperature is 915 degrees F.

1.3.5.2 Statistical-Hot-Channel Factors

The maximum fuel and coolant temperatures that have been calculated during this study were based upon the curves cited in Section 1.3.5.1. Since the computer runs were finished, the authors have been made aware of a different method of calculating the temperature at a point in a fuel pin. When calculating a temperature in a fuel pin, account must be taken of: the coolant temperature rise above inlet temperature, the temperature difference across the coolant film boundary layer, the temperature difference across the oxide layer, the temperature difference across the clad, and the temperature

difference from the fuel centerline to the clad. It is possible to choose mean values for all the above quantities and calculate the temperature at a point on the fuel centerline. This was done to obtain the average hot channel factors. However, the above quantities are subject to uncertainties which, in turn affect the end result. One can use a statistical approach to calculate a probable value for the upper limit of the temperature at a point in the fuel, in which a range of values for the above temperature differences is assigned. This range of values is assigned assuming that each quantity has its values distributed in a normal manner. From probability theory it is known that the value of a quantity has a 99.9 percent probability of lying below three standard deviations above the average value. Therefore, all of the temperature rises are assigned appropriate variations and a probable value of the upper limit of the fuel temperature is computed, with a confidence factor of 99.9 percent. This calculation is presented in APDA 124, Enrico Fermi Atomic Power Plant, January, 1959, p. 48. In Appendix B, Section B.4 of the present report, empirical relations are derived which can be used to calculate the hot-channel temperatures expected with the statistical methods, from the curves given in this report. It must be noted that one of the factors in the calculation is the temperature difference across the coolant film boundary layer. This quantity can change with flow, so these relations should be applied with caution to the cases where primary coolant flow changes. It is assumed in the simulation, that this quantity does not change, so the error is already present in the results of the simulation. The application of the correction factor may or may not compound the error.

1.3.6 Reactor Inlet Coolant Transients

In the previous study, the behavior of the reactor inlet coolant temperature when primary sodium, secondary sodium, and feedwater flow changed was estimated. These estimates were used to program the reactor inlet coolant temperature so that the behavior of the reactor, under such conditions, could be investigated.

Since the last report was prepared, data that originated in the Holley Carburetor Company's control system study have been made available to Bendix by APDA. In the present re-examination the Holley results were used in the computation to give as realistic a simulation as possible, for the cases where secondary sodium and feedwater flow changed.

1.3.7 Computer Diagram

The computer set up used in this study is different from the one used to provide the information presented in Bendix Report 1052. The set up that was used for the present study is shown in Figure 1.3. Some changes have also been made in the internal computer circuits. The circuits that differ from those presented in the previous report are discussed, in this report, in Appendix B, Sections B.3.1 to B.3.5.

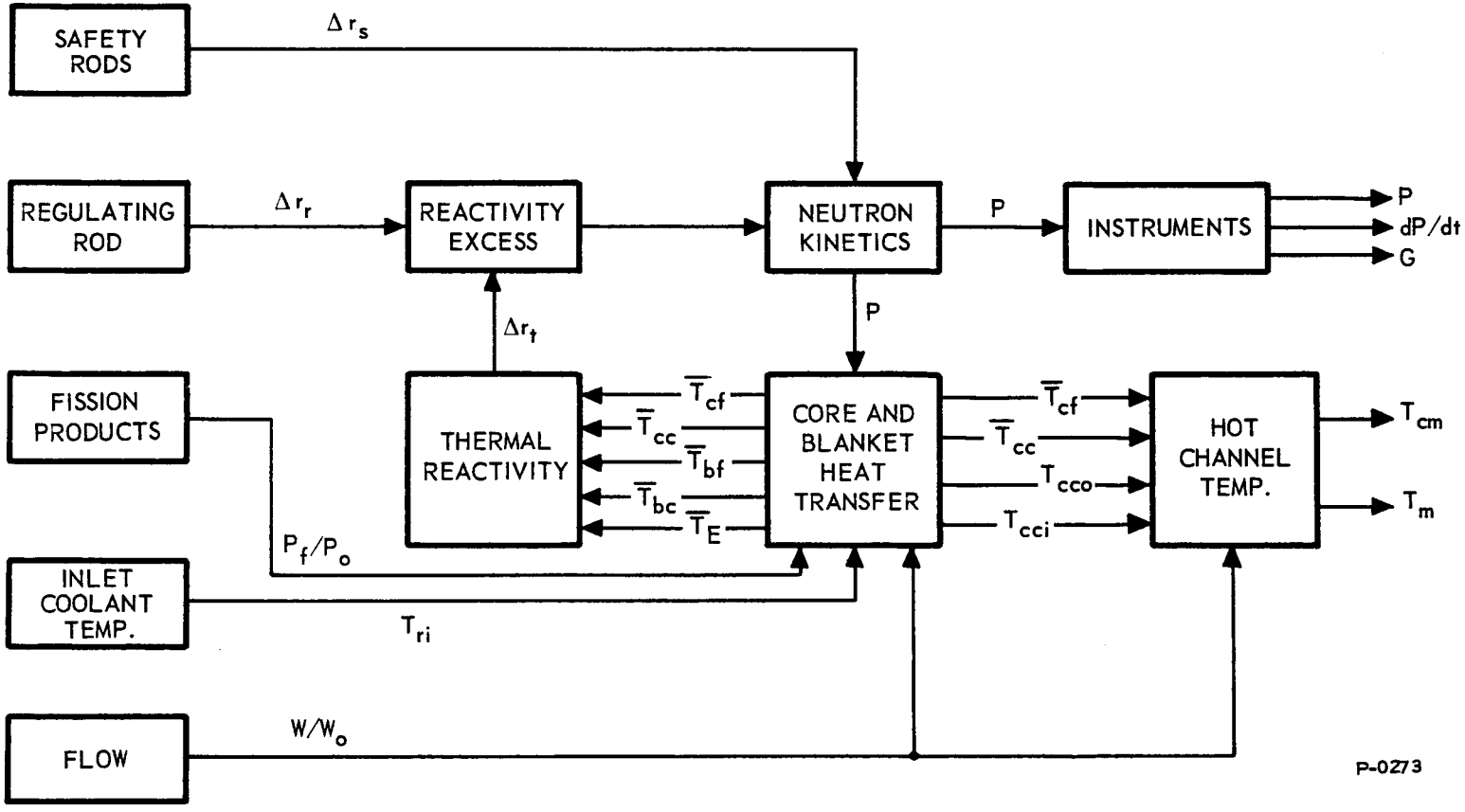

Figure 1.3 - Block Diagram of the Analog Computer Circuit

SECTION 2

CONDITIONS REQUIRING ACTION BY THE POWER-LIMITING SYSTEM

2.0 GENERAL

During start up and operation of the atomic power plant, certain fluctuations in power are to be expected which are not dangerous and should be considered normal. The power-limiting system should not respond to signals induced by such changes; their control lies in the domain of the regulating system.

This section presents considerations of fluctuations in coolant temperatures, coolant flow rates, and reactivity to see under what conditions the power-limiting system must respond. There are two parts to this section. The first part deals with fluctuations during full-power operation, and the second with transients during start up.

2.1 TRANSIENTS DURING FULL-POWER OPERATION

When the plant is operating at full power, there are several causes of fluctuations that the power-limiting system will be required to arrest. Here we will consider a situation that will result in the insertion of positive reactivity at the rate of one cent per second, to a total of 92 cents; a complete primary coolant flow failure, partial failure of primary coolant flow, and some disturbances of secondary-coolant and feedwater flow that give rise to reactor-inlet-coolant temperature changes.

2.1.1 Positive Reactivity Insertion

It is assumed that some combination of circumstances has caused positive reactivity to be inserted at the rate of one cent per second, until 92 cents has been inserted. A computer run has been made to determine the effects on the reactor and primary coolant temperatures when such a reactivity transient takes place. Figure 2.1 shows the maximum fuel and coolant temperatures, in the hottest channel of the core, during such an excursion. In this figure, curves for three values of the temperature coefficient of reactivity have been presented. The curve labeled ρ_o corresponds to the calculated

temperature coefficient of reactivity. The curves labeled $\rho o/2$ and $3\rho o/2$ correspond to one-half and one-and-one-half times the calculated temperature coefficient of reactivity respectively.

The simulation is not meaningful after sodium boiling takes place Of course, the computer continues to operate, but the data are no longer valid, as indicated by the dotted parts of the curves. This calculation assumes that heat produced in the reactor is removed by the steam system, so that the reactor inlet temperature does not change during the computer run. The correction for statistical hot-channel factors, described in Appendix B, can be applied to the curves in Figure 2 1 Figure 2.2 shows the behavior of the reactor power and the average reactor outlet coolant temperature during the same excursion as described above. For convenient comparison, the corresponding results from the previous report are given in Figure C1, of Appendix C, of this report

2.1 2 Complete Primary Flow Failure

An occurrence that will surely damage the reactor if corrective measures are not taken, is one where all three primary coolant pumps fail at once. It is expected that the negative temperature coefficient of reactivity will help to shut the reactor down, but such high temperatures will be reached that the fuel will still melt. A computer run was made in which the coolant flow at any time, W(t), was given by

$$\frac{W(t)}{Wo} = 0.72e^{-t/1.5} + 0.26e^{-t/10} + 0.02,$$

where Wo is the flow at normal operating conditions, and t is the time in seconds. This equation is not the same as the one used in the last study. In particular, the flow decays to two percent of its initial value; instead of four percent as was previously the case. This final flow value was suggested by the APDA engineering staff. The equation used in the last report is reproduced in Appendix C, Section C.2.2, of this report The power contributed by the decay of fission products at any time after shut-down, t, was assumed to be given by,

$$\frac{P_f(t)}{Po} = \frac{0.141}{t + 3.44} - (4.85 \times 10^{-5})t + 0.034,$$

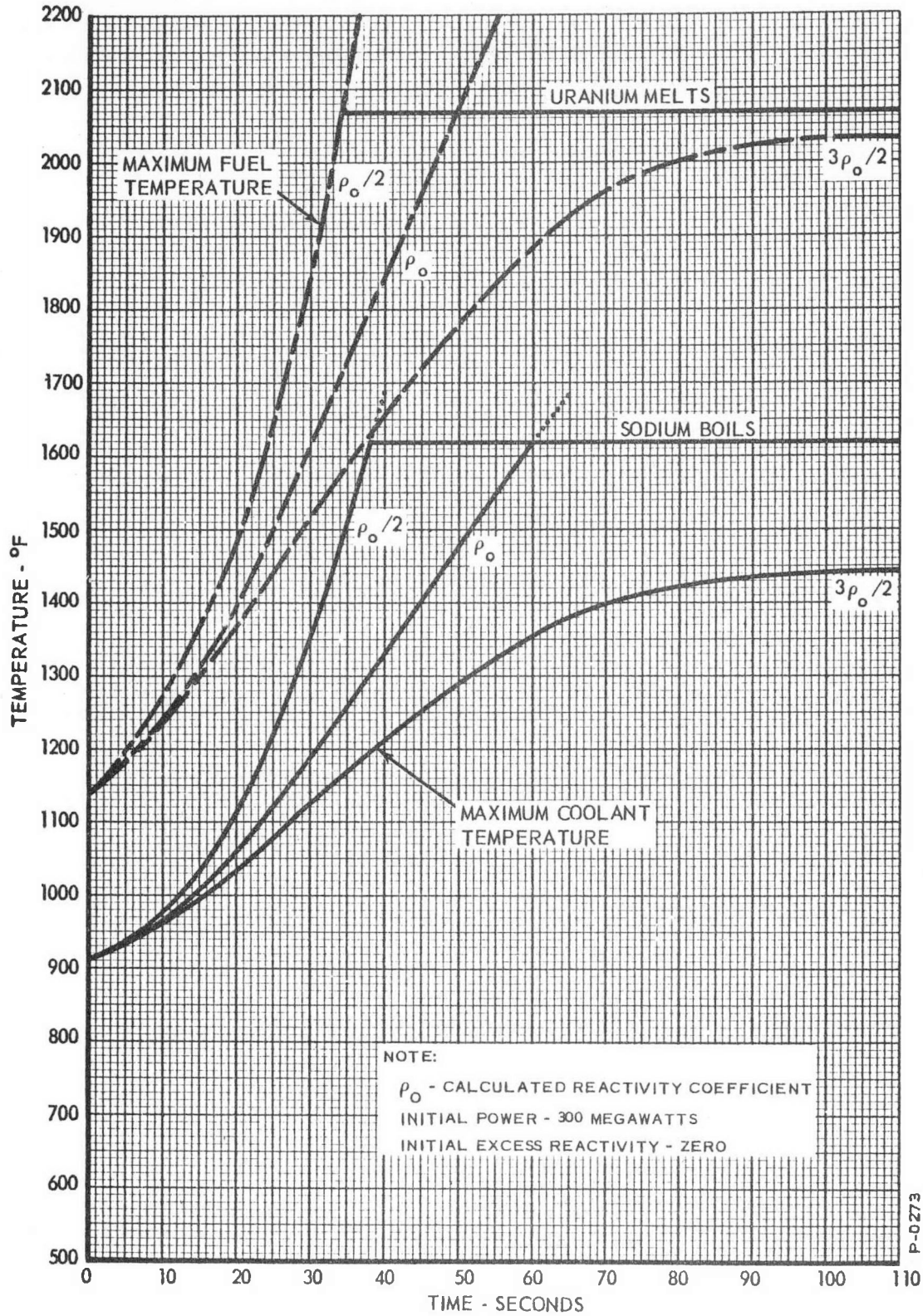

Figure 2.1 - Excursion from Full Power: Maximum Hot-Channel Temperatures

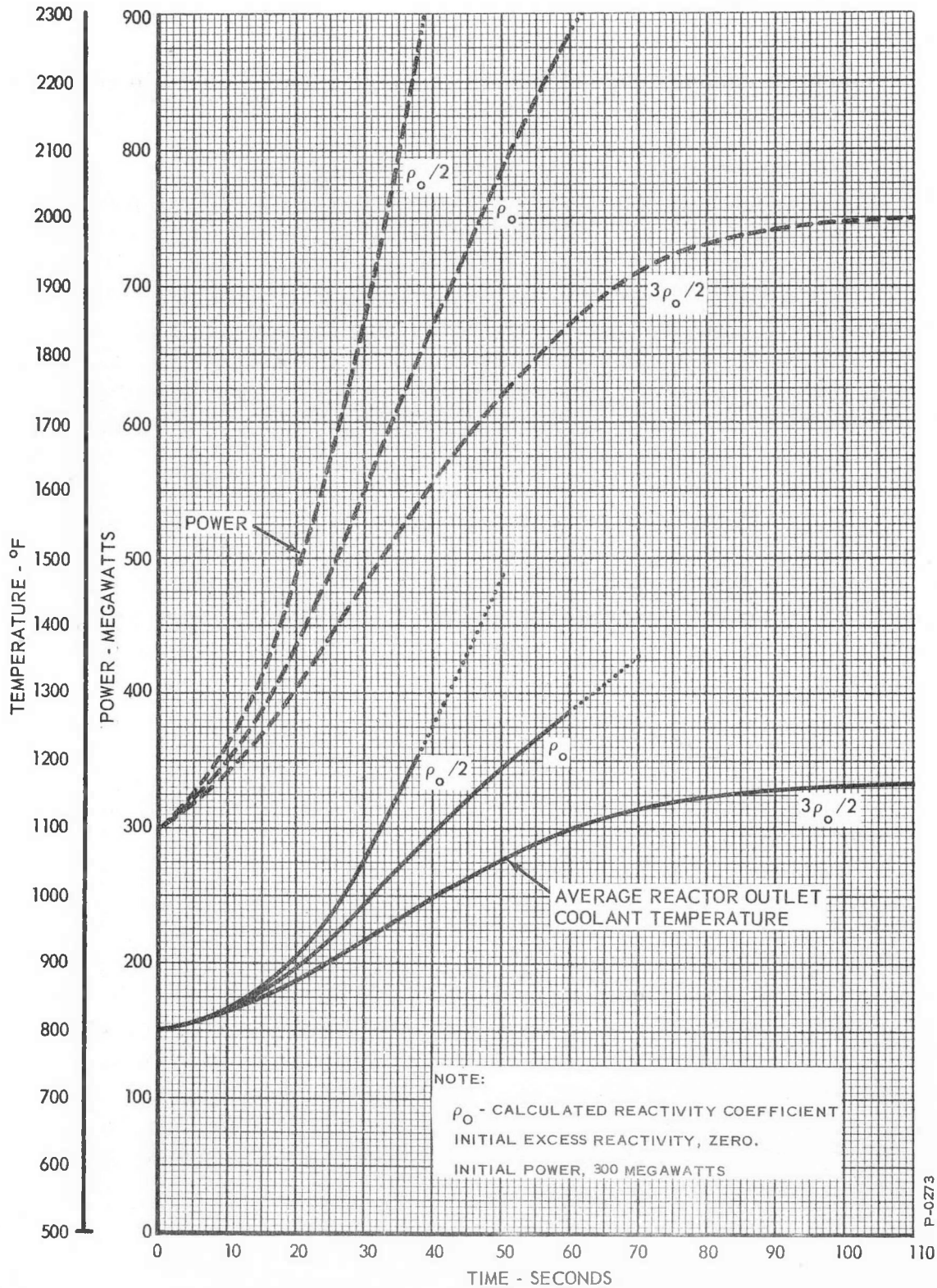

Figure 2.2 - Excursion from Full Power: Power and Reactor Outlet Coolant Temperature

where Po is the normal operating power of the reactor; 300 megawatts. This equation, used to simulate the effect of fission product delay on a power shut-down, is an approximation of the Way-Wigner Law. The details of this approximation are given in Bendix Report 1052, Appendix B, Section 13. The approximation is compared to the Way-Wigner Law in Figure B-13.2 in the above reference. The results of the computer run for maximum fuel and coolant temperatures in the hottest channel are shown in Figure 2.3. The symbol ρo identifies the curve corresponding to the calculated value of the temperature coefficient of reactivity. The curves labeled $\rho o/2$ and $3\rho o/2$ correspond to one-half and one-and-one-half times the calculated temperature coefficient of reactivity respectively. The dotted parts of the curves are meaningless because boiling has occurred in the hottest channel. The correction for statistical-hot-channel factors described in Appendix B can be applied to the curves in Figure 2.3; but because the flow is changing, the results may be only qualitative. The results of the computer run for power and average reactor outlet coolant temperature are shown in Figure 2.4. The dotted portions of the curves are meaningless since coolant boiling has occured in the hottest channel.

For convenient comparison, the corresponding results from the previous report are shown in Figure C2, of Appendix C, of this report.

2.1.3 Reactor Inlet Coolant Temperature Changes

The coolant entering the inlet plenum of the reactor can undergo temperature changes from a variety of causes. One of the primary pumps can fail, resulting in flow stopping in one loop and flowing faster in the operative loops. If it is assumed that the flow does not change in the secondary loop, increased flow in the primary of an intermediate heat exchanger will result in an increase in the temperature of the outlet sodium at the heat exchanger primary, which increases the temperature of the primary coolant entering the reactor inlet plenum. If a secondary coolant pump fails, the outlet coolant temperature at the primary of the intermediate heat exchanger will undergo an increase which will feed into the reactor. Similarly, changes in feedwater flow will induce temperature changes in the reactor inlet coolant.

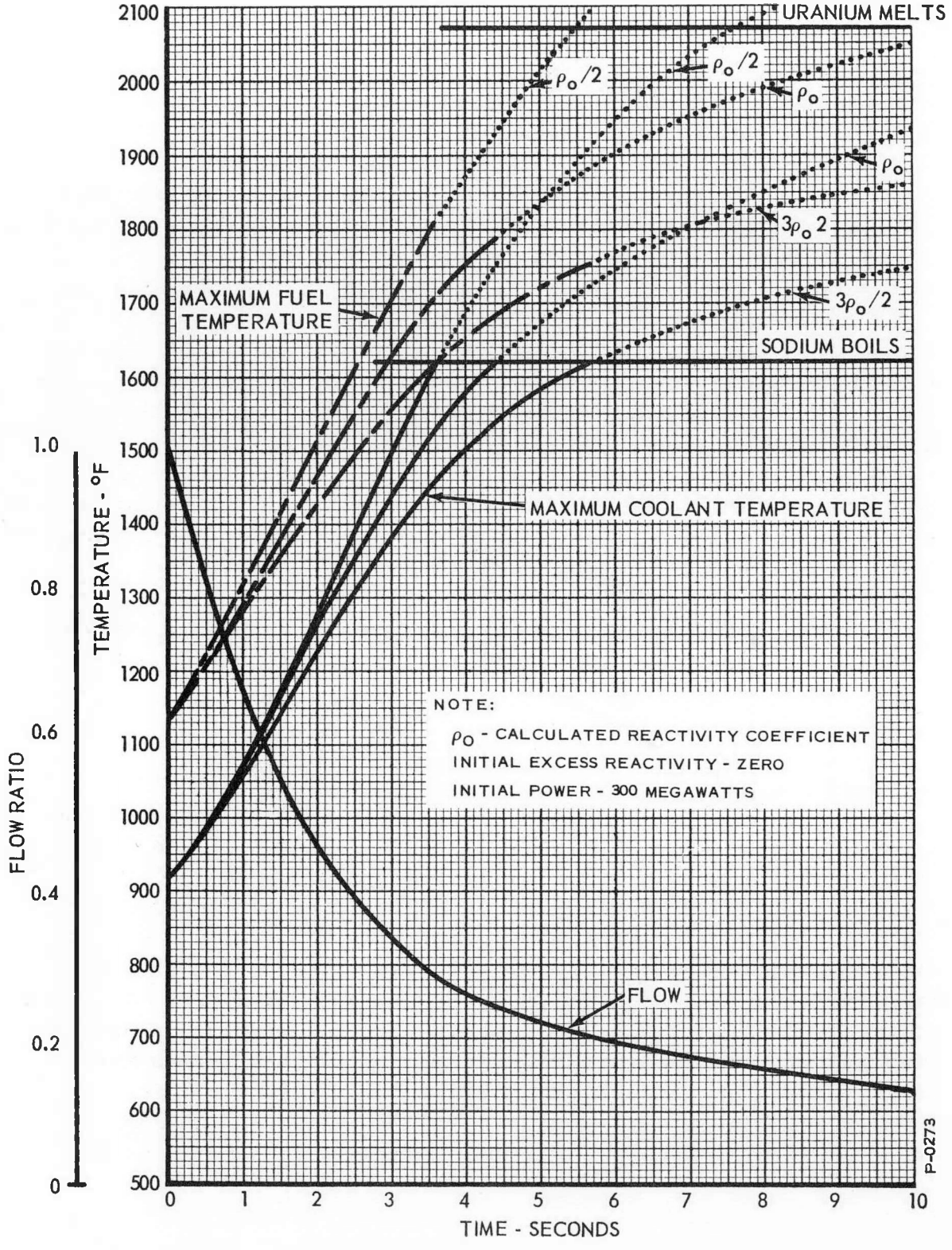

Figure 2.3 - Complete Primary Flow Failure: Hot-Channel Temperature

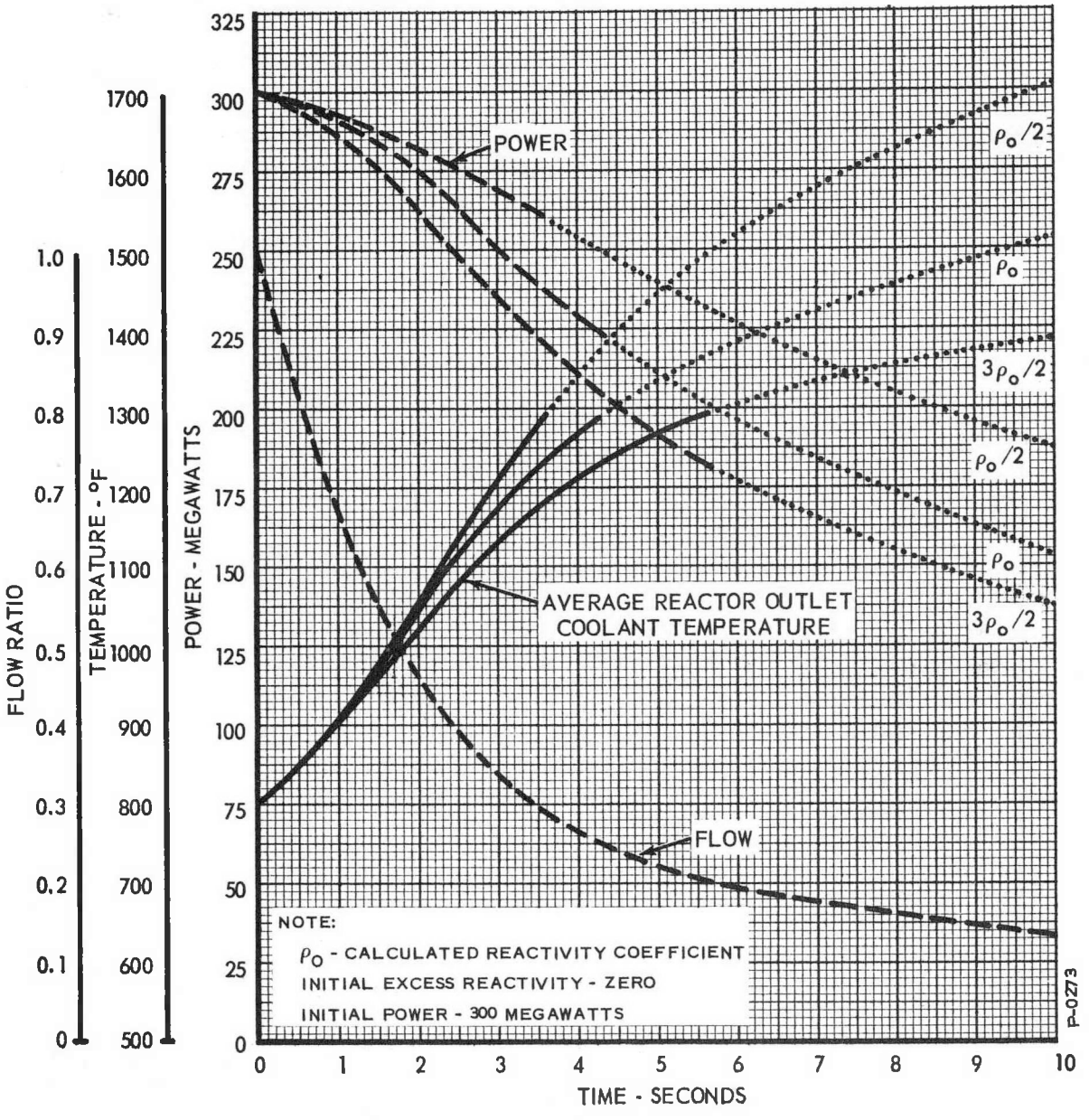

Figure 2.4 - Complete Primary Flow Failure: Power and Reactor Outlet Coolant Temperature

2.1.3.1 Loss of One Primary Coolant Pump

When the reactor is operating at full power, one of the primary coolant pumps can conceivably fail. Because of the hydraulic characteristics of the pumps and the coolant system, the flow will increase through the operative loops. The total primary flow drops to 83 percent of its full value, due to the hydrodynamics of the system, in two seconds after the failure of one primary pump. This flow change has two causes: the flow in the disabled loop drops to zero in two seconds, while the other two loops each increase their flow by 25 percent, with no change in pump speed. The temperature of the primary coolant leaving the operative intermediate heat exchanger primaries increases to a value given by,

$$T_{po} = T_{pi} + \frac{(T_{si} - T_{pi})\left\{1 - \exp\left[\frac{-H}{C}\left(\frac{W_s - W_p}{W_s W_p}\right)\right]\right\}}{1 - \frac{W_p}{W_s}\exp\left[\frac{-H}{C}\left(\frac{W_s - W_p}{W_s W_p}\right)\right]}$$

Here T_{pi} is the primary inlet temperature, T_{si} is the secondary inlet temperature, W_p and W_s are the weight flow rates of the primary and secondary coolants respectively, H is the heat transfer coefficient, and C is the specific heat of the two coolants when they are the same fluid. This equation is derived in Appendix C of Bendix Report 1052. Using the above flow values, we find the temperature rise to total 30 degrees F. For purpose of calculation, the temperature is assumed to rise as a step filtered by a 3.6 second first order lag (due to the effect of the inlet plenum) in cascade with a 4.6 second first order time delay (due to the time constant of the heat exchanger). Figure 2.5 shows the results of the computer run made to study this situation. The temperature of the reactor inlet coolant is assumed to begin to increase, by a total of 30 degrees F., with the appropriate time constant, about five seconds after the flow begins to drop. The five second delay is introduced to account for the transport lag in the primary coolant loop. It is to be noted that the changes in temperature in the reactor are not severe. As expected, the reduction in power caused by the temperature coefficient of reactivity compensates for the inlet coolant temperature change to a large extent. It appears that, from the point of view of the reactor alone, no corrective action is needed. It is to be noted that the data are not correct

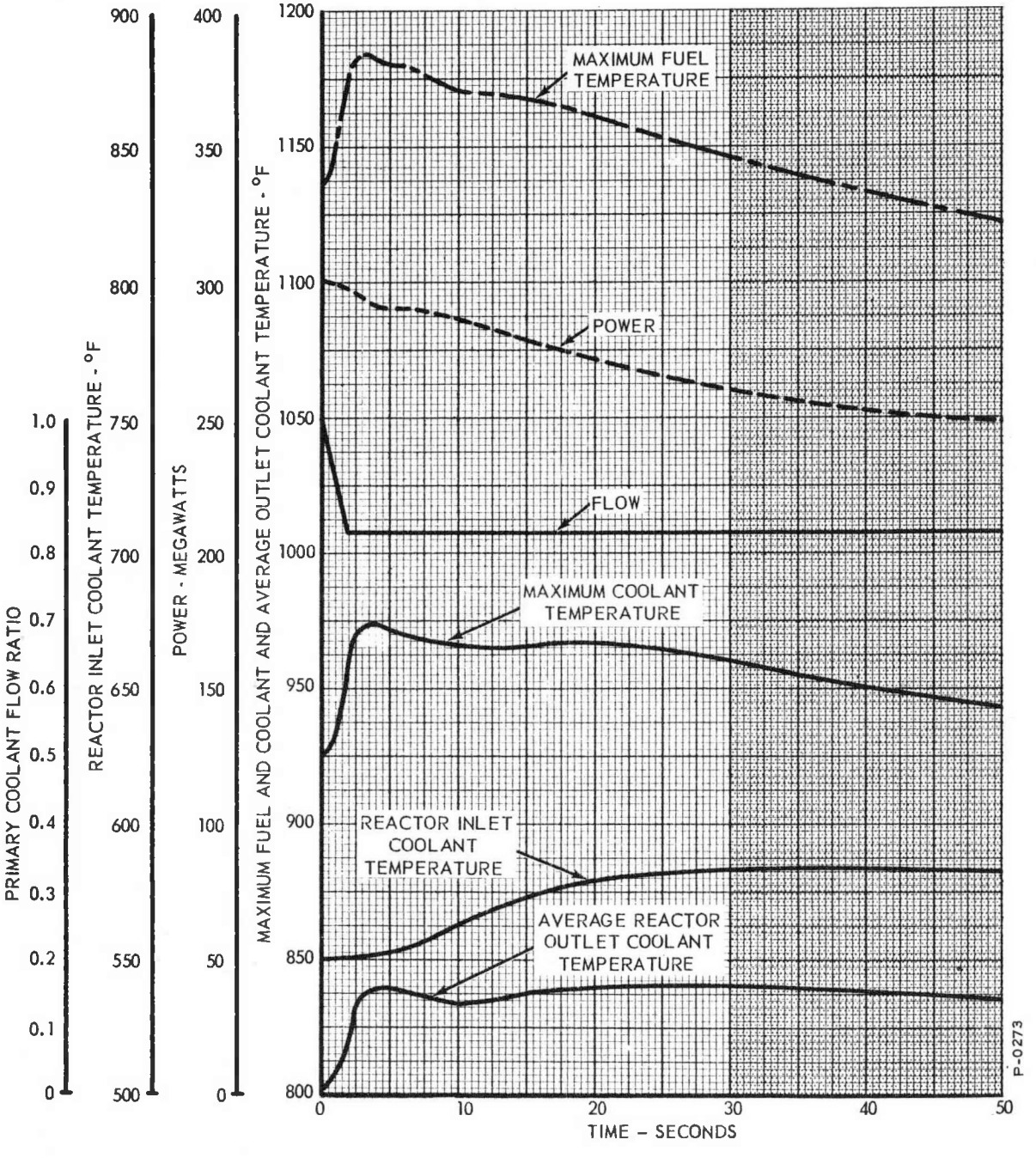

Figure 2.5 - Failure of One Primary Pump: Power and Reactor Temperature

for times longer than 30 seconds because the effect of the recirculation of the coolant around the primary loop has not been simulated. The statistical-hot-channel factors, discussed in Appendix B may be applied to the fuel and coolant temperature, but may provide only qualitative information because the flow is not constant.

For convenient comparison, the corresponding results from the previous report are shown in Figure C3, of Appendix C, of this report.

2.1.3.2 Loss of All Secondary Pumps

The effect, of the loss of all secondary pumps, on the reactor inlet temperature has been studied by the Holley Carburetor Company. Their results are shown in Figure 2.6. The Holley Carburetor Company chose the final value of the flow to be 15 percent of its initial value instead of zero, to account for convective circulation. The effect on the reactor was simulated by introducing the temperature change given by Figure 2.6 into the reactor inlet coolant while the reactor is initially operating at full power. The primary coolant flow was maintained at its full value. Only the calculated temperature coefficient was used. The results of this computer run are shown in Figure 2.7. From the point of view of the reactor proper, damage is not immediate as the negative temperature coefficient serves to reduce the power. The statistical-hot-channel factors described in Appendix B, can be applied to the maximum fuel and coolant temperature curves shown in Figure 2.7. The Holley Carburetor Company curve, shown in Figure 2.6, includes the effect of the recirculation of the coolant around the primary loop, so the curves in Figure 2.7 are qualitatively significant for times longer than 30 seconds.

Because of interlocks between associated primary and secondary pumps, this situation has a very low probability of occurring. The statistical-hot-channel factors corrections, described in Appendix B, can be applied to the maximum fuel and coolant temperature curves.

For convenient comparison, the corresponding results from the previous report are shown in Figure C4, of Appendix C, of this report.

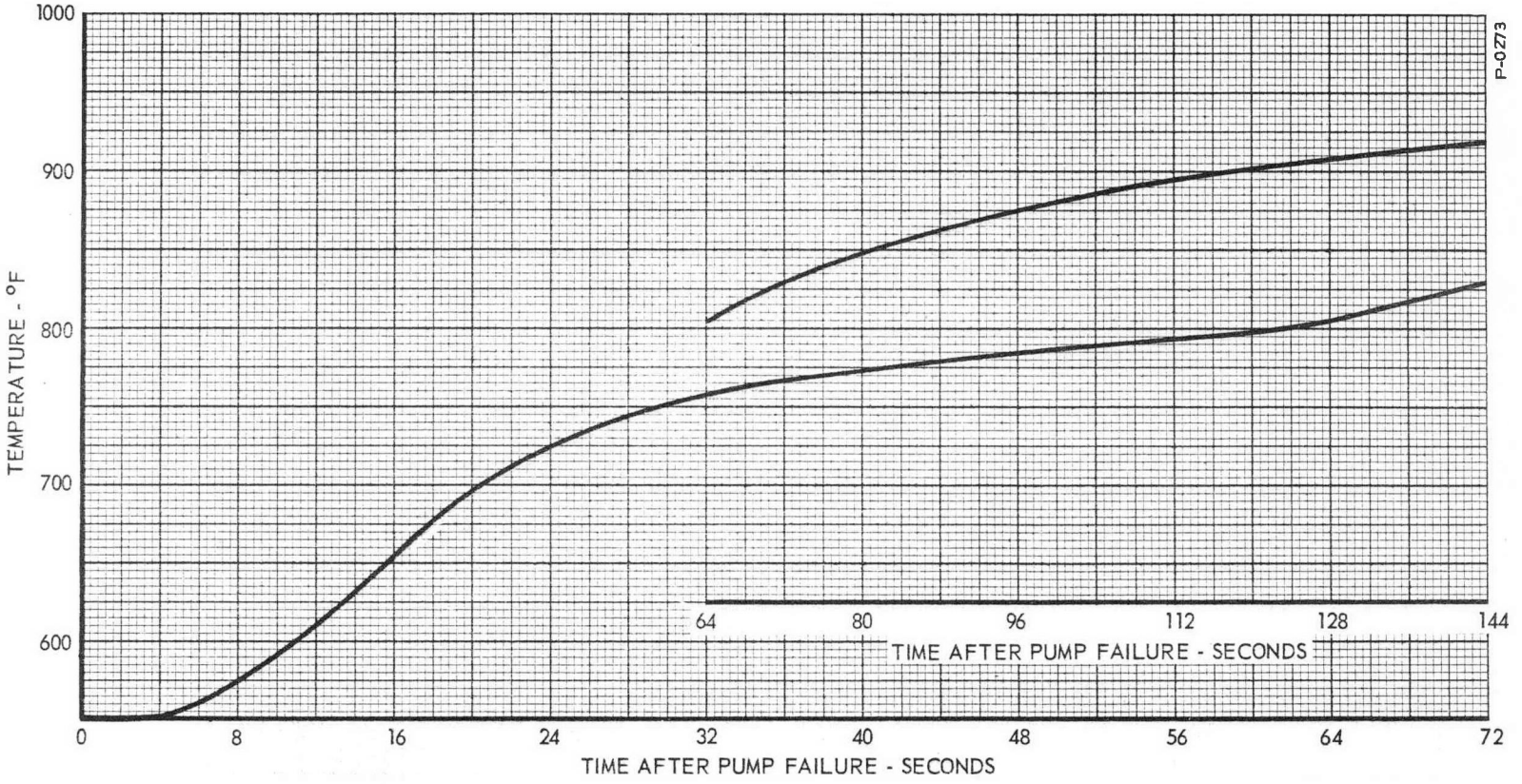

Figure 2.6 - Complete Secondary Flow Failure: Reactor Inlet Coolant Temperature (From Holley Carburetor Company)

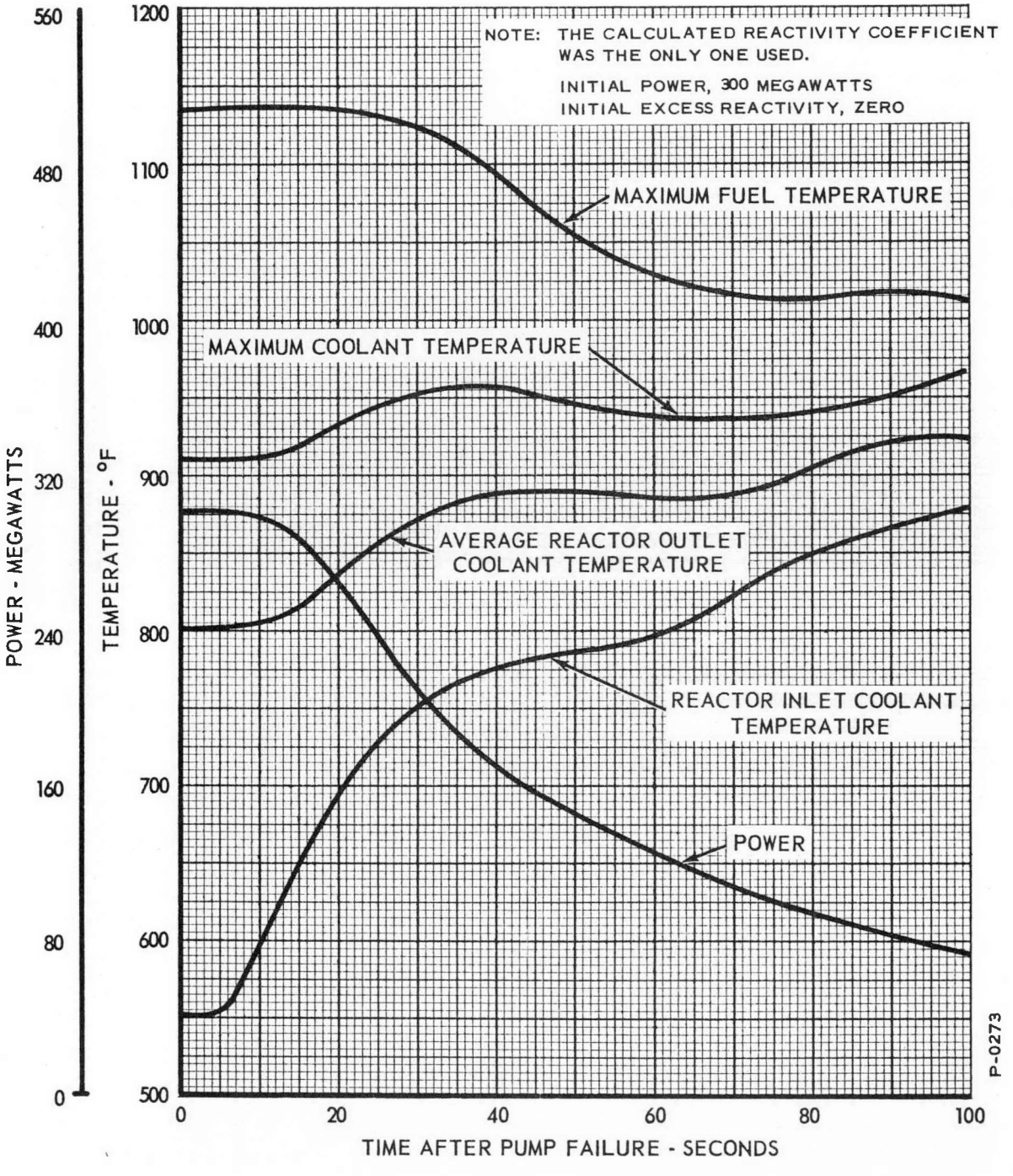

Figure 2.7 - Complete Secondary Flow Failure: Power and Reactor Temperature

2.1.3.3 Loss of One Secondary Pump

When one secondary pump fails, the resulting temperature change in the reactor inlet coolant is assumed to be one third as great as for the case of a total secondary flow failure. A computer run was made programming the reactor inlet temperature in accordance with Figure 2.6, but with the magnitude of the temperature reduced to one third of that shown in the figure. The results of the computer run are shown in Figure 2.8. Only the calculated value of the temperature coefficient was used. Again we see that the transient is smoothed out by the reactor. So, from the point of view of the reactor, no corrective action needs to be taken. The statistical-hot-channel factors described in Appendix B can be applied to the maximum fuel and coolant temperature curves shown in Figure 2.8. The Holley Carburetor Company data take into account the effect of the recirculation of the coolant around the primary and secondary loops, so that data in Figure 2.8 are qualitatively significant for times longer than 30 seconds.

For convenient comparison, the corresponding results from the previous report are shown in Figure C5, of Appendix C, of this report.

2.1.3.4 Changes in Feedwater Flow

Feedwater flow changes can affect the temperature of the reactor inlet coolant by influencing the amount of power removed by the steam generator. The Holley Carburetor Company has computed this effect for two cases: loss of feedwater flow, and increased feedwater flow. In the previous study, computer runs corresponding to those in this section, were not made. In Section C.2.3.4, of Appendix C, of this report, a discussion of the qualitative considerations presented in Bendix Report 1052 is given.

2.1.3.4.1 Loss of Feedwater Flow -- Figure 2.9 is a plot of the data from the Holley Carburetor Company showing the effect on reactor inlet coolant temperature of a reduction of feedwater flow to ten percent of its nominal value. These data were used to program the temperature of the reactor inlet coolant, starting with the reactor at full power. The results of the computer run are shown in Figure 2.10. Again, it is seen that damaging temperatures will not be reached immediately. The statistical-hot-channel correction factors described in Appendix B can be applied to the maximum fuel and

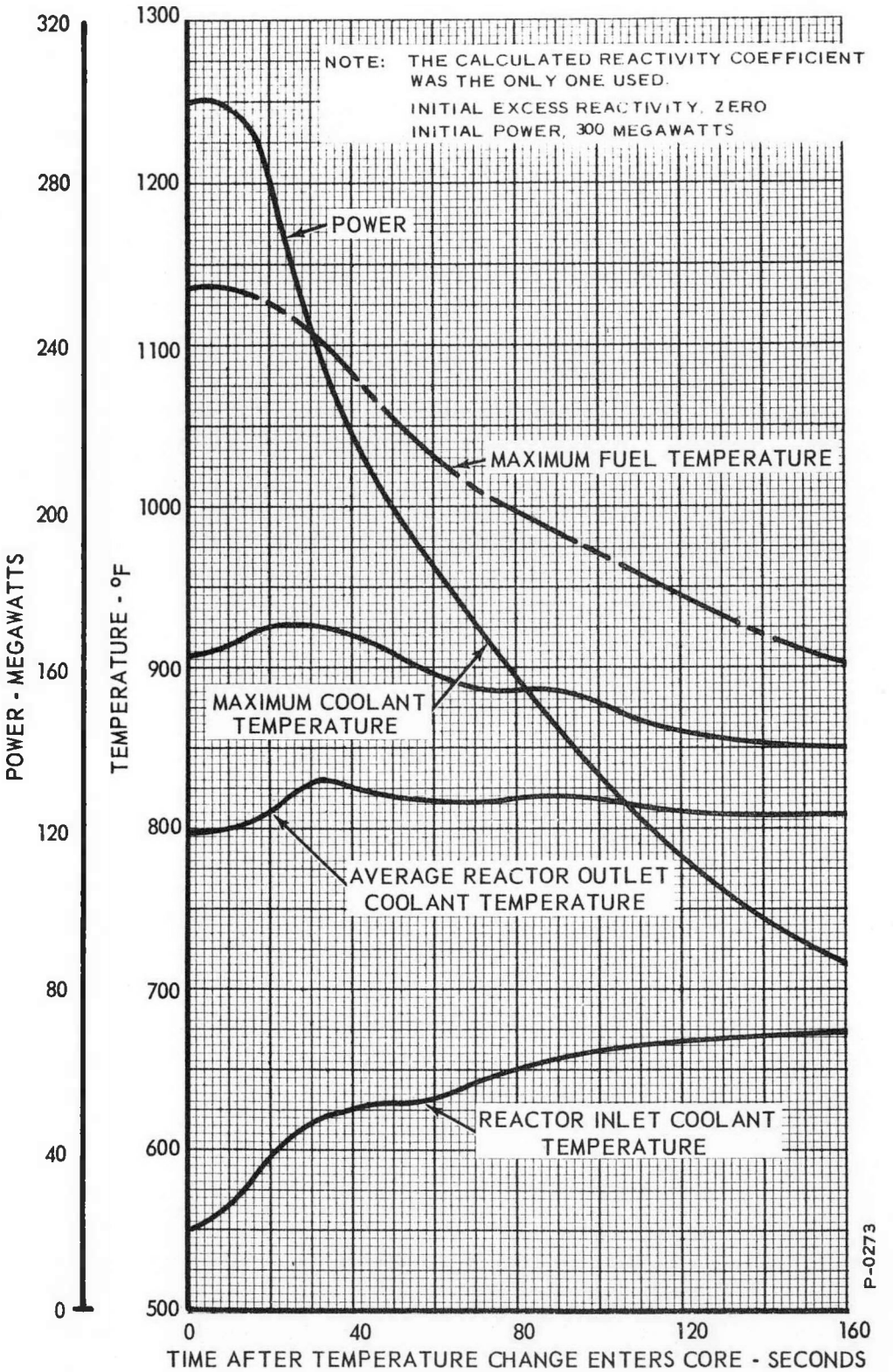

Figure 2.8 - Failure of One Secondary Pump. Power and Reactor Temperatures

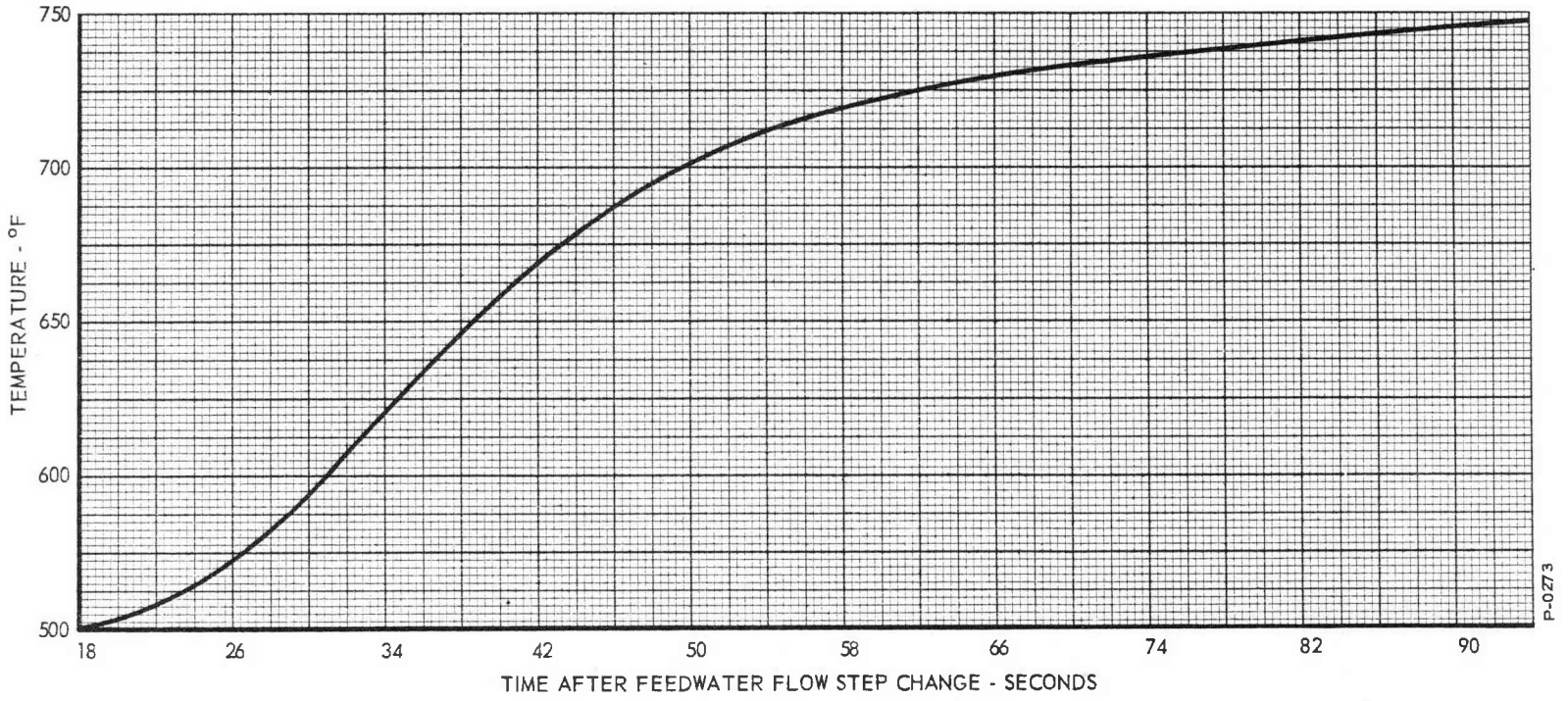

Figure 2.9 - Feedwater Flow Decrease: Reactor Inlet Coolent Temperatures (From Holley Carburetor Company)

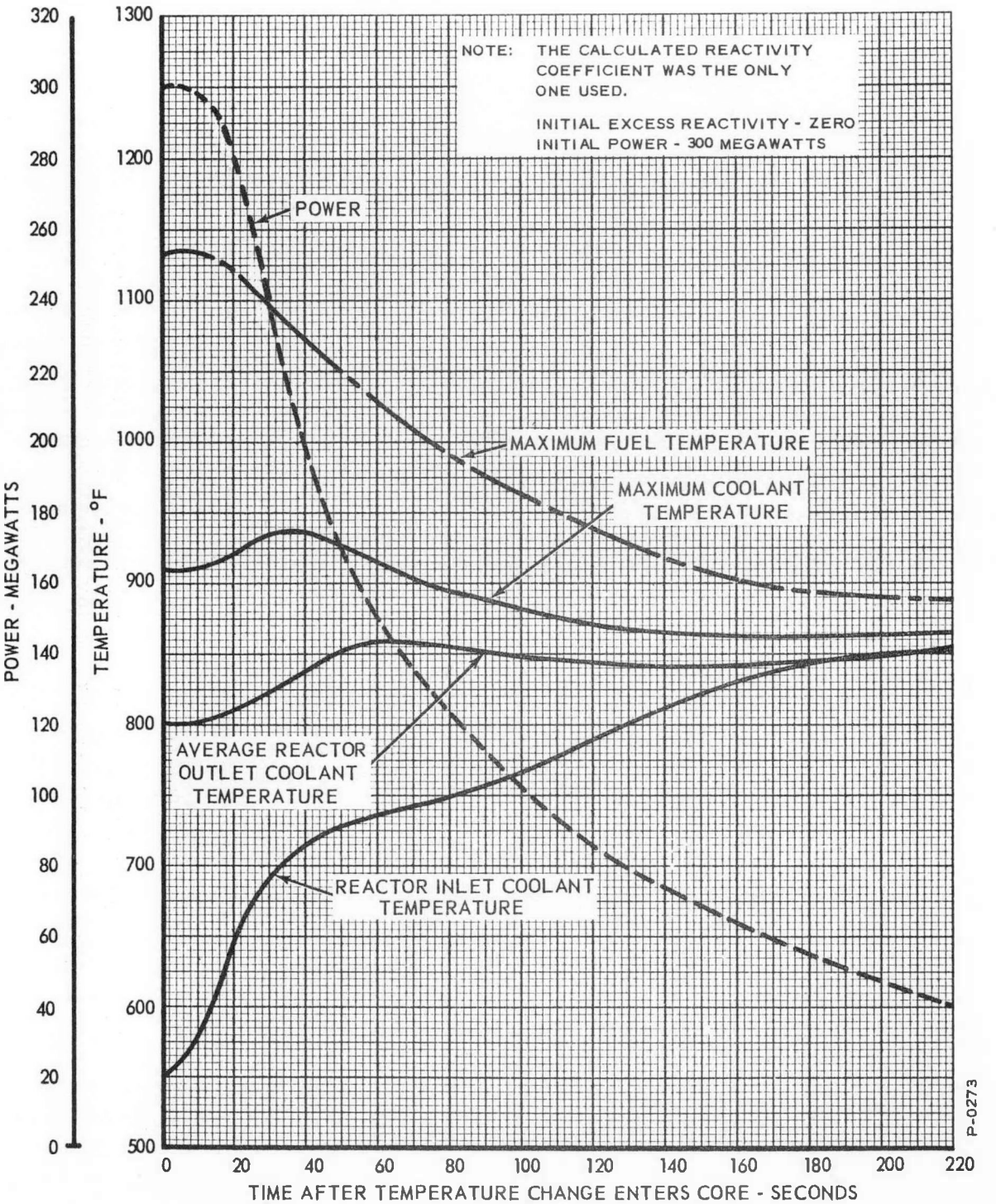

Figure 2.10 - Feedwater Flow Decrease: Power and Reactor Temperature

coolant temperature curves shown in Figure 2.10. The Holley Carburetor Company data take into account the effect of the recirculation of the coolant, so the data in Figure 2.10 are qualitatively significant for times longer than 30 seconds.

2.1.3.4.2 Increase in Feedwater Flow -- Figure 2.11 is a plot of the data from the Holley Carburetor Company showing the effect, on the reactor coolant inlet temperature, of an increase of feedwater flow to 150 percent of its nominal value. These data were used to program the temperature of the reactor inlet coolant, starting with the reactor at full power. The results of the computer run of this case are shown in Figure 2.12. As expected, the reactor smooths out this transient also. The statistical-hot-channel factor corrections discussed in Appendix B can be applied to the curves for the maximum fuel and coolant temperatures. Again, the data are qualitatively correct for times longer than 30 seconds, since the Holley Carburetor Company study included the effect of the recirculation of the primary and secondary coolant.

2.2 TRANSIENTS DURING LOW-POWER OPERATION

When the reactor is being brought to power, a malfunction of the equipment can put the reactor on a fast transient which can be damaging. Two transients of this kind have been studied. In one case, the reactor is assumed to be completely shut down when the positive reactivity insertion begins. In the other case, the, reactor is initially operating at one percent of full power, with a growth factor equal to zero, when the excursion begins. In both cases the shut-down temperature is assumed to be 550°F, instead of 600°F as in the previous study. If the shut-down temperature is lowered still more, faster transients will result but the maximum temperature reached will not increase.

2.2.1 Start-Up Excursion

A computer run was made to determine the temperatures when positive reactivity was inserted, from zero power, at the rate of one cent per second. An analog computer can only simulate the behavior of the reactor over a range of less than three decades of power in one run, so only the range from one-percent-of-full-power to full power was studied. Digital computations made by NDA, and reported in NDA 014-190, indicate that for a start-up transient, the reactor power goes through the one-percent-of-full-power level with a growth

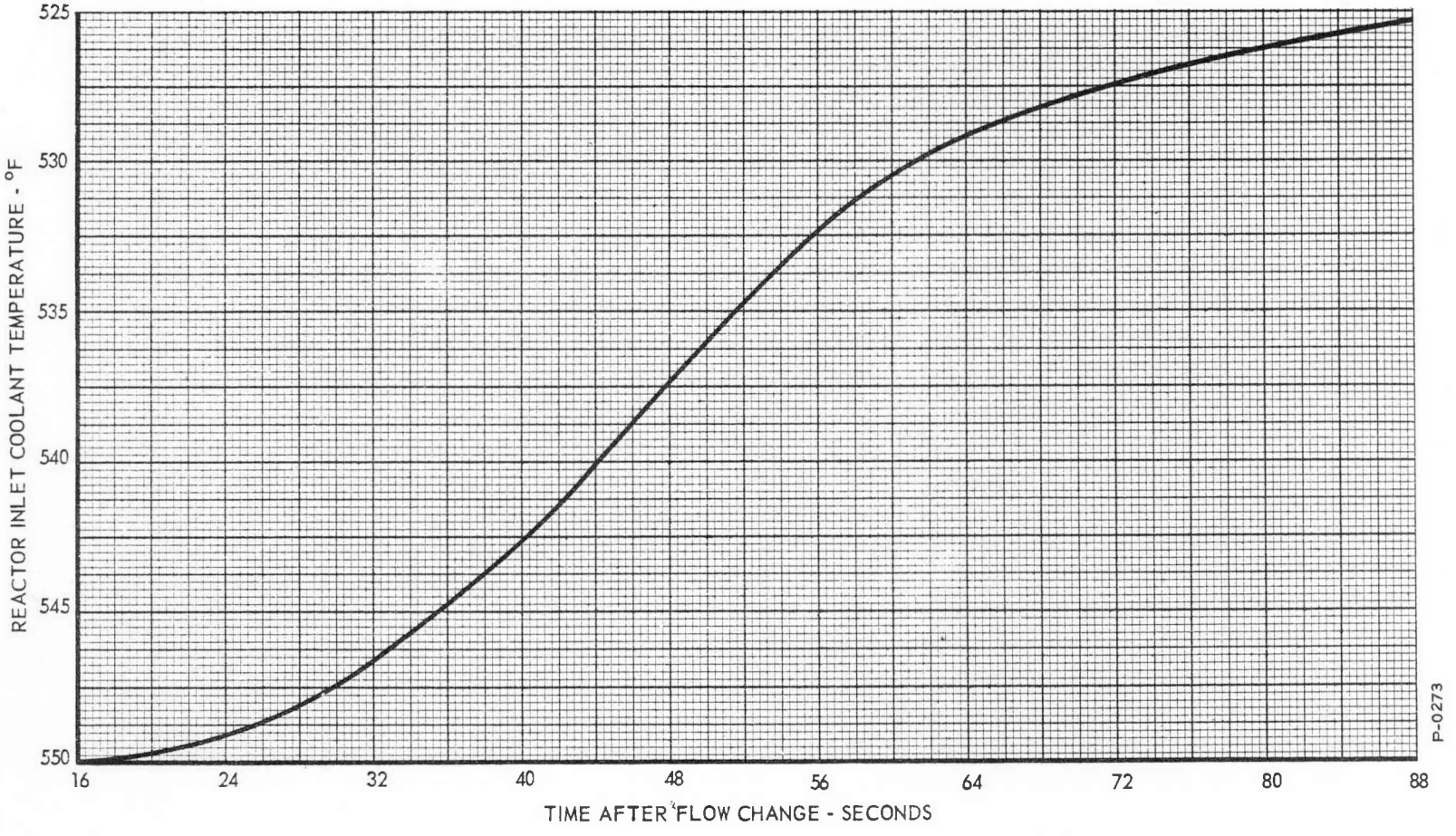

Figure 2.11 - Feedwater Flow Increase: Reactor Inlet Coolant Temperature (From Holley Carburetor Company)

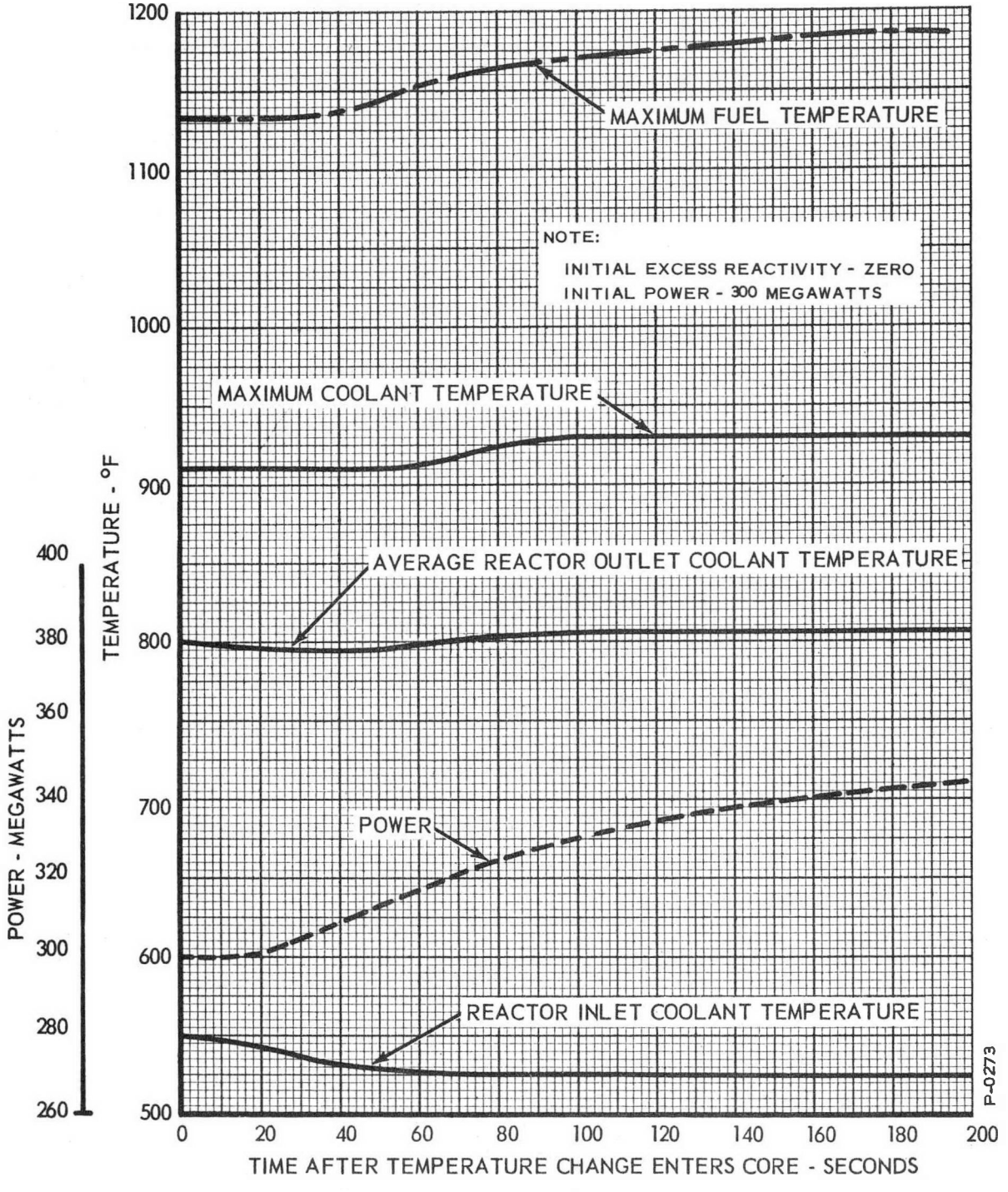

Figure 2.12 - Feedwater Flow Increase: Power and Reactor Temperatures

factor corresponding to 70 cents worth of excess reactivity. Figure 2.13 shows the effect on the fuel temperature in the hottest channel for such an excursion. Note that three values of the temperature coefficient of reactivity have been used. The curve labeled ρo corresponds to the calculated temperature coefficient. The curves labeled $\rho o/2$ and $3\rho o/2$ correspond to one-helf and one-and-one-half times the calculated temperature coefficient of reactivity respectively. Figure 2.14 shows the behavior of the temperature of the coolant in the hottest channel during the excursion. The labels on the curves have their usual significance. Note that the simulation is no longer valid after the sodium boiling temperature is reached in the hottest channel, as shown by the dotted parts of the curves. The statistical-hot-channel correction factors discussed in Appendix B, can be applied to the curves in Figures 2.13 and 2.14. Figure 2.15 shows the behavior of the reactor power, during the above excursion. The dotted parts of the curves show that coolant boiling has occurred in the hottest channel. Figure 2.16 shows the behavior of the average reactor outlet coolant temperature during the excursion. Again, the dotted portions of the curves show where coolant boiling has occurred in the hottest channel.

For convenient comparison, the corresponding results from the previous study are shown in Figure C6, of Appendix C, of this report. It is to be noted that the shut-down temperature used before was 600°F instead of the present value of 550°F. A further reduction in this temperature will result in a faster transient but the maximum temperatures reached will not be changed.

2.2.2 Excursion from One-Percent-of-Full-Power

A computer run was made to determine the temperatures when positive reactivity was inserted, from one-percent-of-full-power at the rate of one cent per second. The reactor was assumed to have a growth factor equal to zero at the start of the excursion. Figure 2.17 shows the effect of such a transient on the fuel temperature in the hottest channel. Note that three values of the temperature coefficient of reactivity have been used. The curve labeled ρo corresponds to the calculated temperature coefficient. The curves labeled $\rho o/2$ and $3\rho o/2$ correspond to one-half, and one-and-one-half times the calculated temperature coefficient respectively.

Figure 2.18 shows the behavior of the coolant temperature in the hottest channel during the same excursion. The labels on the curves have the usual meanings. The curves are meaningless after

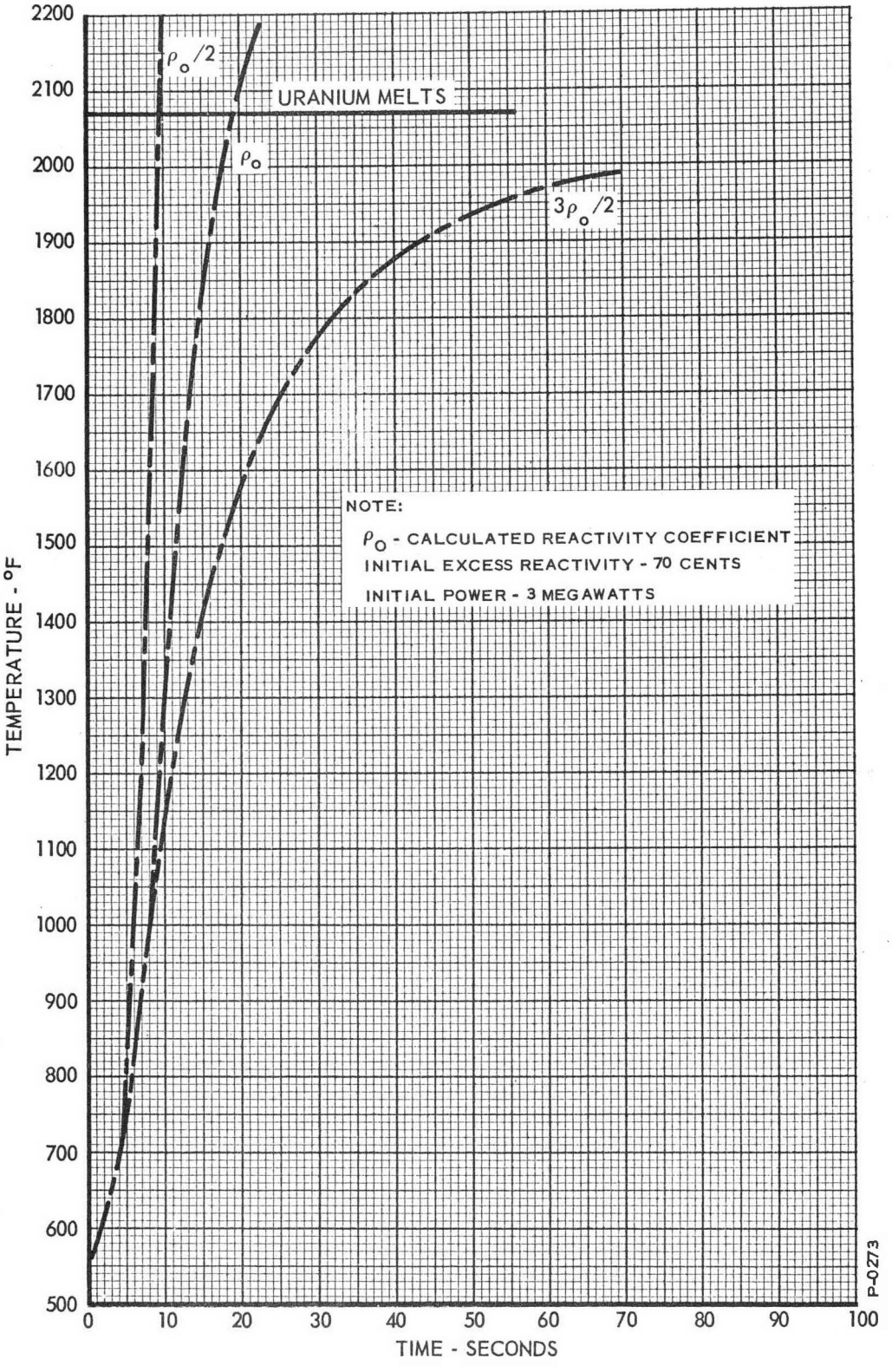

Figure 2.13 - Start-Up Excursion: Maximum Hot-Channel Fuel Temperature

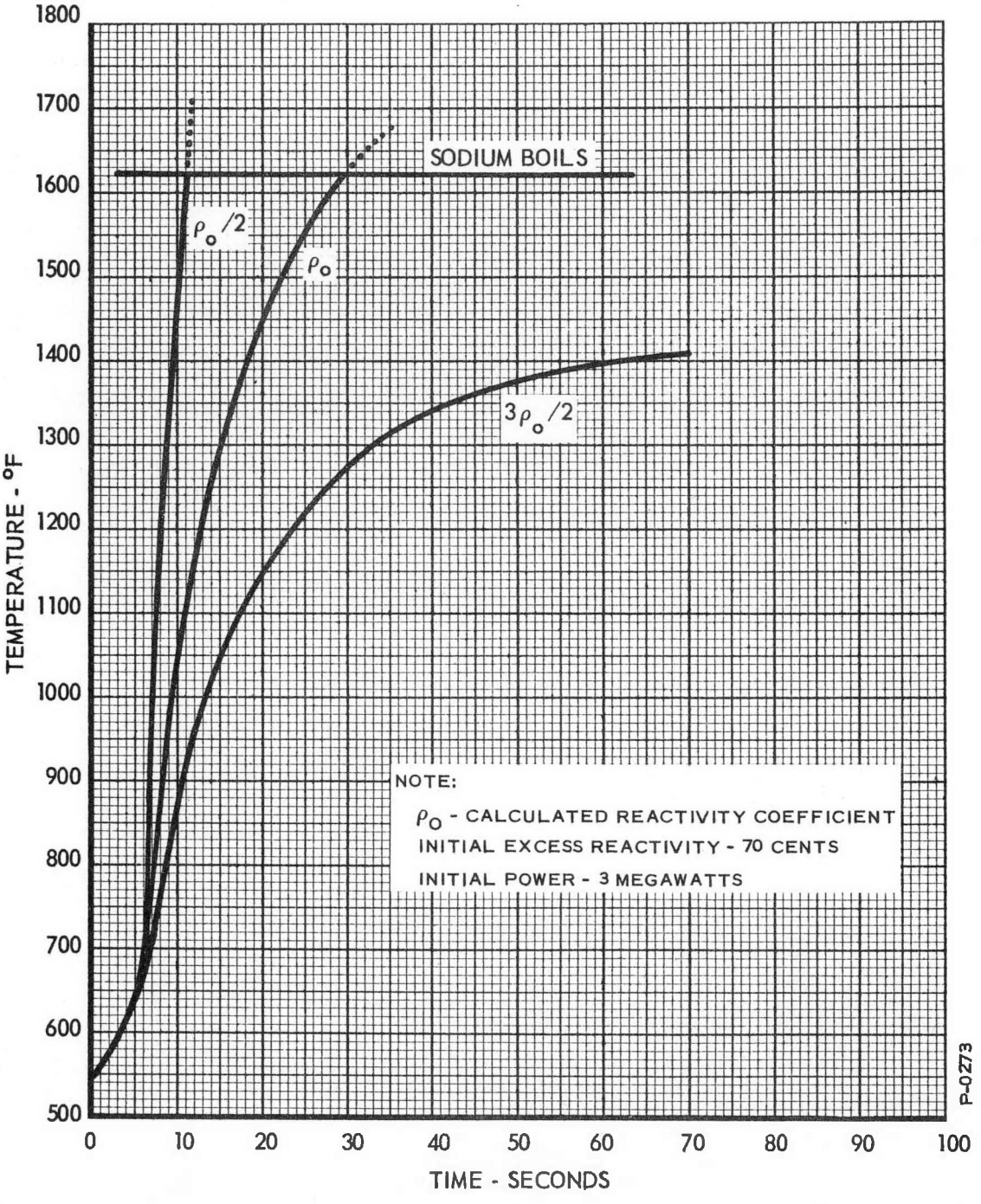

Figure 2.14 - Start-Up Excursion: Maximum Hot-Channel Coolant Temperature

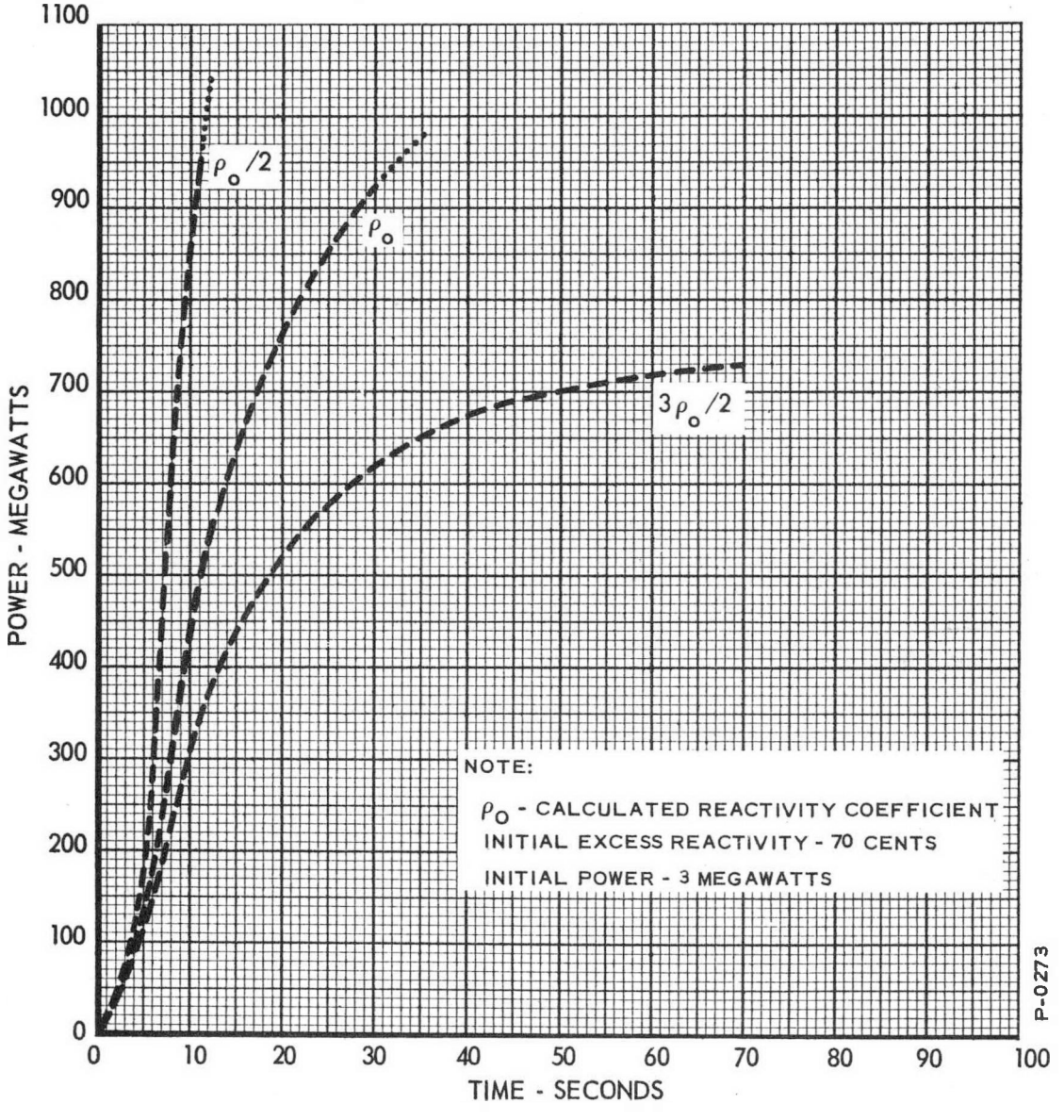

Figure 2.15 - Start-Up Excursion: Power

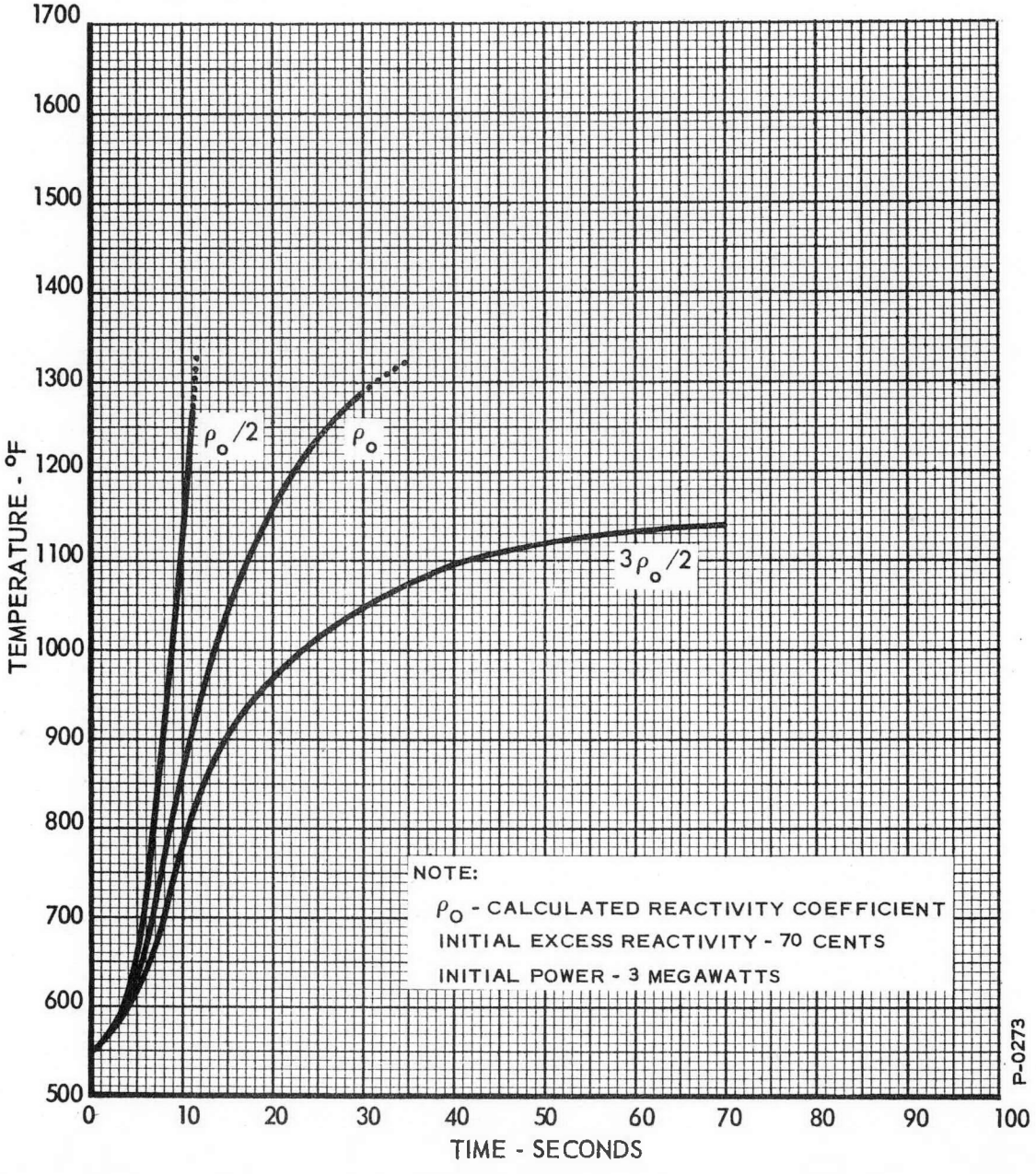

Figure 2.16 - Start-Up Excursion: Reactor Outlet Coolant Temperature

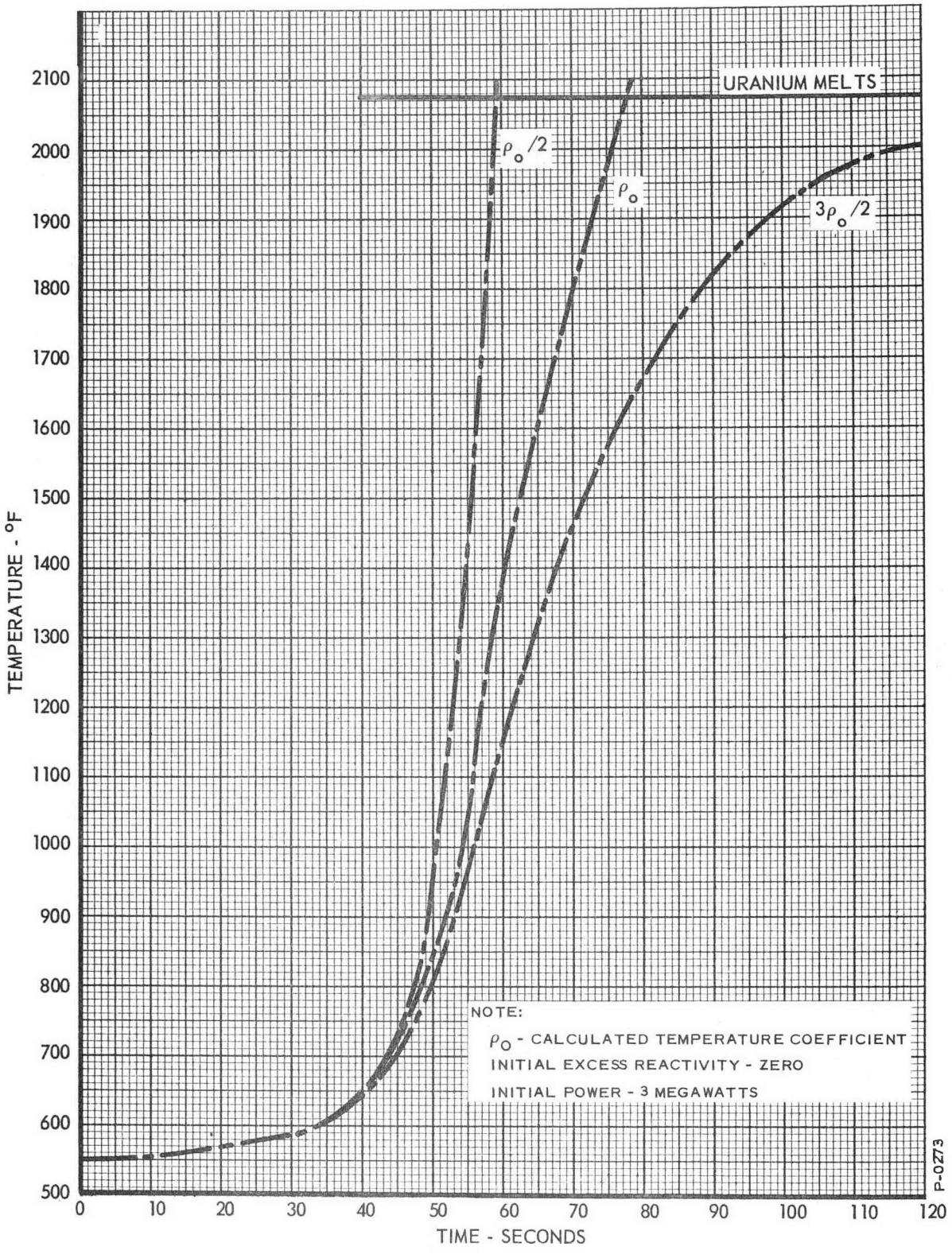

Figure 2.17 - Excursion from Low Power: Maximum Hot-Channel Fuel Temperature

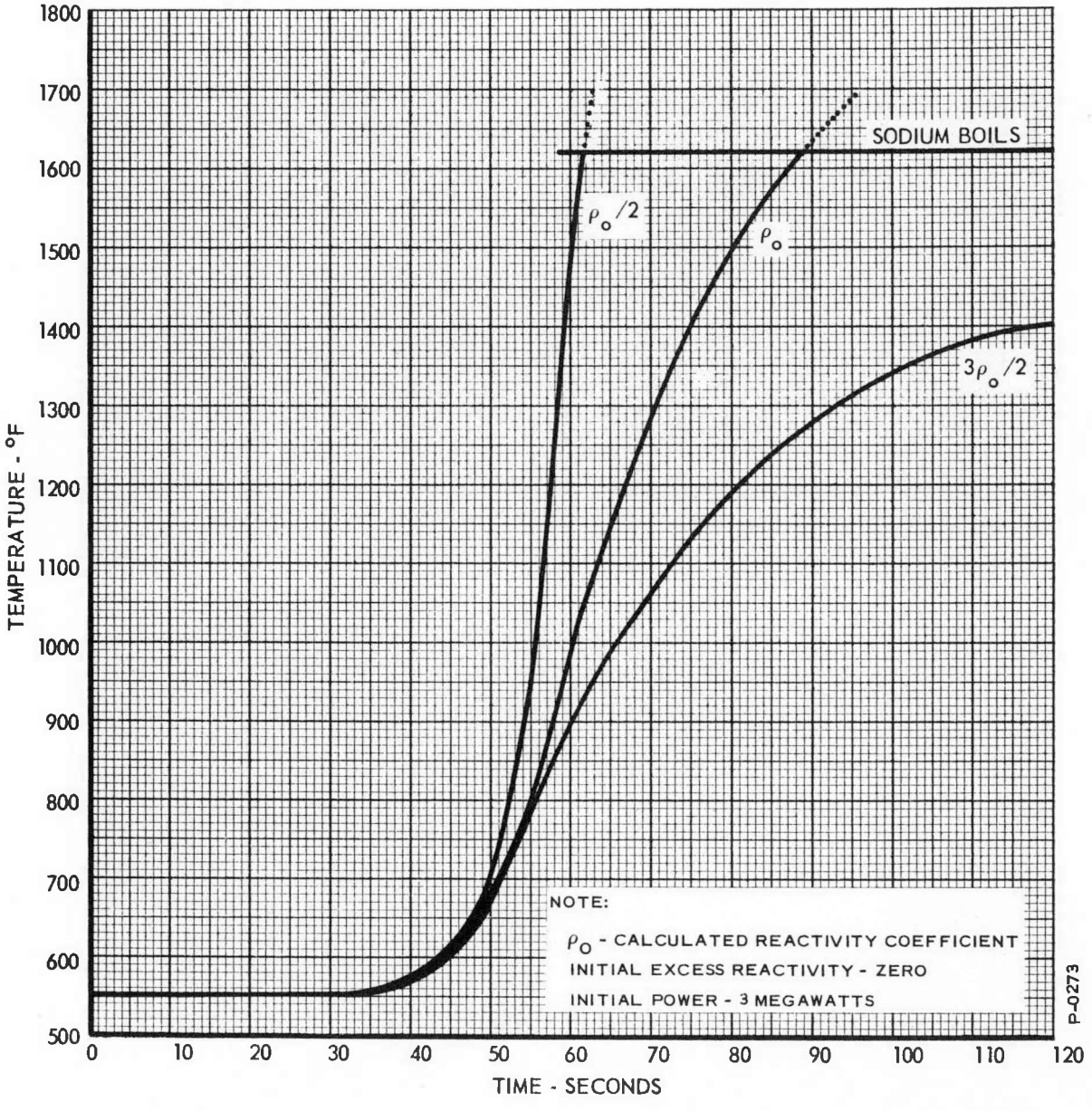

Figure 2.18 - Excursion from Low Power: Maximum Hot-Channel Coolant Temperature

the coolant boils in the hottest channel, as shown by their dotted portions. The average hot channel factor has been used during the computation of the curves shown in Figure 2.17 and 2.18. The statistical hot channel correction factors discussed in Appendix B, can be applied to the fuel and coolant temperatures shown in the last two figures. Figure 2.19 shows the behavior of the power, and Figure 2.20 the behavior of the average reactor outlet temperature during the excursion. The dotted parts of the curves show that coolant boiling has occurred in the hottest channel, and these parts of the curves have no meaning.

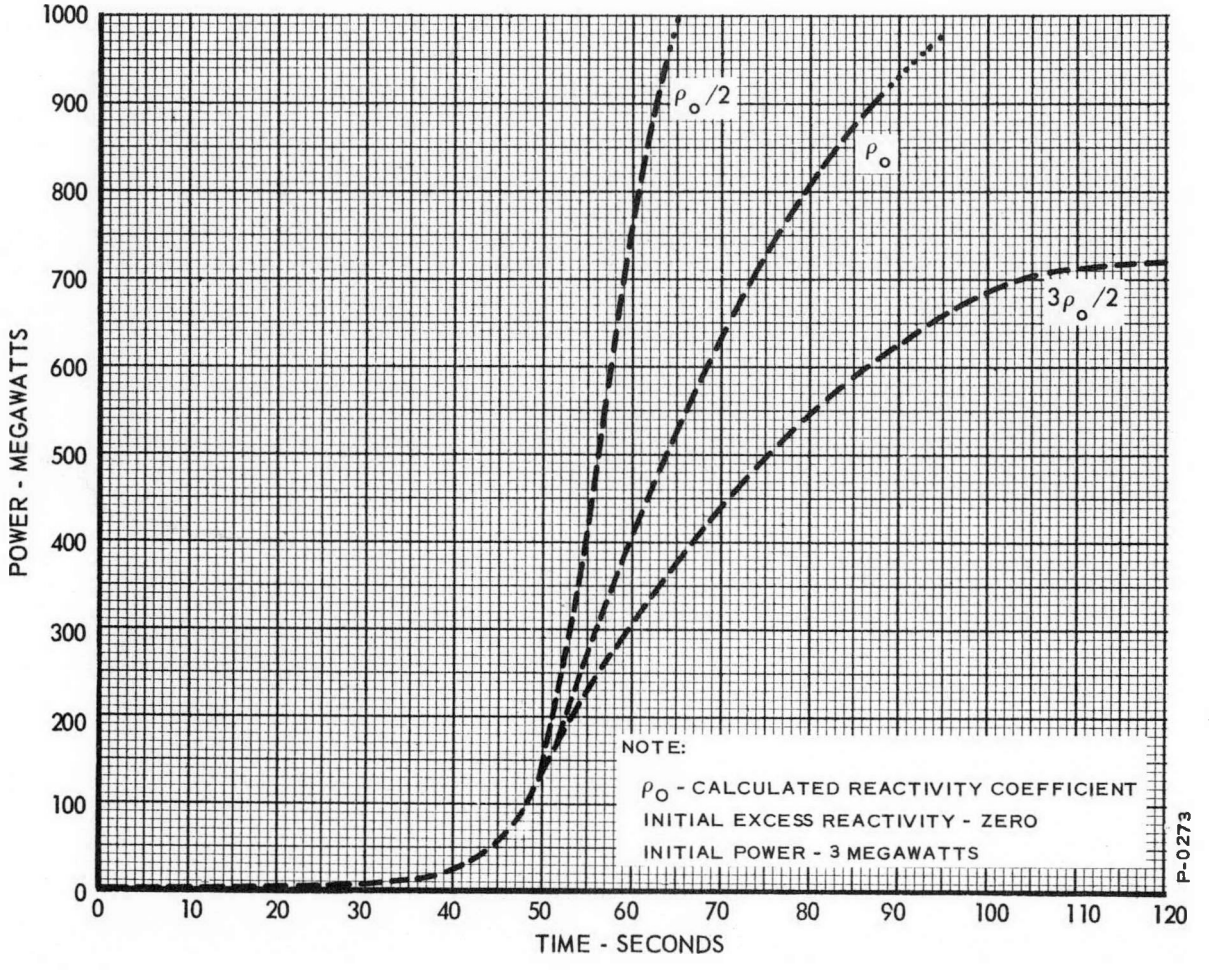

Figure 2.19 - Excursion from Low Power: Power

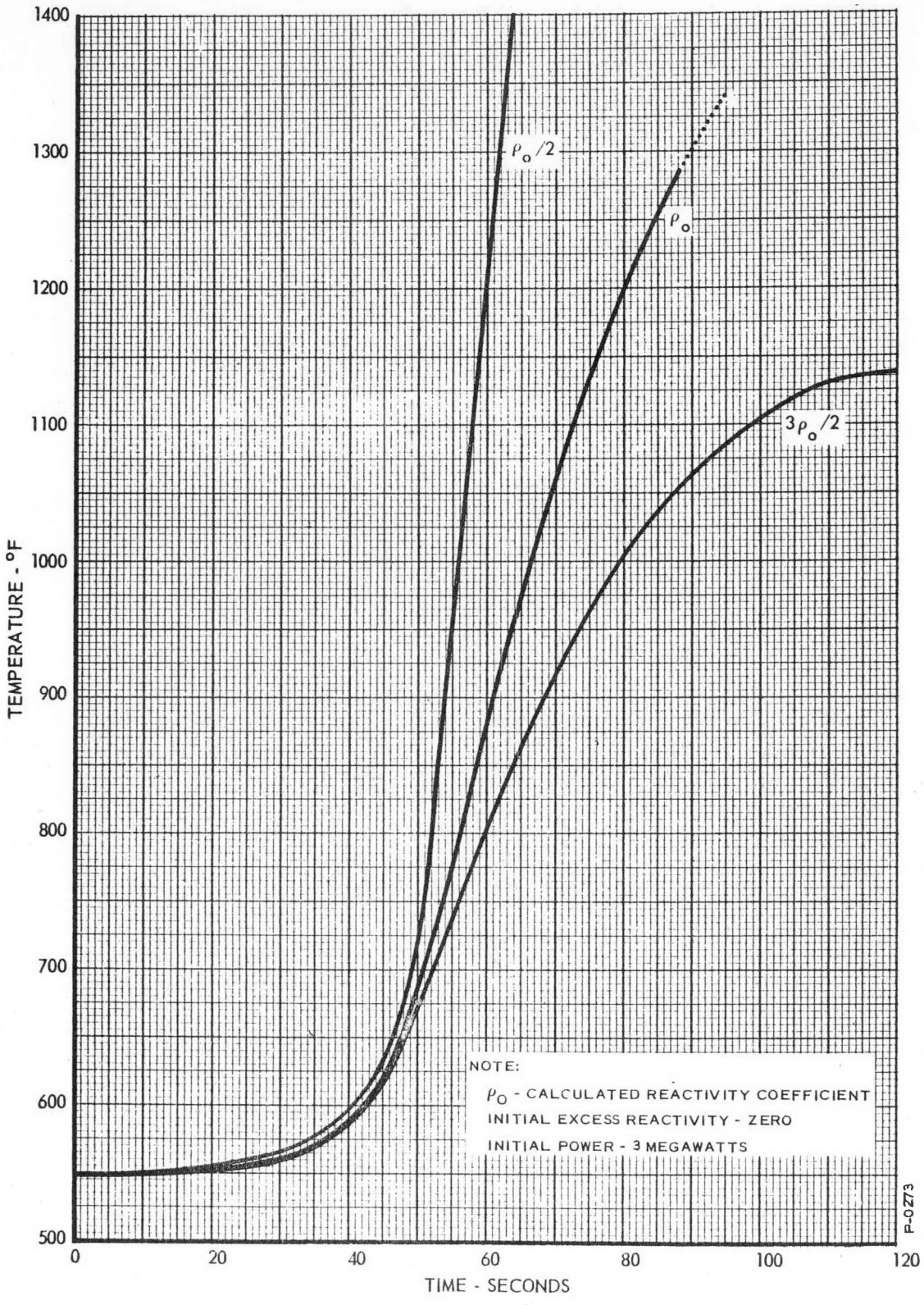

Figure 2.20 - Excursion from Low Power: Reactor Outlet Coolant Temperature

SECTION 3

CONCEPTUAL DESIGN OF THE POWER-LIMITING SYSTEM AND TRIP LEVEL SETTINGS

3.0 GENERAL

In this section we will present discussions of the philosophy governing the design of the power-limiting system, its responses, the signals available to operate the system, and trip level settings.

3.1 POWER-LIMITING SYSTEM PHILOSOPHY

3.1.1 Previous Philosophy

The primary function of a power-limiting system is to prevent fuel melting, and to prevent damage to the reactor structure. As mentioned in Section 1.2.2, the power-limiting system was previously designed in such a manner as to minimize thermal shocks to parts of the reactor structure. To alleviate these shocks the power-limiting system was designed to have three modes of response: Setback sequential scram and scram. The setback made use of an insertion of negative reactivity by the regulating rods to keep the reactor at some safe power level in case of a slow, positive excursion. The sequential scram inserted negative reactivity with the safety rods, in a programmed manner so as to hold the outlet temperature relatively constant in the event of a complete primary flow failure. The scram was considered a last resort, and the thermal shock would not be alleviated.

3.1.2 Elimination of Sequential Scram

APDA has now acquired information which shows that the reactor structure can withstand repeated scrams. Thus, the sequential scram is sacrificed for simplicity and reliability of the power-limiting system. The present philosophy calls for the use of the scram to arrest severe positive transients, to shut the reactor down in the event of a complete primary flow failure, and in case of severe secondary and feedwater flow changes. The design, recommended in this report is based upon this philosophy.

3.1.3 Setback

It is recommended that a setback be one of the modes of controlling the reactor if its power level, or rate of increase of power, exceeds the limits of the regulating system. The protection given by the setback response is desirable at low power levels, since it takes a minimum of 27 minutes to withdraw the safety rods. A great saving in time results if inadvertent scrams can be prevented during start up. Thus, it is recommended that the setback should be provided with a growth-factor trip that is effective at low power levels, if the saving in time is important.

The setback is also the mode of response of the power-limiting system that will take care of relatively small fluctuations in power, that exceed the limits considered as normal, while the reactor is operating at full power. Since normal power fluctuations of about ten percent are expected, the setback power trip should not be set lower than 120 percent of full power. The setback is not a mode of operation that will shutdown the reactor. Rather, it is a response that will gently keep the reactor from exceeding some preset power level. When the power-limiting system is called upon to act, it is recommended that the regulating rods be used on setback. The use of the safety rods for this purpose would make the safety rod drive mechanism complex, and hence less reliable. The setback will introduce negative reactivity, with the regulating rods, at the maximum rate until the initiating signal falls below the trip level. Control of the rods will be returned to the regulating system with a manual reset switch.

In the previous study, the effect of a setback operated by a power trip, set at 120 percent of full power, was investigated. A copy of the results obtained then, is presented in Figure C7, of Appendix C of this report. No computer runs investigating the setback have been made during this study.

3.1.4 Flow Trips

The present philosophy of initial operation requires that any major coolant flow disturbance greater than the loss of one cooling system, will scram the reactor. Any pump failure in a coolant loop will cause all the other pumps in that system to stop. Thus a multiple interlock circuit failure will have occurred, in addition to the stopping of a pump, for the temperature effects resulting from a secondary or

feedwater flow disturbance to reach to core. So, the transients that the reactor undergoes because of such disturbances have a very low probability of occurrence.

3.2 GENERAL DISCUSSION OF SIGNALS

In this section a discussion of the electrical signals that can be obtained, to measure the behavior of the neutron flux in reactors in general, will be presented. The signals which are proportional to rates of change of neutron flux are analyzed in terms of their magnitudes, ranges of applicability, and statistical fluctuations.

3.2.1 Definitions and Advantages

Here we will only be concerned with electrical signals, from neutron detectors, that are related to the neutron flux level and its rate of change. The level of the current coming from a neutron detector is proportional to the neutron flux and hence, the power of the reactor. This is known as the "power signal", and has units, megawatts. The rate of change of this current is proportional to the rate of change of power, and is known as the "rate signal". The rate signal has units, megawatts per second. From the neutron flux measurement another quantity, known as the "growth factor, G" may be inferred. The growth factor is defined by the equation,

$$P = P_o \, e^{Gt},$$

and has units, nepers per second. In this equation: P is the power at any time, t is the time, and P_o is the initial power at time to equal to zero. The term "period" is often used for the reciprocal of the growth factor. The period has the units, seconds per neper.

The use of the growth factor is advantageous because information can be obtained over many decades of reactor power. It has disadvantages because the growth factor signal is small and the statistical fluctuations in the signal are large and do not decrease with power. The rate signal is large and its statistical fluctuations decrease with power, but it can only be used in the power range. It was shown in the previous report that these two signals can be used to advantage, each in its own range of maximum utility.

3.2.2 Comparative Magnitudes of Signals

In the previous report, the circuit shown in Figure 3.1 was analyzed to determine the relative magnitudes, in terms of voltages, of the rate and growth-factor signals that it provides. This circuit is equally applicable to the measurement of rates or growth factors. In the latter application, the resistor, R_1, is replaced with a diode to obtain a logarithmic relation between the current through the diode and the voltage across it. The ionization chamber was assumed to provide 10^{-4} amperes at full power. R_1 was assumed to be 10^6 ohms, C_1 was 10^{-9} farad, and R_1C_1 was 0.1 second. Two values of R_2C_2 were examined, 0.1 and 0.01 second. Table 3.1 is copied from Bendix Report 1052.

Table 3.1 - Magnitude of Signals

Rate, Mw/sec	Growth-Factor, nepers/sec	Rate Signal, volts	Growth-Factor Signal, volts
10	0.033	3.3×10^{-1}	3.0×10^{-4}
7	0.023	2.3×10^{-1}	2.0×10^{-4}
2	0.007	6.0×10^{-2}	6.0×10^{-5}

The rates and growth factors shown in the table only correspond at a power level of 300 megawatts. It is to be noted that a gain of a factor of one thousand in signal level is achieved by using the rate signal.

The reader is referred to Bendix Report 1052, Section 6.4.1, p. 58 et seq. for the details of the calculations leading to the values given in Table 3.1.

3.2.3 Statistical Fluctuations of Signals

The circuit shown in Figure 3.1 was also analyzed to determine the statistical fluctuations in the rate and growth factor signals when the reactor is operating at a constant power level. In Appendix D of the previous report a detailed derivation of equations for the standard deviation of the fluctuations was given. The equations which result are:

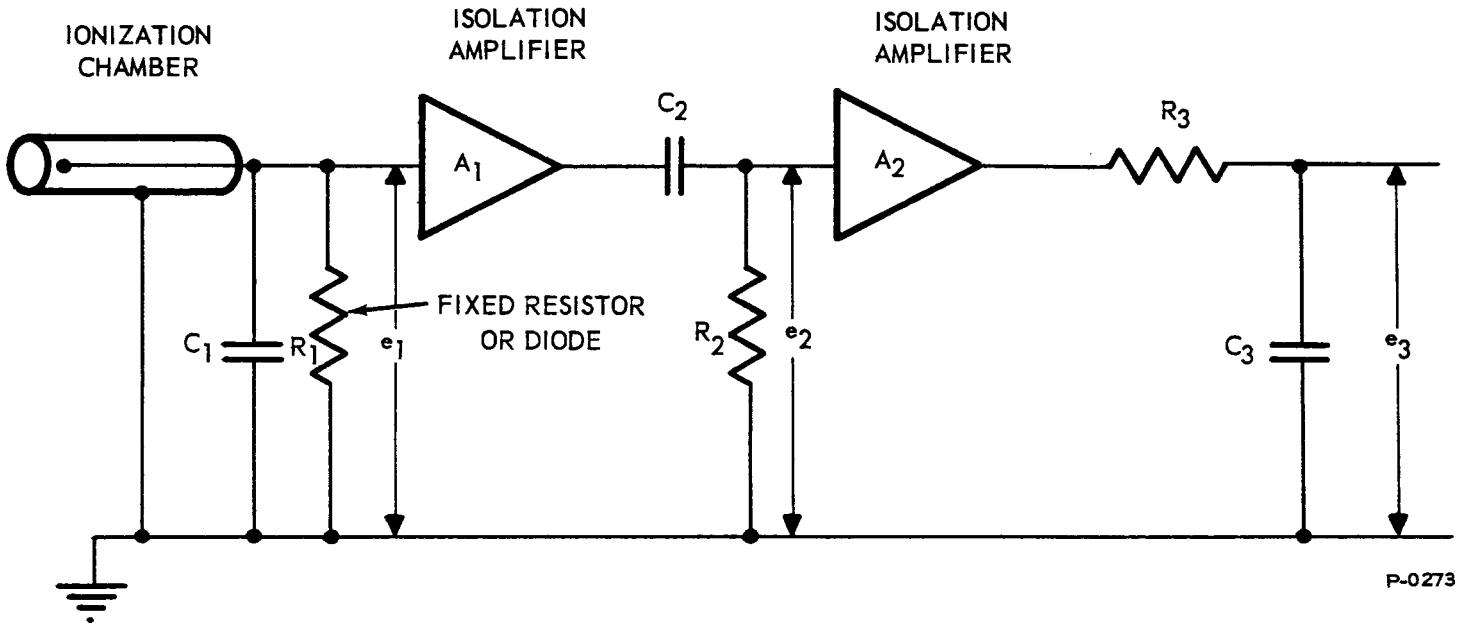

Figure 3.1 - Schematic Diagram of a Typical Circuit for Determining the Rate and Growth-Factor from Ionization Chamber Current

$$\sigma(G) = \sqrt{\frac{1}{2n}} \left[\frac{1}{\left[\frac{K}{nq} C_1 + R_2C_2\right]\left[\frac{K}{nq} C_1 + R_3C_3\right]\left[R_2C_2 + C_3\right]} \right]^{1/2},$$

and

$$\sigma(\text{Rate}) = \sqrt{q\frac{n}{2}} \left[\frac{1}{(R_1C_1 + R_2C_2)(R_1C_1 + R_3C_3)(R_2C_2 + R_3C_3)} \right]^{1/2},$$

In these equations: $\sigma(G)$ is the standard deviation of the growth-factor signal in nepers per second, $\sigma(\text{Rate})$ is the standard deviation of the rate signal in amperes per second, nq is the ionization chamber current in amperes, n is the pulse rate in pulses per second, and K is the diode constant in volts per neper. The other quantities are identified in Figure 3.1. $\sigma(\text{Rate})$ (amperes per second) can be converted into $\sigma(\text{Rate})$ (megawatts per second) by multiplying it by $3 \times 10^6 \frac{\text{mw}}{\text{sec}} / \frac{\text{amp}}{\text{sec}}$ at full power only.

Six times the standard deviations given by the above equations are plotted in Figure 3.2; as a function of power level. Six times the standard deviation is the signal level that will not be exceeded more than once in 188 months of continuous operation. (For an analysis of this point, see Section D.2, of Appendix D, of Bendix Report 1052). The figure presented here, as Figure 3.2, has been copied from the previous report. The values for the rate signal have been plotted in percent of full power change per second, and illustrate the effect of changing R_2C_2.

One conclusion that can be drawn from this analysis, is that it is the magnitude of the fluctuations at low power that determines the minimum setting of the growth-factor trips. We see from Figure 3.2 that a growth-factor trip must not be set lower than about 0.03 nepers per second if accidental trips are to be avoided, during low-power operation, when the time constants shown in the figure are used. Note that these signals are present when the actual reactor growth factor is zero, corresponding to reactor operation at a constant power level. Thus any growth-factor signal that the reactor introduces when it changes power, will add to these signals.

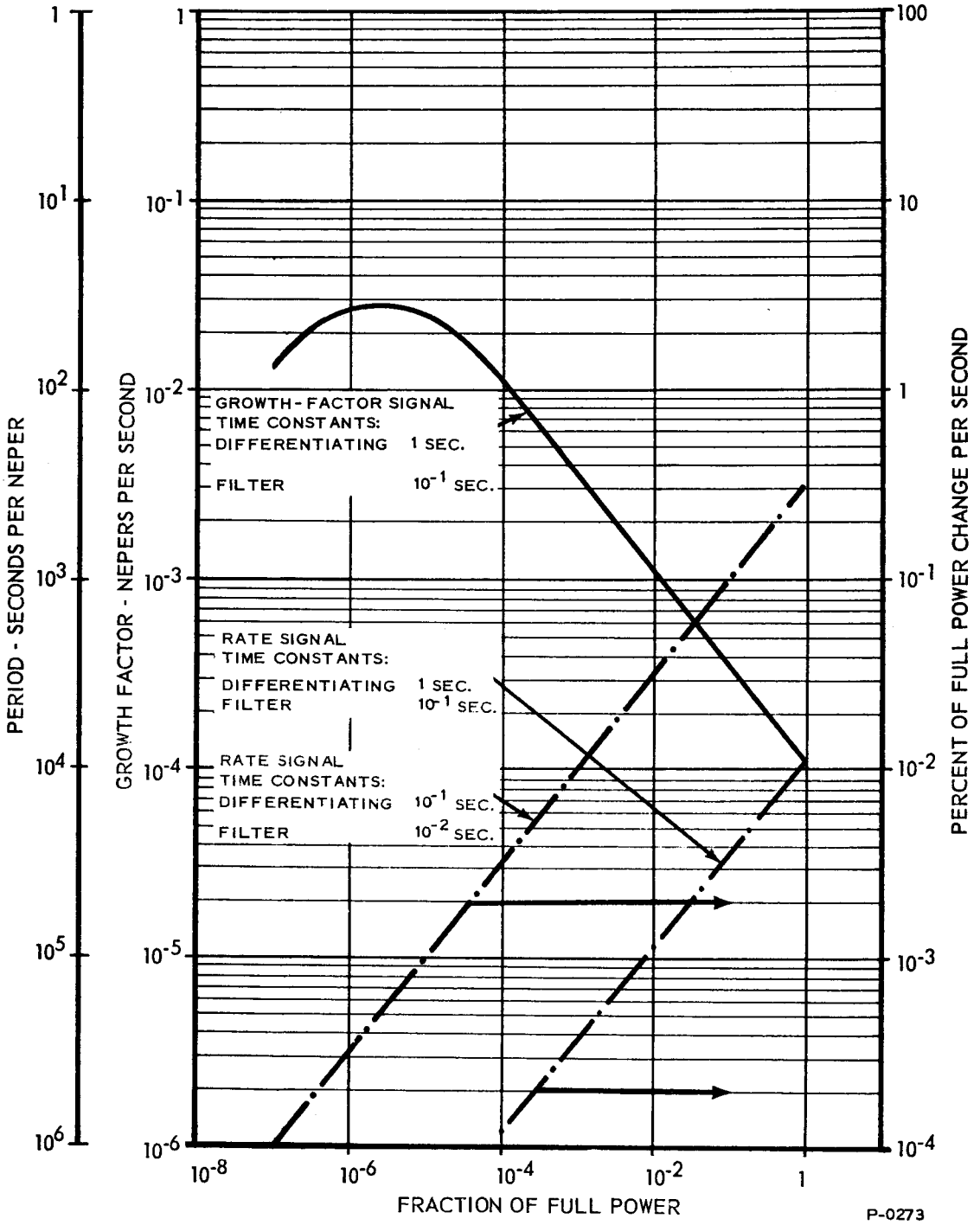

Figure 3.2 - Statistical Fluctuations: Reactor Power Constant

Another conclusion that can be drawn from Figure 3.2 is that the full-power fluctuations determine the minimum setting of the rate trip, since the fluctuations decrease with decreasing power. If the time constants shown in the figure are used, the rate trips must not be set lower than 0.01 percent of full power change per second, or 0.03 megawatt/sec when R_2C_2 is 0.1 second, or 0.3 percent of full power change per second when R_2C_2 is 0.01 second. Now, having the limits of the minimum trip settings in mind, we proceed to examine the signals that are available during transients so as to see where the trips can be set to protect the reactor.

3.3 SIGNALS GENERATED BY TRANSIENTS AND TRIP LEVEL SETTINGS

In Section 2, the results of computer runs for various transients were presented. In that section, the figures only showed the curves for temperature, power, and in some cases flow. When the runs were made, the rate and growth-factor signals corresponding to each transient were recorded. The graphs of these signals will now be presented, and used to set the trip levels which will protect the reactor.

3.3.1 Full-Power Operation

3.3.1.1 Reactivity Insertion at Full Power

In Figure 3.3, the rate and power signals generated by the excursion caused by inserting positive reactivity at one cent per second, starting from full power, are presented. Here the power curves are the same as those shown in Figure 2.2. In Figure 3.4, the growth-factor signals for this excursion are shown. In the same figure, curves of the effective reactivity are also shown. Three values of the temperature coefficient of reactivity were used. ρo represents the calculated value of the coefficient, while $\rho o/2$ and $3\rho o/2$ represent one-half and one-and-one-half times the calculated value respectively.

For convenient comparison, the corresponding results from the previous study are shown in Figure C8 of Appendix C of this report.

It is seen that if the temperature coefficient is $3\rho o/2$, the smallest rate and growth-factor signals will result. Thus, we must base our analysis of trip settings using these signals on this case. We see from Figure 3.3 that a maximum rate signal of about 9.2 megawatts per second will result when the temperature coefficient is $3\rho o/2$. We have seen, in Section 3.2.3 that the minimum rate trip setting that can be used, when the largest time constant in the circuit is 0.1 second, is 0.03 megawatt per second so this signal is excellent for controlling the reactor. If we set the rate scram trip at six megawatts per second (the value chosen in the previous report) we see from Figure 3.3 that the transient will be stopped long before the fuel can melt, even if the temperature coefficient of reactivity is $\rho o/2$, one-half its calculated value.

We see from Figure 3.4 that a maximum growth-factor signal of about 0.021 nepers per second will be obtained. We have seen, in Section 3.2.3 that a growth-factor trip cannot be set at a value less than 0.03 nepers per second, if accidental trips are to be avoided during low power operation. Then, if the temperature coefficient is $3\rho o/2$, it will be impractical to try to arrest a transient of this kind with a scram tripped by a growth-factor signal, if the trip is not to be adjusted as power is changed. If the temperature coefficient of reactivity is ρo, the use of the growth-factor scram trip will be marginal. Clearly if the temperature coefficient of reactivity is $\rho o/2$, a growth-factor scram trip will be quite effective, if it is at the minimum setting of 0.03 nepers per second. However, the temperature coefficient of reactivity is expected to be near $3\rho o/2$, so the rate-scram trip is relied upon to stop severe excursions starting from full power.

In Section 3.1.3, it was recommended that the setback mode be retained. In the previous study, it was recommended that the setback rate trip be set at two megawatts per second. It appears that this setting should not be changed.

In the previous report, it was recommended that the power-scram trip be set at 150 percent of full power, or 450 megawatts. The trip was set at this high value because the sequential-scram power trip was set at 130 percent of full power, between the setback and scram power trips. Considerations of the accuracy requirements for the power level instruments made it impractical to space the trip levels any closer together. Since the sequential scram has now been eliminated, the scram power trip can set at a lower value to give better protection in the event of a start-up transient. The

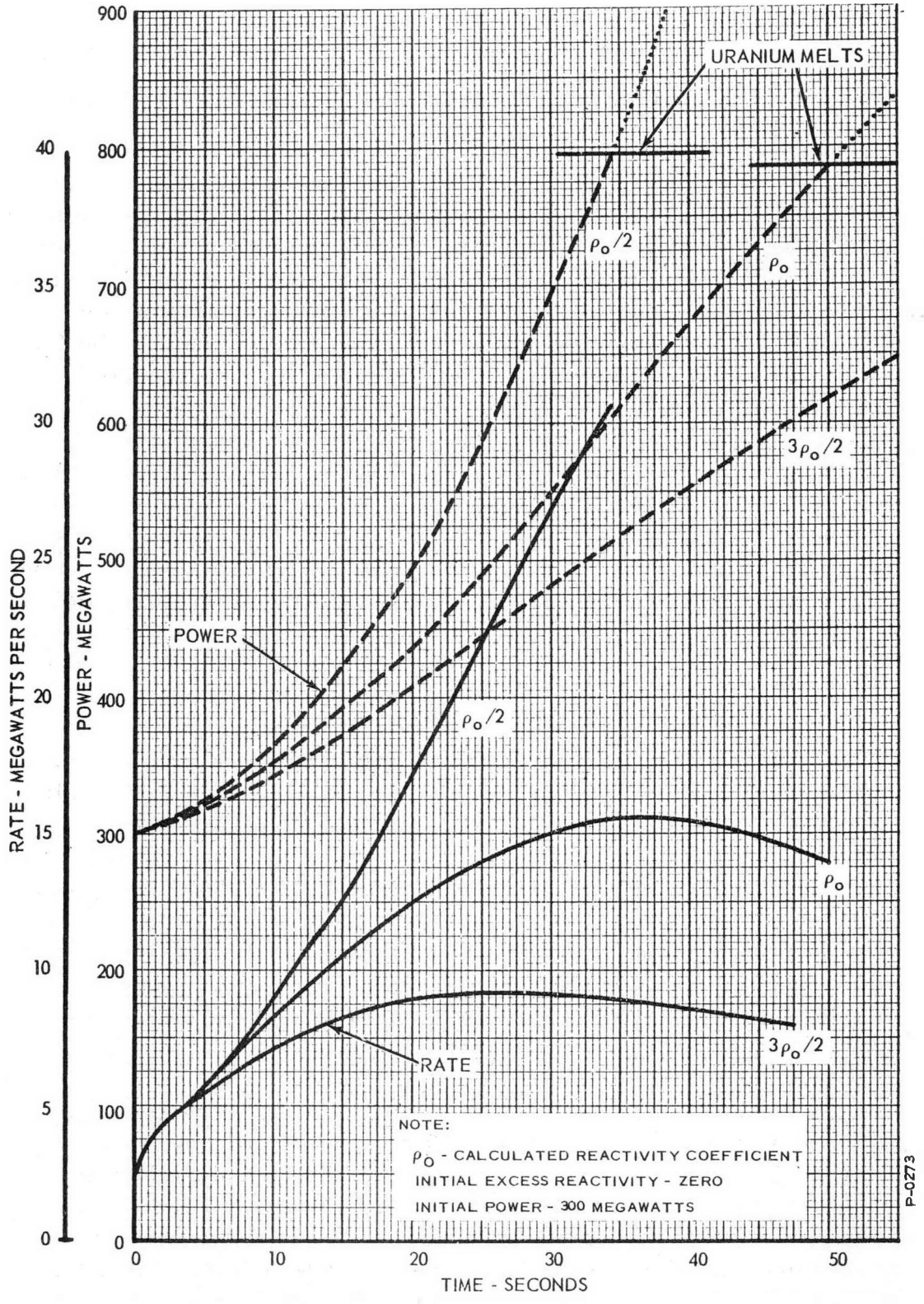

Figure 3.3 - Excursion from Full Power: Rate Signal and Power

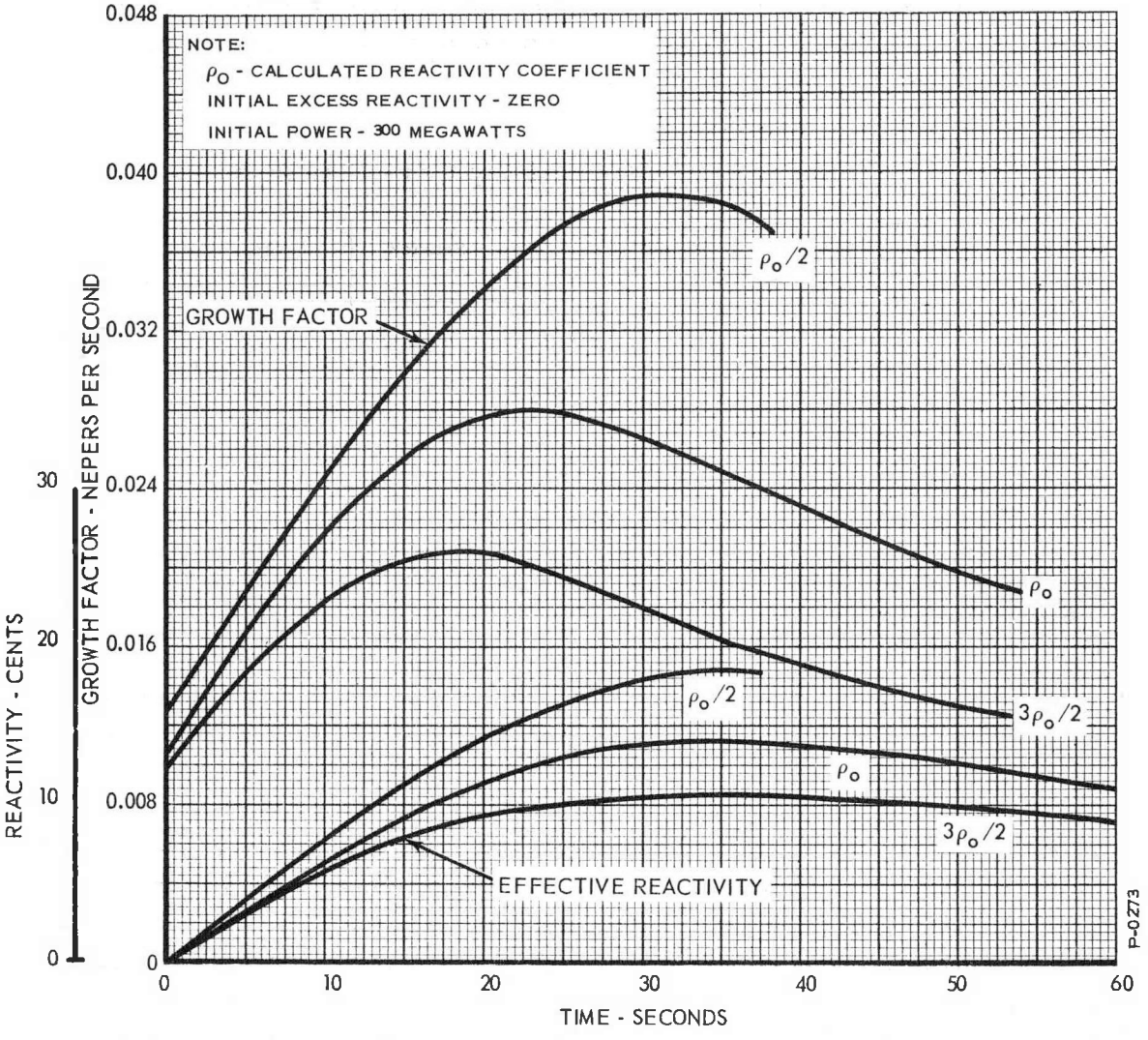

Figure 3.4 - Excursion from Full Power: Growth-Factor Signal and Effective Reactivity

setback power trip must be left at 120 percent of full power because of normal fluctuations in reactor power level. So it is recommended that the scram power trip be set at 130 percent of full power. Setting it higher weakens the protection given, and setting it lower increases the accuracy requirements imposed on the power-measuring equipment. These settings are to be considered tentative until the transients caused by flow changes, and those caused by reactivity insertions at low power are examined. For convenience, these tentative settings are presented in Table 3.2.

Table 3.2 - Tentative Trip Level Settings

Response / Signal	Alarm	Setback	Scram
Power	110%	120%	130%
Rate	1 Mw/sec	2 Mw/sec	6 Mw/sec

The alarm trip settings are the same as those recommended in the previous report.

3.3.1.2 Flow Changes at Full Power

In this section we will analyze the signals generated by the reactor when it is influenced by sodium flow changes in the primary and secondary coolant loops, and by feedwater flow changes.

3.3.1.2.1 Complete Primary Flow Failure -- In Figure 3.5, the power and rate signals caused by a complete primary coolant flow failure are shown. The power curves are the same as those shown in Figure 2.4. In Figure 3.6 the growth-factor signals for the same transient are shown. In the same figure, curves of the effective reactivity are shown also. Three values of the temperature coefficient of reactivity were used. ρo represents the calculated value of the coefficient and $\rho o/2$ and $3\rho o/2$ represent one-half and one-and-one-half times the calculated value respectively.

For convenient comparison, the corresponding results from the previous study are shown in Figure C9, of Appendix C, of this report.

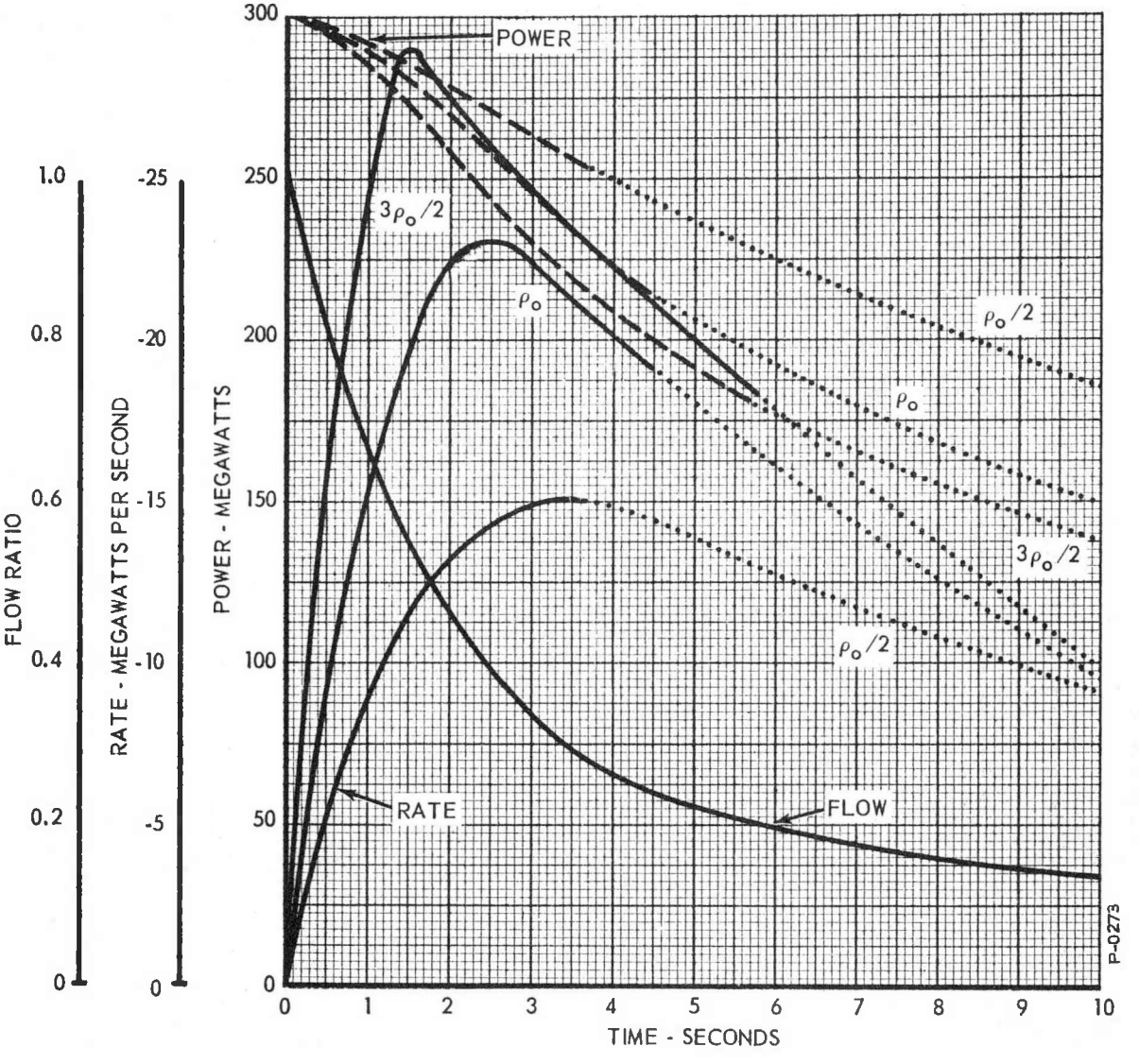

Figure 3.5 - Complete Primary Flow Failure Rate Signal and Power

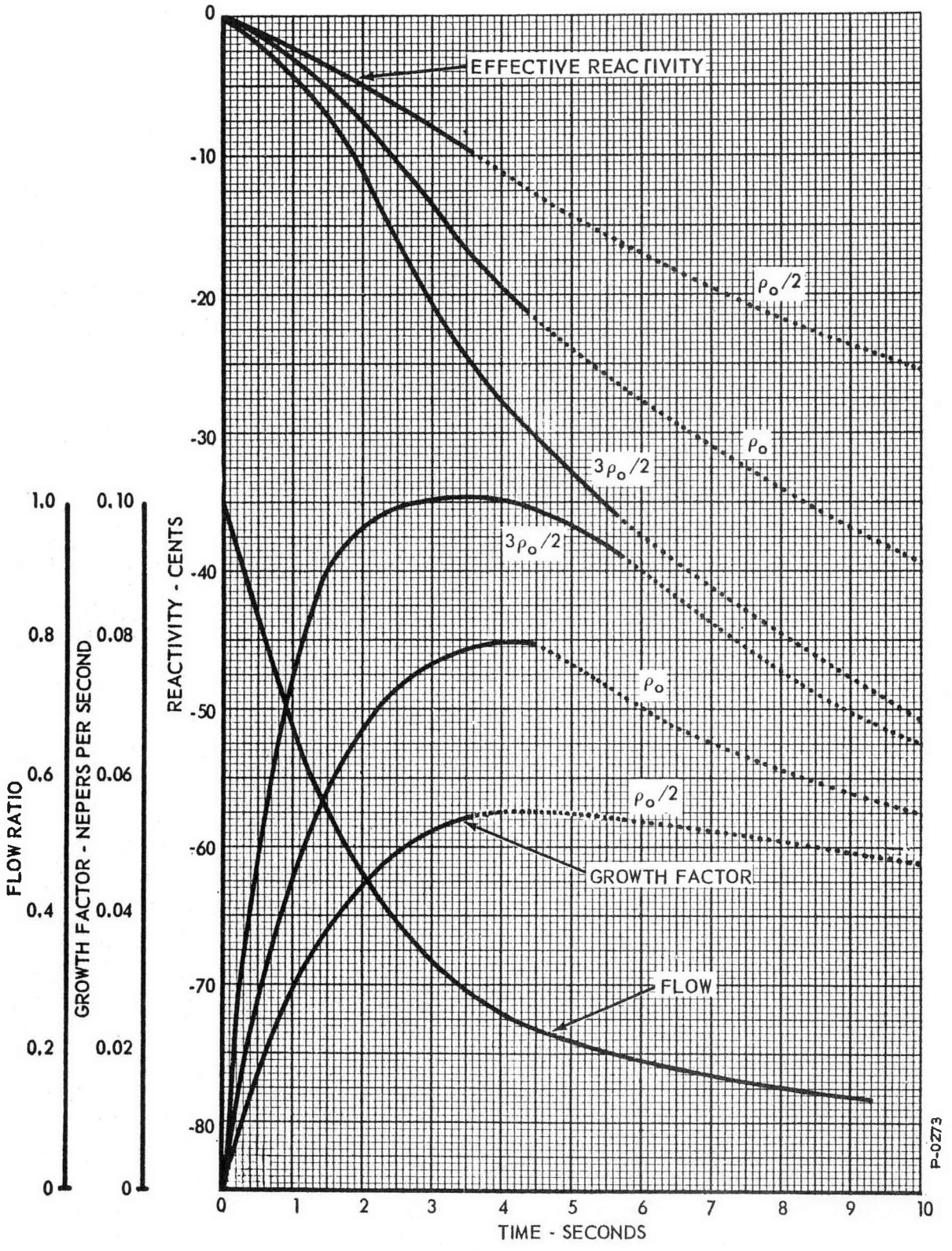

Figure 3.6 - Complete Primary Flow Failure: Growth-Factor Signal and Effective Reactivity

It is seen from Figures 3.5 and 3.6 that the power decreases, and so the rate and growth-factor signals are negative. Thus, the trips set in the last sections will not be operated by this transient. However some means of protecting the reactor must be provided, because, as we see from Figure 2.3, the coolant will boil in the hottest channel between 3.6 and 5.7 seconds after the pumps stop. This range is dependent upon the value of the temperature coefficient of reactivity, and upon the choice of hot-channel factors. Since the failure of all primary pumps is seen to require very fast action by the power-limiting system, it is important to investigate the effect of using the statistical-hot-channel factors. Figure 3.7 shows the behavior of the temperature of the coolant in the hottest channel when the statistical-hot-channel factors are used. Figure 3.7 was obtained from Figure 2.3 by means of the equation,

$$T_{cm}(3\sigma) = T_{cci} + 1.192\,(T_{cm} - T_{cci}),$$

which is derived in Appendix B, Section 4. The results are only qualitative, because the factor depending on coolant flow may change with flow in this range. We see from the Figure that the coolant will now boil in the hottest channel between 2.7 and 3.5 seconds after the pumps stop. This means that the power-limiting system must sense, and respond very quickly to, a complete primary flow failure.

The only reasonable way in which all three primary pumps can fail at once, is for the electrical power for the pumps to fail. In principle, this failure in power could be used to trigger a scram. In the reference design the feedwater pumps are connected to the same bus as the sodium pumps. The inertia of the feedwater pumps will cause the voltage on the common bus to decay with a time constant of about two seconds, if the power fails. Thus, if a device which senses the voltage on the bus, or the current drawn by the primary pumps, is used to trigger the scram the response is much too slow to protect the reactor. It is therefore recommended that the negative rate trip, suggested in the previous report be used to protect the reactor in the event of a complete primary flow failure. Referring to Figure 3.5 we see that if a scram trip is set at minus ten megawatts per second, the reactor will be adequately protected, even if the temperature coefficient of reactivity is $\rho o/2$.

When a complete primary flow failure takes place, it is assumed that the regulating system is operative. The

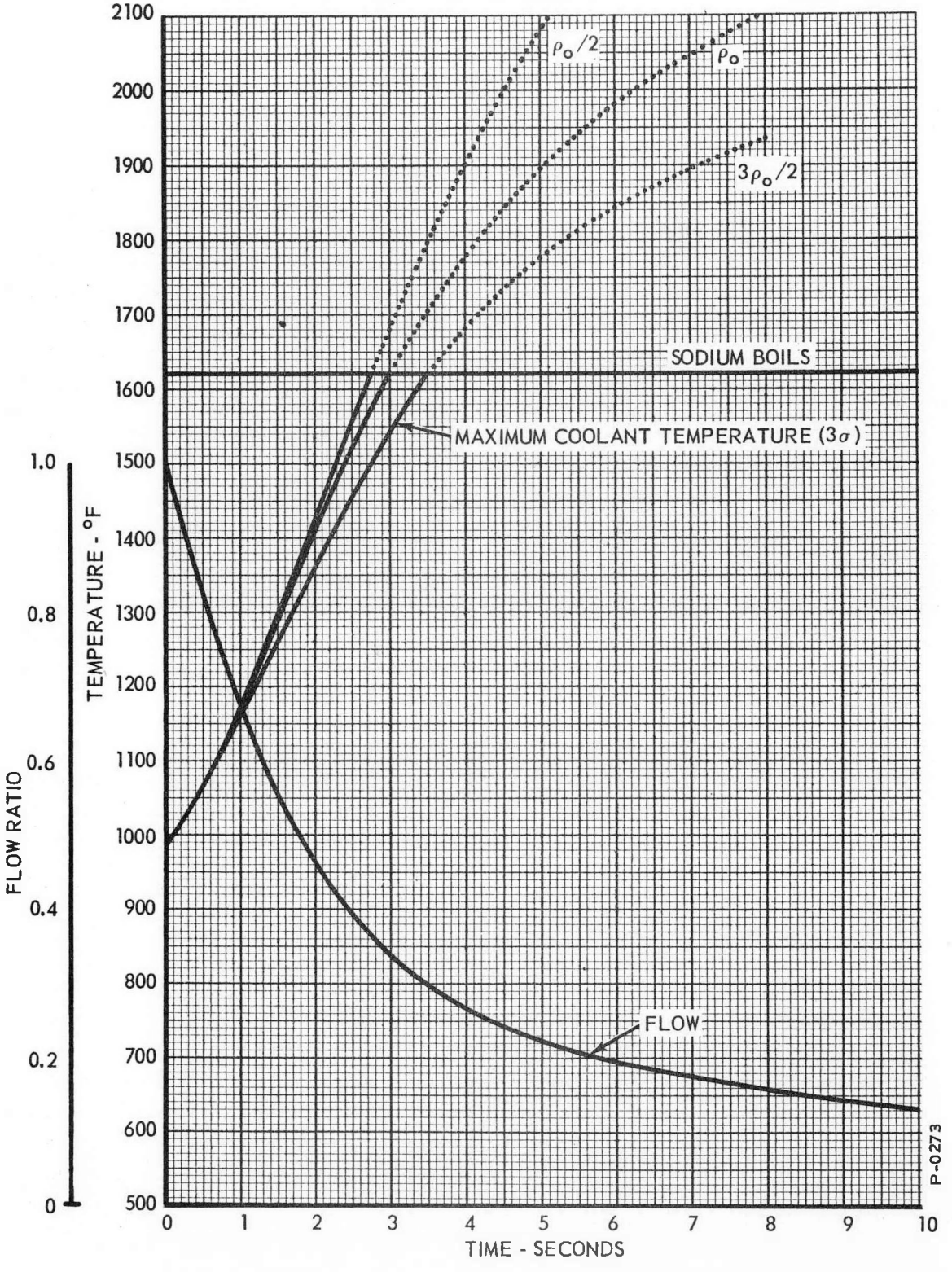

Figure 3.7 - Complete Primary Flow Failure: Maximum Hot-Channel Coolant Temperature, Statistical Hot-Channel Ractor

regulating system will sense the power decrease, and will call for a positive reactivity insertion. If we assume that the regulating system inserts positive reactivity at the maximum rate of one cent per second, the reactivity will not decrease at the rate shown by Figure 3.6. If we consider that the flow decay has been in progress for two seconds, and that the reactivity coefficient is $3\rho o/2$, Figure 3.6 shows that the temperature increase will have reduced the reactivity by eleven cents. However, by this time, the regulating system will have introduced two cents worth of positive reactivity; leaving a net reduction of nine cents. Thus the net reactivity curve will be between the curves labeled ρo and $3\rho o/2$ shown in Figure 3.6, and the rate and growth-factor signals will be between the values given for ρo and $3\rho o/2$. We see from Figure 3.5 that the minus ten-megawatt-per-second rate will be present some time between 0.3 and 0.65 seconds after the flow begins to decay. Clearly, if the rate trip actuated the scram, someplace in this range, the reactor will still be adequately protected. It follows that the regulating system will not significantly interfere with the generation of a negative rate signal large enough to scram the reactor in the event of a complete primary coolant flow failure.

3.3.1.2.2 Loss of One Primary Pump -- In Section 2.1.3.1 the simulation of the effect of the failure of one primary coolant pump has been discussed. Figure 2.5 shows the results of the simulation for temperatures, flow, and power. Figure 3.8 shows the signals that result when the pump fails. Only the calculated value of the temperature coefficient of reactivity was used. It is seen that the power decreases, and that the rate and growth-factor signals are negative, and so will not actuate the trips set to protect the reactor from positive excursions. Although the rate signal is negative, it is not large enough to trip the scram which protects the reactor in the event of a complete primary flow failure. No corresponding curves were obtained in the previous study. In that study the value of the rate signal was inferred from the power curve shown in Figure C3, of Appendix C in this report.

3.3.1.2.3 Loss of All Secondary Pumps -- In Section 2.1.3.2 the effect of a complete secondary flow failure, on power, and temperatures has been examined. The data obtained from the computer run are shown in Figure 2.7. The power, rate, and growth-factor signals accompanying this transient are shown in Figure 3.9. only the calculated value of the temperature coefficient of reactivity was used. It is noted that the rate and growth-factor signals are

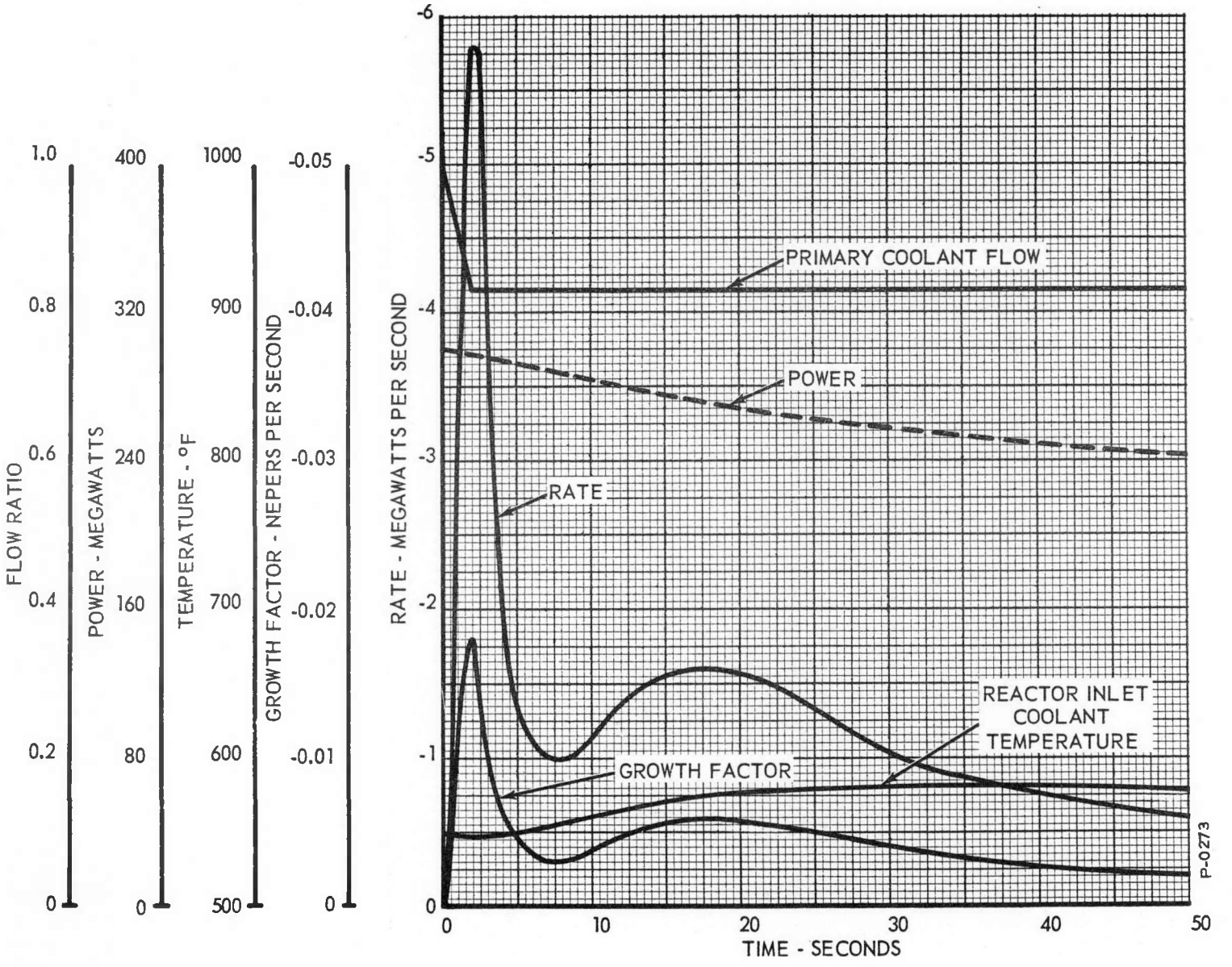

Figure 3.8 - Failure of One Primary Pump: Power, and Rate and Growth-Factor Signals

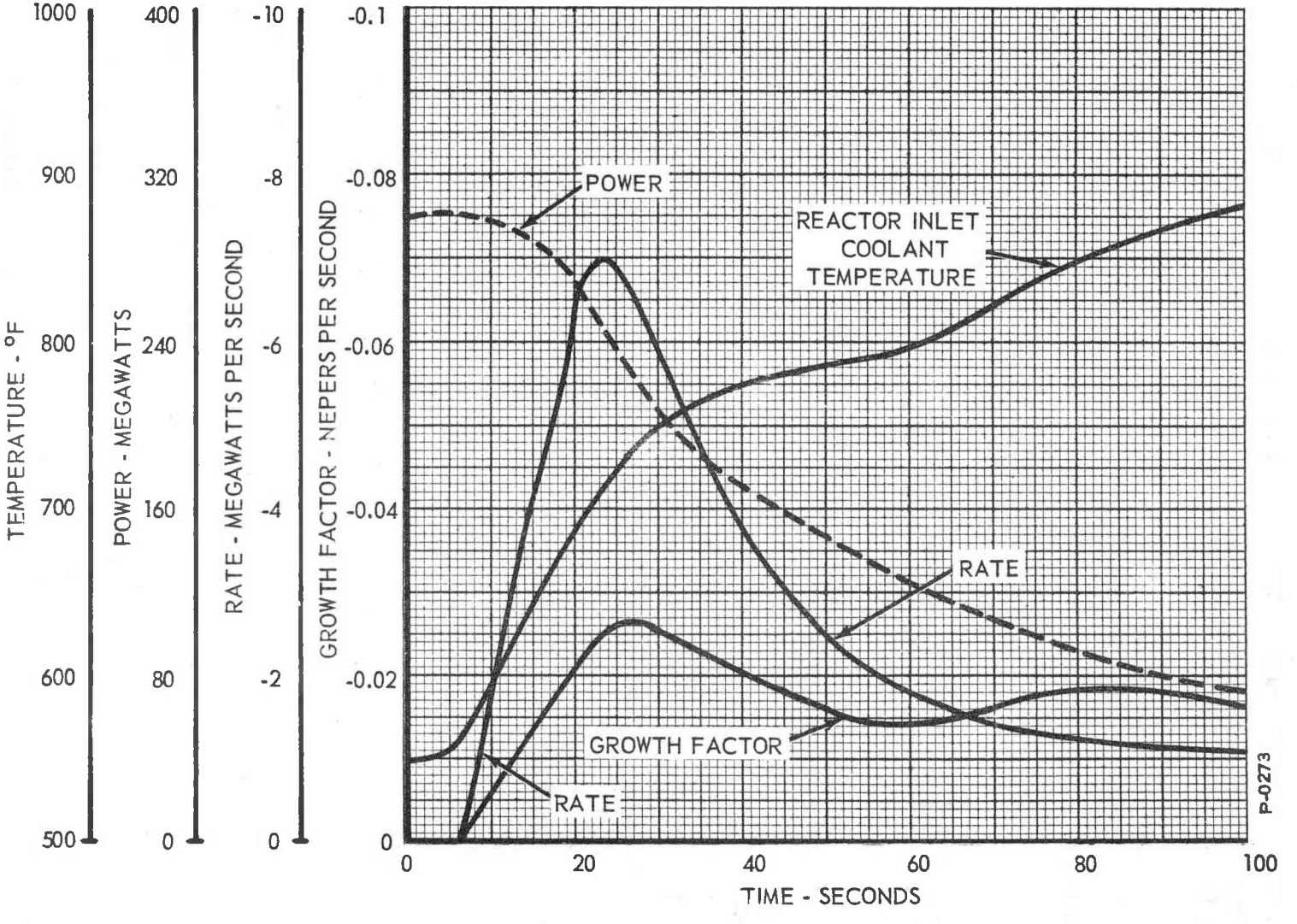

Figure 3.9 - Complete Secondary Flow Failure. Power, and Rate and Growth-Factor Signals

negative so none of the trips which protect the reactor from positive excursions will operate. The rate signal is not large enough to trip the scram that protects the reactor in the event of a complete primary flow failure.

No corresponding curves were obtained in the previous study. There, the value of the rate signal was inferred from the power curve that is shown in Figure C4, of Appendix C, of this report.

3.3.1.2.4 Loss of One Secondary Pump -- In Section 2.1.3.3, the effect on power and on fuel and coolant temperatures, of the failure of one secondary coolant pump was discussed, and the results of the computer run were shown in Figure 2.8. The power, rate and growth-factor signals accompanying such a failure are shown in Figure 3.10. Only the calculated value of the temperature coefficient of reactivity was used. Again, we note that the signals are negative and will not operate any of the trips set so far to protect the reactor from positive transients. Although the rate signal is negative, it is not large enough to trip the scram, set at minus ten megawatts per second, that protects the reactor in the event of a complete primary flow failure.

No corresponding curves were obtained in the previous study. There, the value of the rate signal was inferred from the power curve that is shown in Figure C5, of Appendix C, of this report.

3.3.1.2.5 Loss of Feedwater Flow -- In Section 2.1.3.4.1, the simulation of the effects of a step decrease in feedwater flow from 100 to ten percent of full flow has been discussed. The results of the computer run showing the effects on temperatures and power were shown in Figure 2.10. The power, rate, and growth-factor signals corresponding to this transient are shown in Figure 3.11. Only the calculated value of the temperature coefficient of reactivity was used. No corresponding runs were made during the previous study. We note that the signals are negative and will not operate any of the trips set thus far, to protect the reactor from positive excursions. Although the rate signal is negative, its maximum value is less than ten megawatts per second; so the scram trip will not be operated. It takes 18 seconds for the temperatuee change in the primary coolant, induced by the step change in feedwater flow, to enter the core.

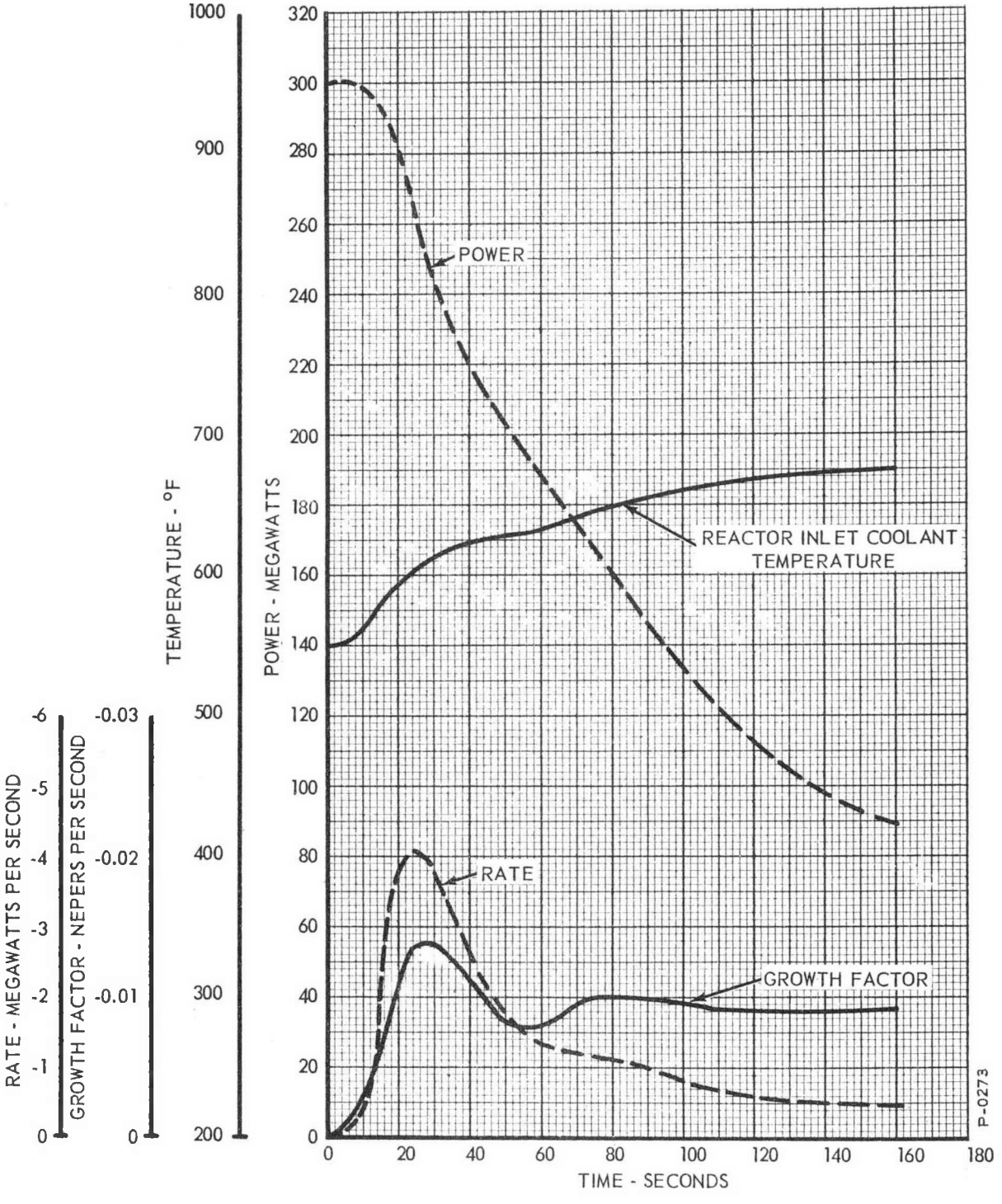

Figure 3.10 - Failure of One Secondary Pump Power, and Rate and Growth-Factor Signals

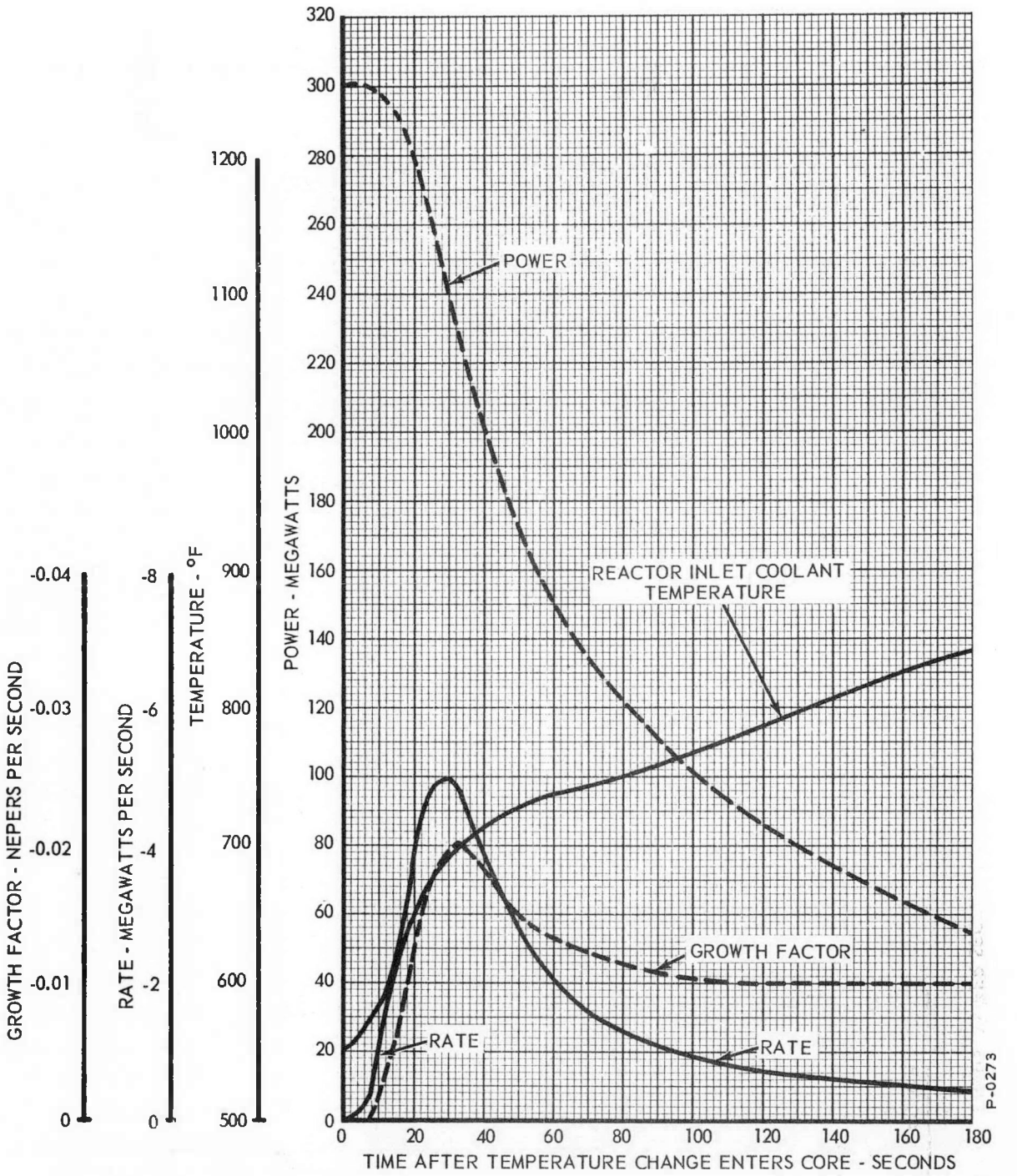

Figure 3.11 - Feedwater Flow Decrease Power, and Rate and Growth-Factor Signals

3.3.1.2.6 Increase in Feedwater Flow -- The effect of a step increase in feedwater flow on power, and on temperatures was presented in Figure 2.12. The feedwater flow was assumed to undergo a step increase from full flow to 150 percent of full flow. The computer run was made using only the calculated temperature coefficient of reactivity. The power, rate and growth-factor signals induced by the transients are shown in Figure 3.12. No corresponding run was made during the previous study. It takes 18 seconds for the temperature change in the primary coolant, induced by the change in feedwater flow, to enter the core. We see that even through the rate and growth-factor signals are positive, their maximum magnitudes are such that no trips will be operated. The power does not increase enough to actuate the setback power trip; which is set at 360 megawatts.

3.3.2 Low-Power Operation

3.3.2.1 Start-Up Transient

In Figure 3.13, the power and rate signals generated by the excursion caused by inserting 92 cents worth of positive reactivity at the rate of one cent per second, starting from zero power are shown. The transient is only simulated in the power range; above one percent of full power. The initial growth factor is assumed to correspond to 70 cents worth of excess reactivity at one percent of full power. The power curves are the same as those shown in Figure 2.15. In Figure 3.14 the growth-factor signals corresponding to this excursion are shown, together with the effective reactivity. Three values of the temperature coefficient of reactivity were used. The curves corresponding to the calculated temperature coefficient of reactivity are identified by the symbol ρo. The curves labeled $\rho o/2$ and $3\rho o/2$ correspond to one-half and one-and-one-half times the calculated value respectively. The corresponding curves obtained during the previous study are shown in Appendix C, in Figure C10. Note that the simulation made during the present study assumed that the shutdown temperature is 550°F, instead of 600°F as in the previous study. Note also, that the simulation of the growth-factor signals, shown in Figure 3.14, is not valid for times shorter than one second, because of lags in the simulator.

We see from Figure 3.13 that the smallest rate signal is obtained when the temperature coefficient of reactivity is $3\rho o/2$. In this case, a rate of six megawatts per second is reached 1.6 seconds

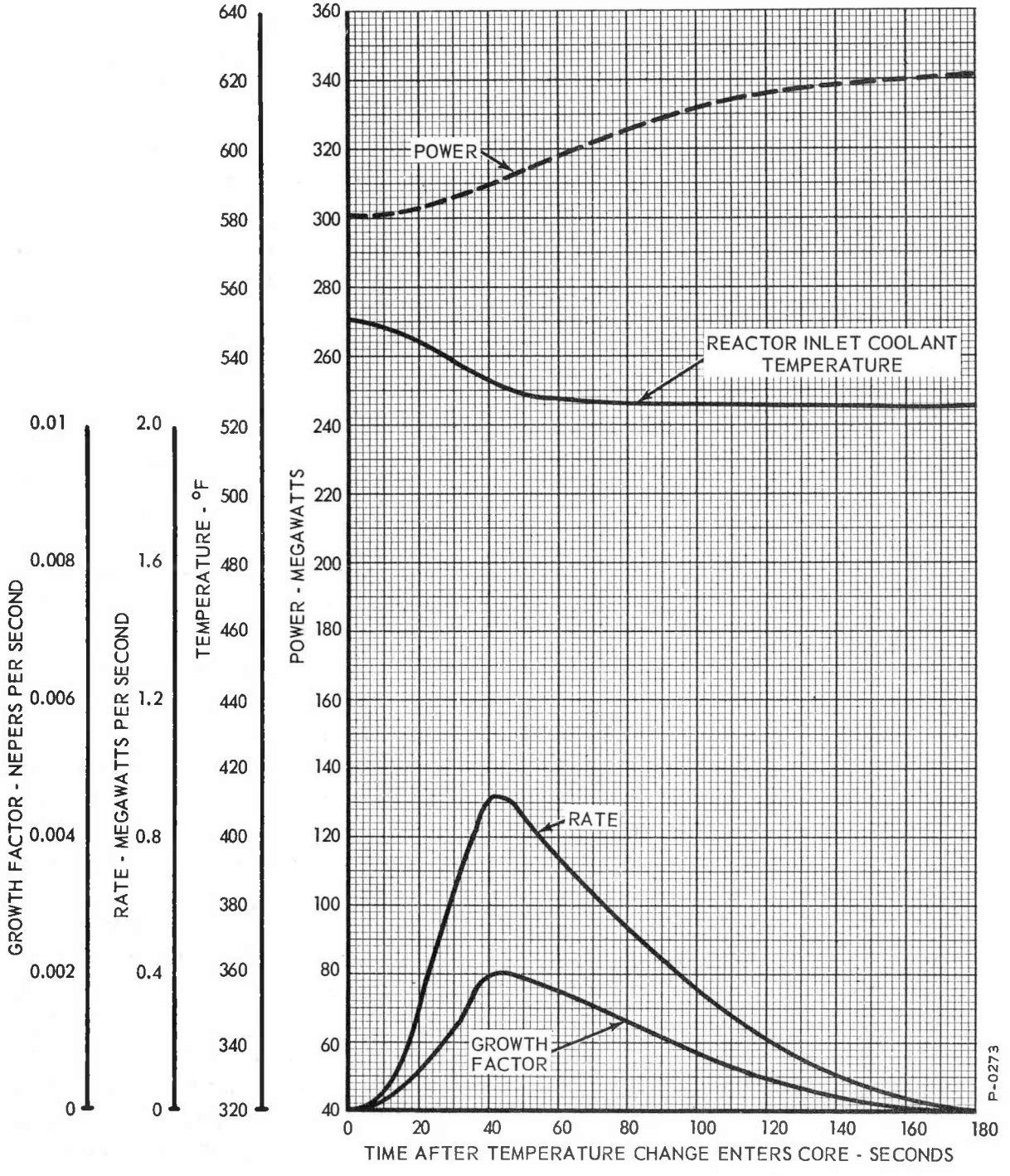

Figure 3.12 - Feedwater Flow Increase: Power, and Rate and Growth-Factor Signals

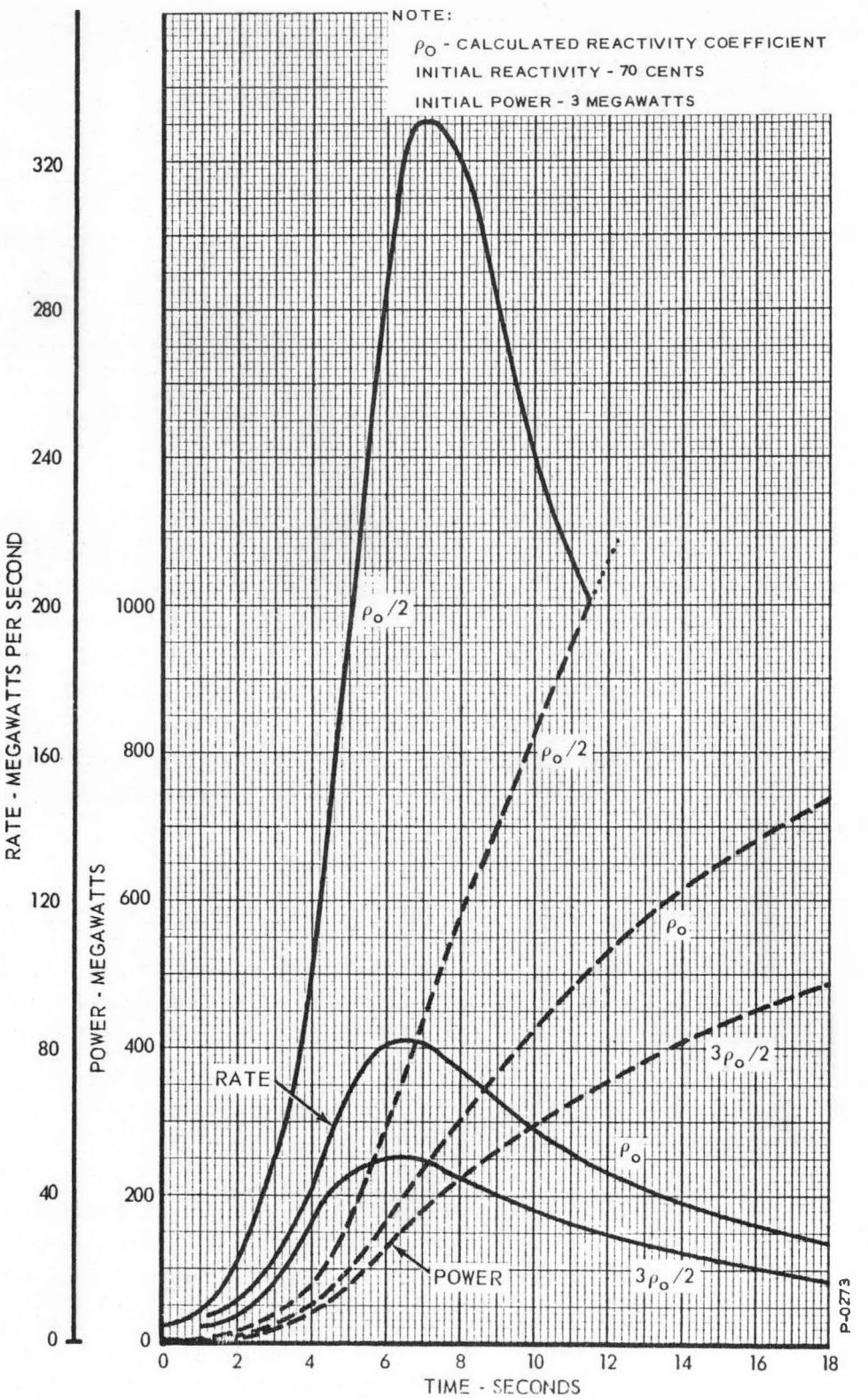

Figure 3.13 - Start-Up Excursion Power and Rate Signal

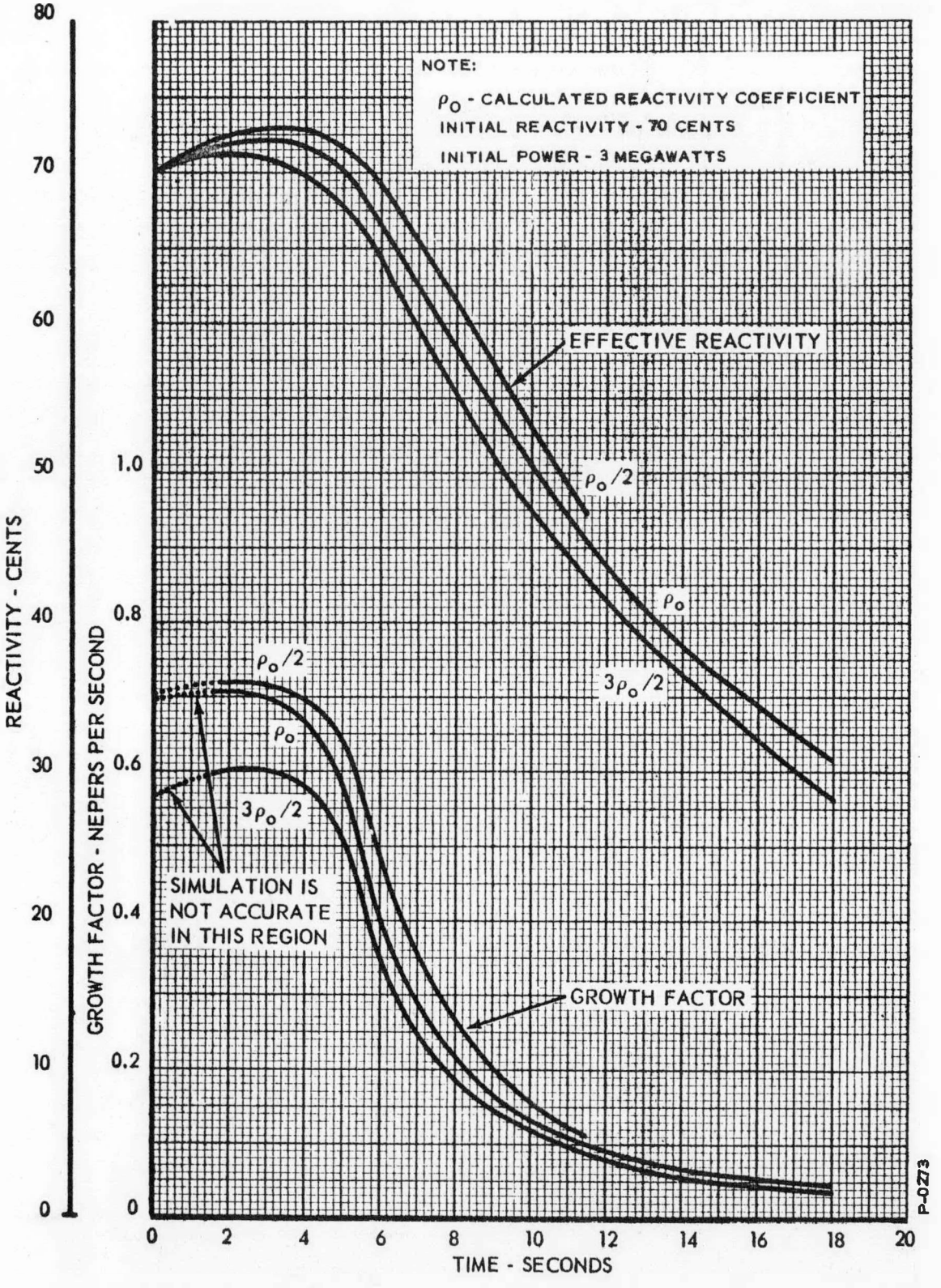

Figure 3.14 - Start-Up Excursion: Growth-Factor Signal and Effective Reactivity

after the reactor power reaches one percent of full power, and the reactor will scram. Thus we see that adequate protection is provided by the rate trip set at this value. Clearly, if the temperature coefficient of reactivity is smaller, the reactor will scram more quickly.

We also see from Figures 2.13 and 2.15 that if the scram power trip is set at 130 percent of full power, 390 megawatts, the reactor will scram about three seconds before fuel melts even if the temperature coefficient of reactivity is $\rho o/2$. Thus it is seen that the scram power trip setting gives good protection.

In the previous report, a scram-growth-factor trip setting of 0.050 nepers per second was chosen. We see from Figure 3.14 that, when the simulation becomes valid, the growth factors range from about 0.6 to 0.72 nepers per second. It follows that a growth-factor scram trip, set at 0.050 nepers per second, will shut the reactor down, far in the sub-power region. This setting of 0.050 nepers per second is well above the minimum setting of 0.030 nepers per second, as discussed in Section 3.2.3.

Previously, a growth-factor alarm trip was set at 0.035 nepers per second. Also a growth-factor setback trip was set at 0.040 nepers per second. It is recommended that these settings not be changed.

3.3.2.2 Excursion from One Percent of Full Power

A computer run was made to determine the behavior of the reactor when positive reactivity was inserted, from one percent of full power, at the rate of one cent per second. The reactor was assumed to have a growth-factor equal to zero at the start of the excursion. In Figure 3.15, the rate and power signals corresponding to the excursion are shown. The power curves are the same as those shown in Figure 2.19. In Figure 3.16 the growth-factor signals and the effective reactivity are shown. The curve labeled ρo corresponds to the calculated temperature coefficient of reactivity. The curves labeled $\rho o/2$ and $3\rho o/2$ correspond to one-half and one-and-one-half times the calculated temperature coefficient of reactivity respectively. No corresponding curves were obtained during the previous study.

Comparing Figures 2.17 and 3.15, we see that the rate signal will reach six megawatts per second 42 seconds after the start of the excursion; about 17 seconds before fuel melting in the

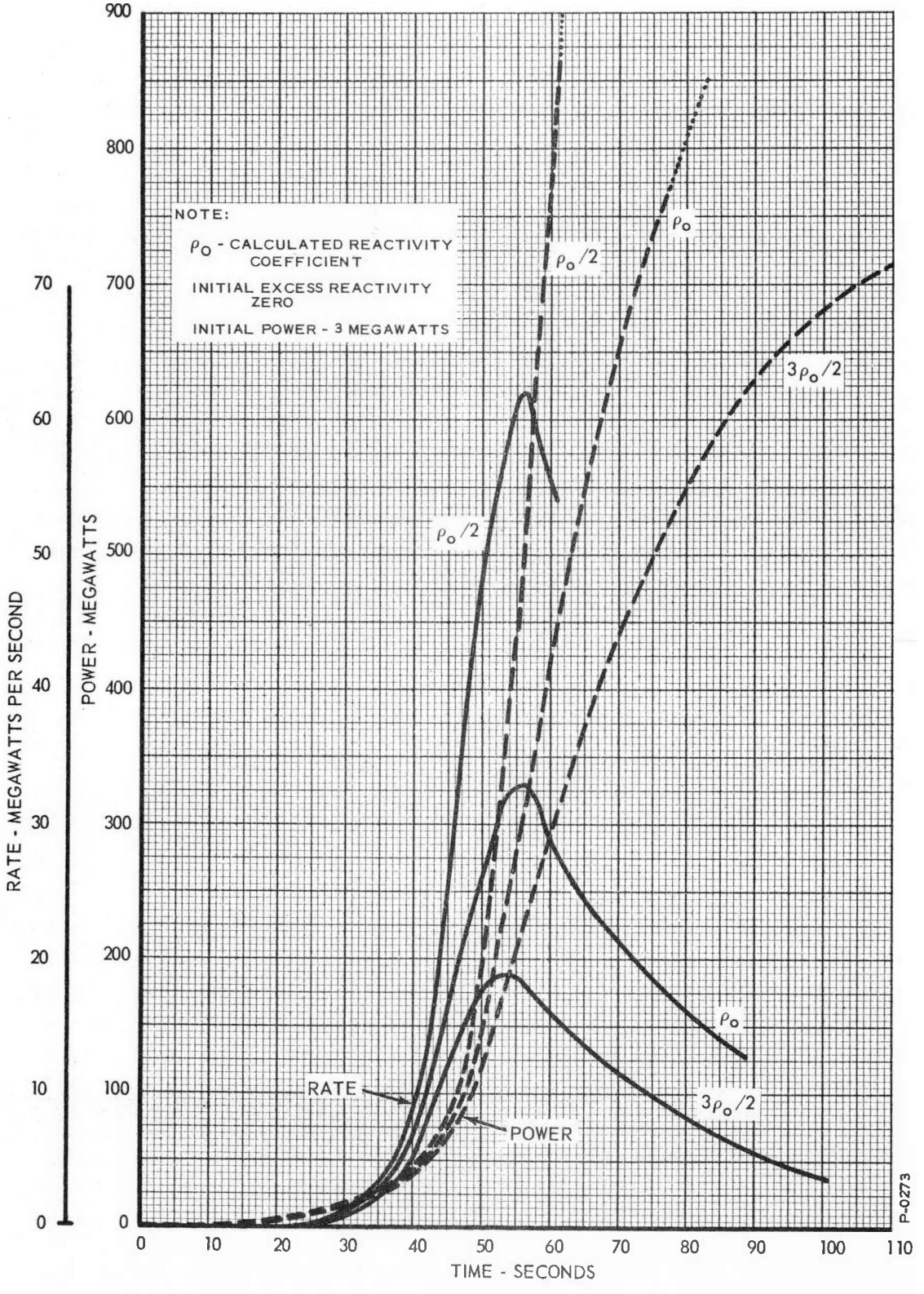

Figure 3.15 - Excursion from Low Power: Power and Rate Signal

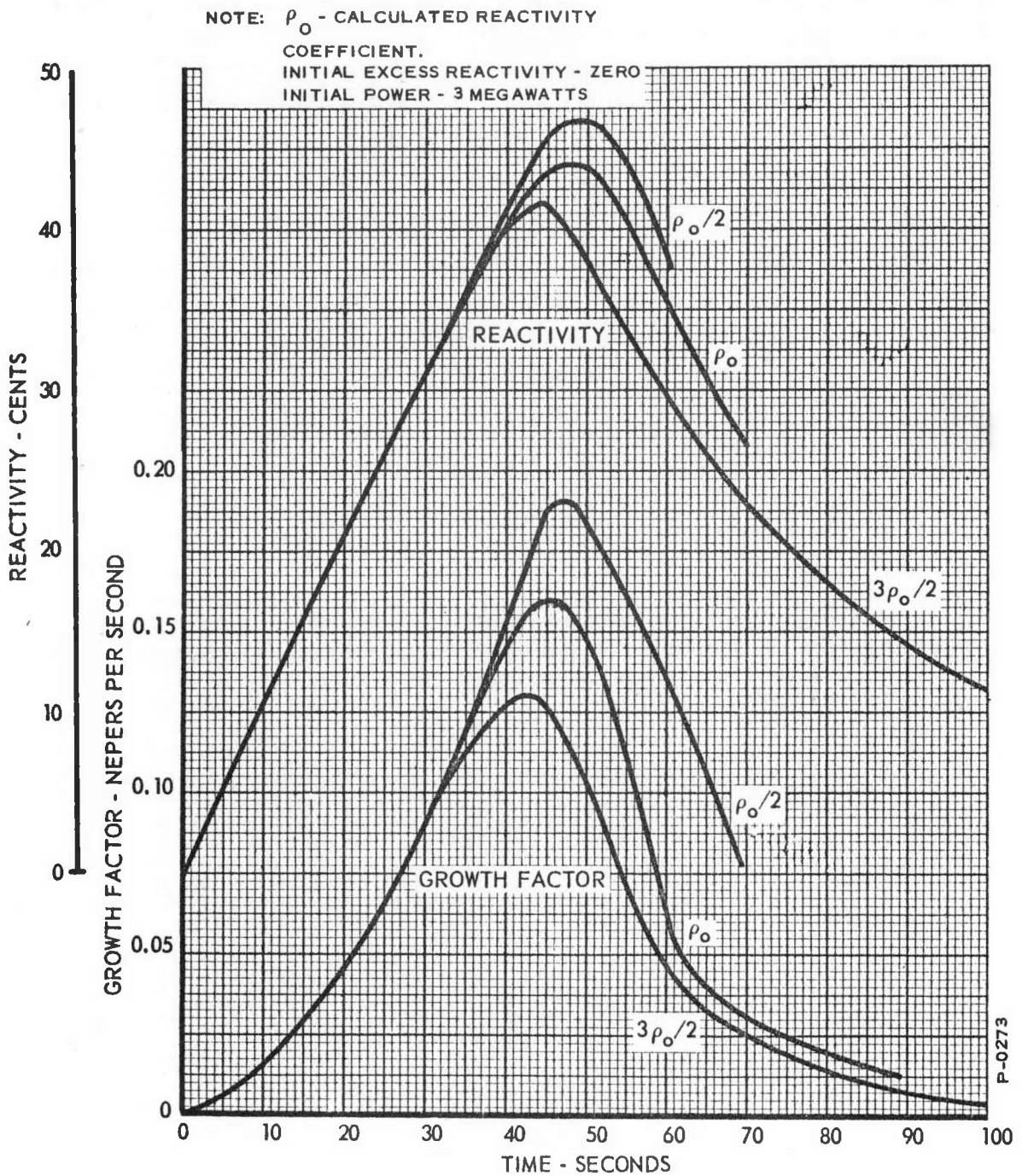

Figure 3.16 - Excursion from Low Power: Growth-Factor Signal and Effective Reactivity

worst case, corresponding to ρo/2. So this trip setting adequately protects the reactor. We see from Figure 3.16 that a growth factor of 0.050 nepers per second is obtained about 22 seconds after the start of the excursion, giving even better protection than the rate scram in the worst case. The power-scram trip will operate about 47 seconds after the start of the excursion, when the temperature coefficient of reactivity is ρo/2, also providing adequate protection.

3.3.3 Summary of Trip Settings

In Sections 3.3.1, and 3.3.2 we have presented information upon which trip level settings were based, together with discussions of the reasons for the individual selections. In this section the trip level settings are summarized for convenient reference. The trip level settings are listed in Table 3.3.

Table 3.3 - Trip Level Settings

Response / Signal	Alarm	Setback	Scram
Power	110%	120%	130%
Rate	+1 MW/sec	+2 Mw/sec	+6 Mw/sec -10 Mw/sec
Growth Factor	+0.035 n/sec*	+0.040 n/sec	+0.050 n/sec

* n/sec = nepers per second

3.3.4 Effect of Temperature Coefficient of Reactivity on Protection

A range of values for the temperature coefficient of reactivity has been investigated since the actual coefficient cannot be completely determined at this time. It is interesting to examine how the change in value of the coefficient affects the degree of protection, against positive excursions, given by the power-limiting system with the trip levels set as shown in Table 3.3. Table 3.4 has been prepared as a convenient method of examining the effect for positive transients. It must be

* n/sec = nepers per second

Table 3.4

Dependence of Scram Protection on Temperature Coefficient: Positive Excursions

TRANSIENT	REACTIVITY COEFFICIENT (ρ_o - CALCULATED COEFFICIENT)	TIME FOR COOLANT BOILING AND/OR FUEL MELTING (4)	TIME FOR POWER TRIP (1) (sec)	TIME FOR GROWTH FACTOR TRIP (2) (sec)	TIME FOR RATE TRIP (3) (sec)	COMMENTS
Excursion at 1¢/sec from Full Power. Excess Reactivity; 0.	$\rho_o/2$ ρ_o $3\rho_o/2$	34.5 50 ?	12.5 15.0 18.0	---- ---- ----	5.5 5.6 6.5	Worst Case: Power Trip Operates 22 sec Before Damage
Feedwater Flow Change, 100% to 150%.	ρ_o	---	----	----	---	No Trips Will Operate
Start Up - 1¢/sec from 3 Mw. Excess Reactivity; 70¢	$\rho_o/2$ ρ_o $3\rho_o/2$	9.5 20 ?	6.5 9.0 12.5	Operates in Sub-Power Region	0.5 0.9 1.0	Worst Case: Power Trip Operates 3 sec Before Damage
Excursion at 1¢/sec from 3 Mw. Excess Reactivity; 0.	$\rho_o/2$ ρ_o $3\rho_o/2$	60 77.7 ?	54.5 59.0 66.0	21.5 21.5 21.5	38 40 41	Worst Case: Power Trip Operates 5.5 sec. Before Damage

(1) Power - Scram Trip Set at 130% of Full Power, or 390 MW.

(2) Growth-Factor - Scram Trip Set at 0.050 Nepers Per Second.

(3) Rate-Scram Trip Set at 6 Mw/sec.

(4) (?) Means That the Simulation Predicts No Damage.

Table 3.5

Dependence of Scram Protection on Temperature Coefficient: Negative Excursions

TRANSIENT	REACTIVITY COEFFICIENT (ρ_o - CALCULATED COEFFICIENT)	TIME FOR COOLANT BOILING AND/OR FUEL MELTING. (sec)	MAXIMUM NEGATIVE RATE SIGNAL (Mw/sec)	TIME SCRAM IS TRIPPED (2) (sec)
Complete Primary Flow Failure	$\rho_o/2$ ρ_o $3\rho_o/2$	2.7(1) 3.0(1) 3.5(1)	15 23 29	1.2 0.7 0.3
Failure of one Primary Pump	ρ_o	-----	5.8	2
Complete Secondary Flow Failure	ρ_o	-----	7	23
Failure of one Secondary Pump	ρ_o	-----	4.1	24
Feedwater Flow Change 100% to 10%	ρ_o	-----	5.0	29

(1) See Figure 3.7.

(2) Negative-rate-scram trip is set at minus ten Mw/sec.

emphasized that a simulation is only an approximation of an actual case. It is seen from the table that the reactor is adequately protected for all positive transients.

Table 3.5 presents similar information for negative transients.

3.4 CORE TEMPERATURE TRIPS

In principle, the hot-channel outlet temperature is determined by the flux and flow. Since the combination of flux and flow is used to operate the power-limiting system in such a manner that the hot-channel temperature does not rise above a preset limit, a temperature measurement is not needed. Of course, the flux and flow do not give information about the malfunction of an individual fuel subassembly and its temperature must be monitored. It is expected that a change in an individual subassembly will take place slowly, so that there is no need to have the power-limiting system respond to this change. It is recommended that the equipment monitoring the temperatures of the subassemblies be provided with an alarm which will advise the operator of an incipient malfunction. Then the operator can take whatever action is needed.

SECTION 4

POWER-LIMITING SYSTEM RESPONSES

4.0 GENERAL

In the previous sections of this report, we have discussed transients with a variety of causes. These included reactivity insertions at one cent per second from three power levels, and sodium-and feedwater-flow disturbances. We noted that all of the excursions resulting from reactivity insertions would be arrested by the power-limiting system well before fuel melting occurred. The only flow disturbance that requires prompt action, from the point of view of the reactor, is a complete primary flow failure. In this section, we will present computer data illustrating the effectiveness of scrams in arresting transients.

4.1 TRANSIENT FROM FULL POWER

Computer runs have been made to examine the effect of scrams triggered by power and rate signals. In both of these cases the reactor is assumed to be undergoing a transient, starting from full power, caused by a positive reactivity insertion at the rate of one cent per second, when the scram occurs.

4.1.1 Scram Actuated by the Power Trip

Figure 4.1 shows the limiting effect on a scram triggered by the power trip set at 390 megawatts (130 percent of full power) on reactor power, and average outlet coolant temperature. The reactor is on an excursion, from full power, caused by the insertion of reactivity at the rate of one cent per second when the scram occurs. The curves for an uncontrolled transient are shown for comparison. Only the calculated value of the temperature coefficient of reactivity was used. Figure 4.2 shows the behavior of the maximum fuel and coolant temperatures under the same conditions.

4.1.2 Scram Actuated by the Rate Trip

Figure 4.3 shows the effect of a scram actuated by a rate trip set at six megawatts per second. The reactor is on an excursion,

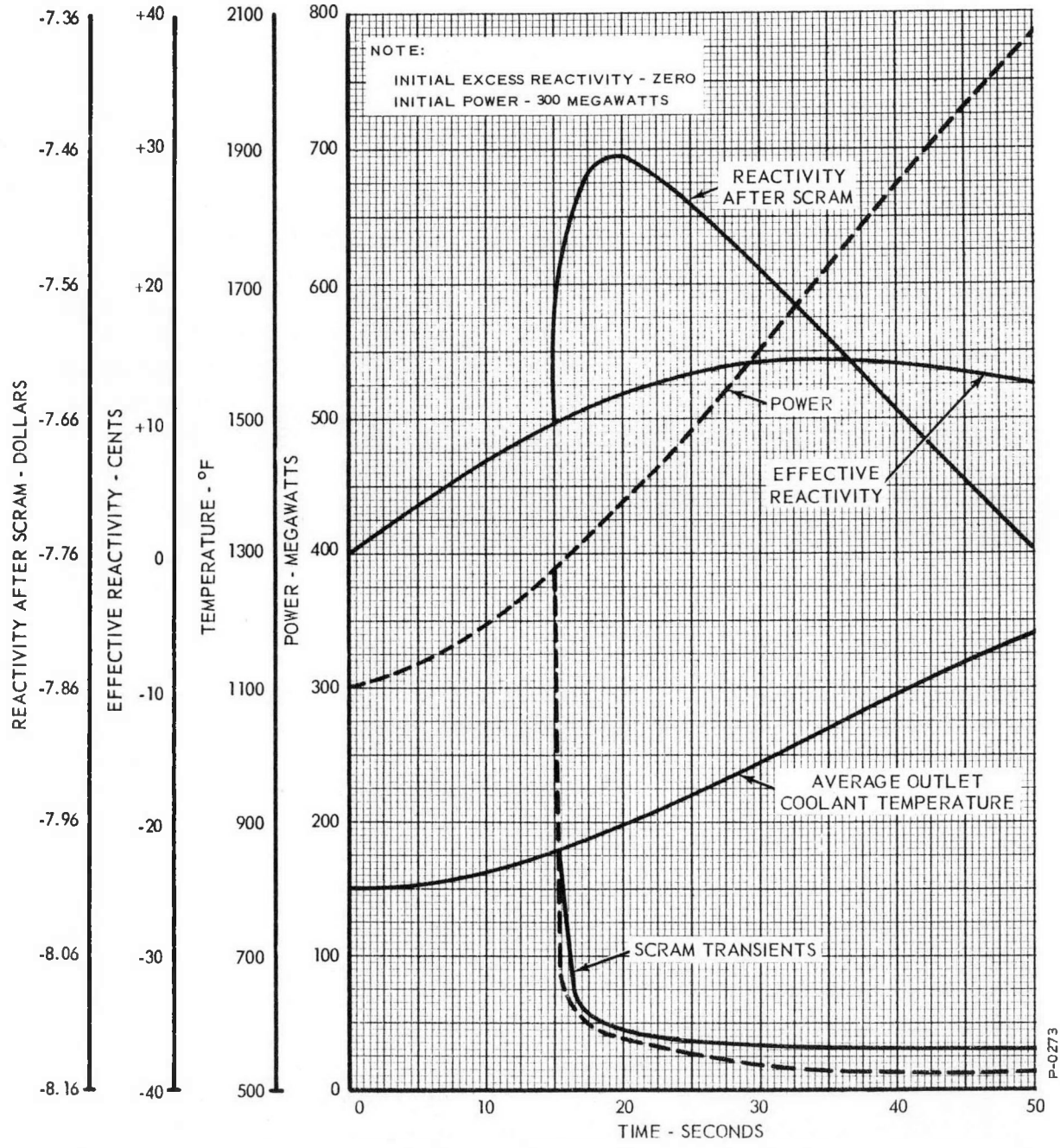

Figure 4.1 - Transient from Full Power at One Cent Per Second Stopped by Scram at 390 Megawatts

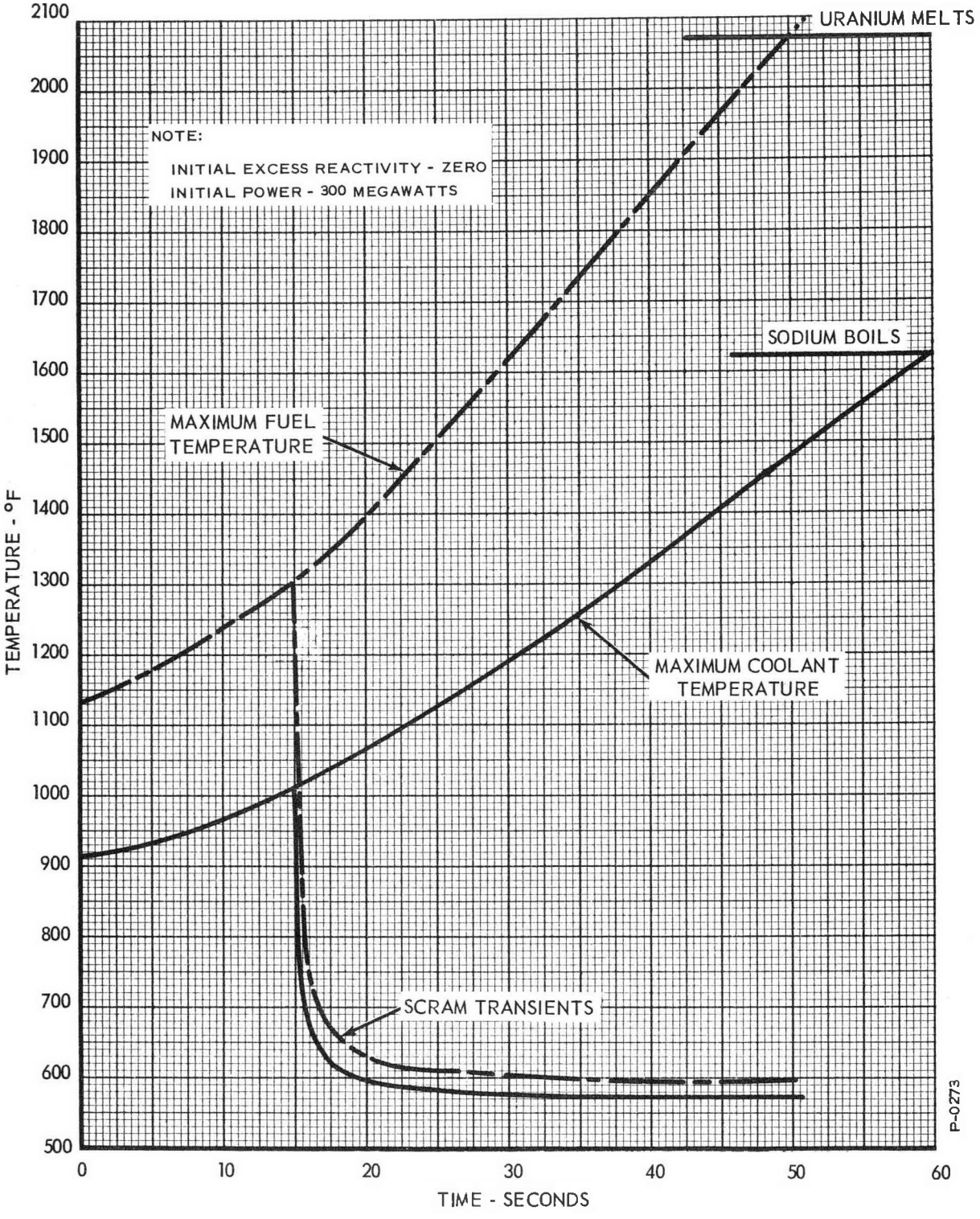

Figure 4.2 - Transient from Full Power at One Cent Per Second Stopped by Scram at 390 Megawatts

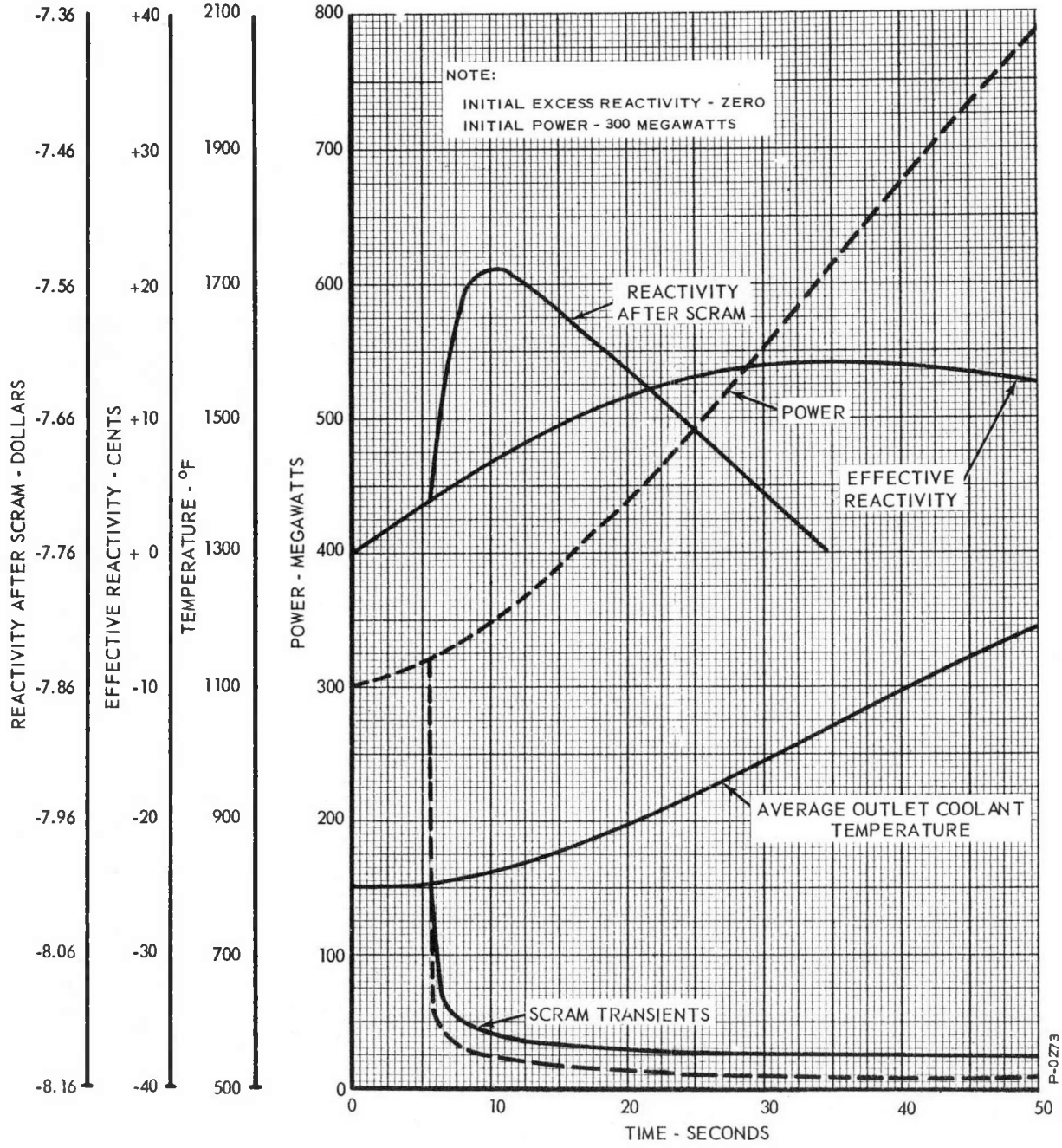

Figure 4.3 - Transient from Full Power at One Cent Per Second Stopped by Scram Set at Six Megawatts Per Second

from full power, caused by the insertion of reactivity at the rate of one cent per second when the scram occurs. The curves for an uncontrolled transient are shown for comparison. Only the calculated value of the temperature coefficient of reactivity was used. Figure 4.4 shows the behavior of the maximum fuel and coolant temperatures under the same conditions.

4.2 START-UP TRANSIENT

The only start-up transient examined for the effect of a scram was the one where the scram was triggered by a power trip set at 390 megawatts (130 percent of full power). The case for the scram triggered by a rate trip set a six megawatts per second was not studied because the scram would occur in less than a second after the reactor power passed one percent of full power. By looking at Figures 2.13 through 2.16, we see that we would not obtain any significant data from such a computer run.

Figure 4.5 shows the effect of a scram, actuated by a trip set at 390 megawatts, on reactor power and average outlet coolant temperature. The reactor is on an excursion from a three-megawatt power level, with an initial reactivity of 70 cents. The excursion is caused by the insertion of positive reactivity, at the rate of one cent per second, from zero power. The data for the uncontrolled transient are shown for comparison. Only the calculated temperature coefficient of reactivity was used. Figure 4.6 shows the behavior of the maximum fuel and coolant temperatures under the same conditions.

4.3 TRANSIENT FROM LOW POWER

Computer runs have been made to study the effectiveness of a scram in limiting a transient from low power. The reactor is undergoing an excursion from a power level of three megawatts, caused by a reactivity insertion at the rate of one cent per second, when the scram occurs. The initial excess reactivity is assumed to be zero. The scrams examined were tripped by power and by rate signals.

4.3.1 Scram Actuated by the Power Trip

Figure 4.7 shows the effect of a scram on power and on average outlet coolant temperature. The scram was actuated by the power trip set at 390 megawatts. The uncontrolled transients are shown for comparison. Only the calculated temperature coefficient of

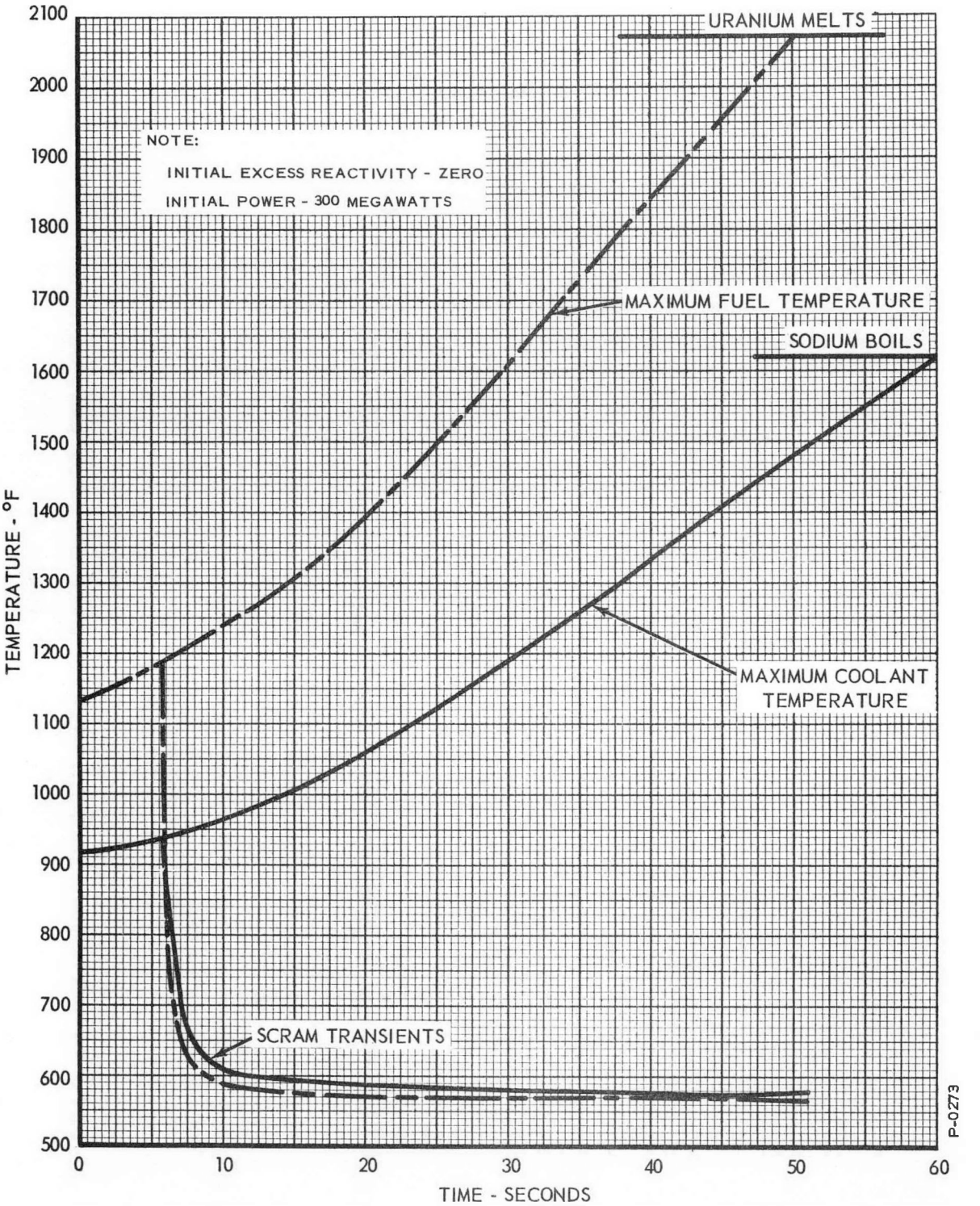

Figure 4.4 - Transient from Full Power at One Cent Per Second Stopped by Scram Set at 6 Megawatts Per Second

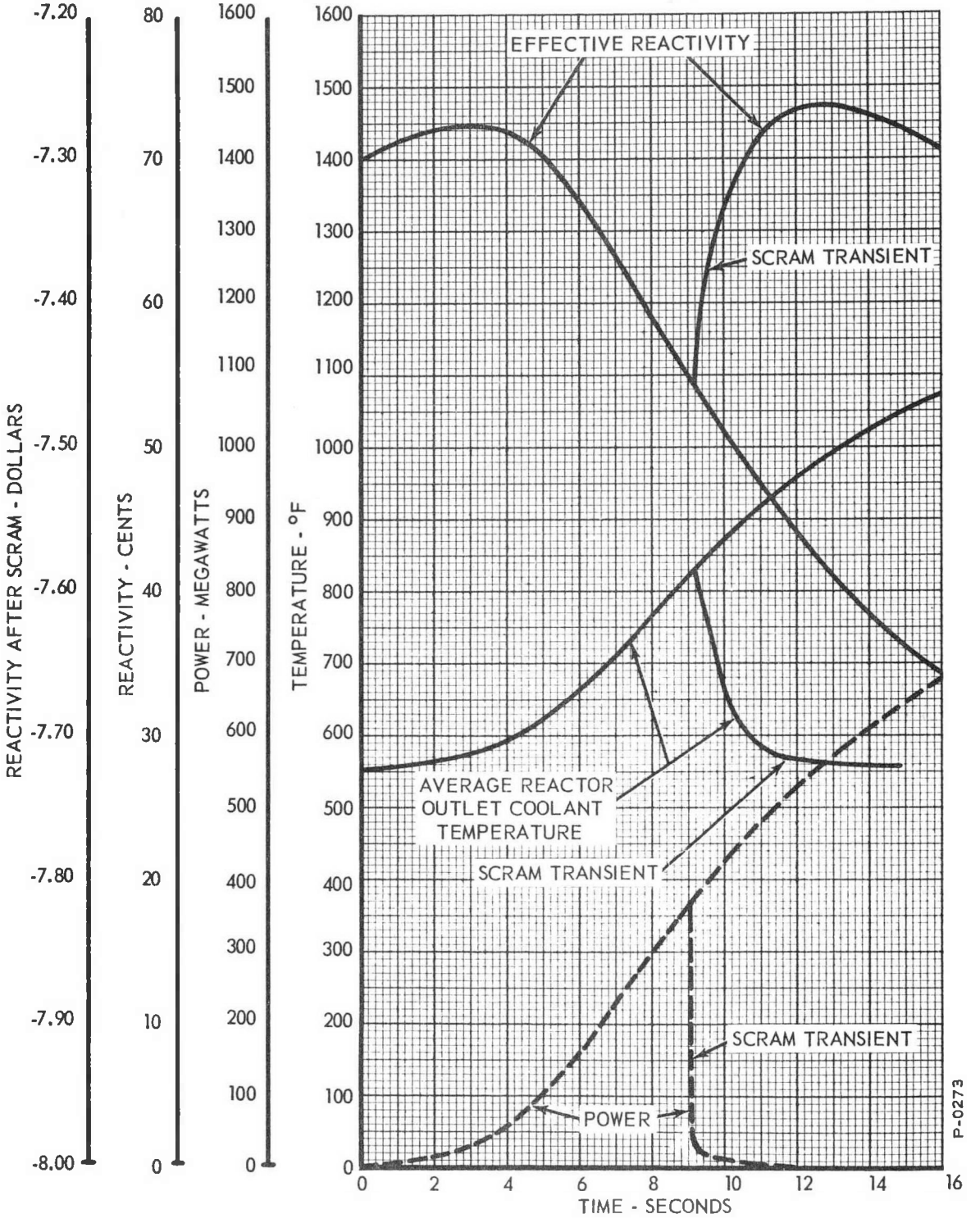

Figure 4.5 - Start-Up Transient Stopped by Scram at 390 Megawatts

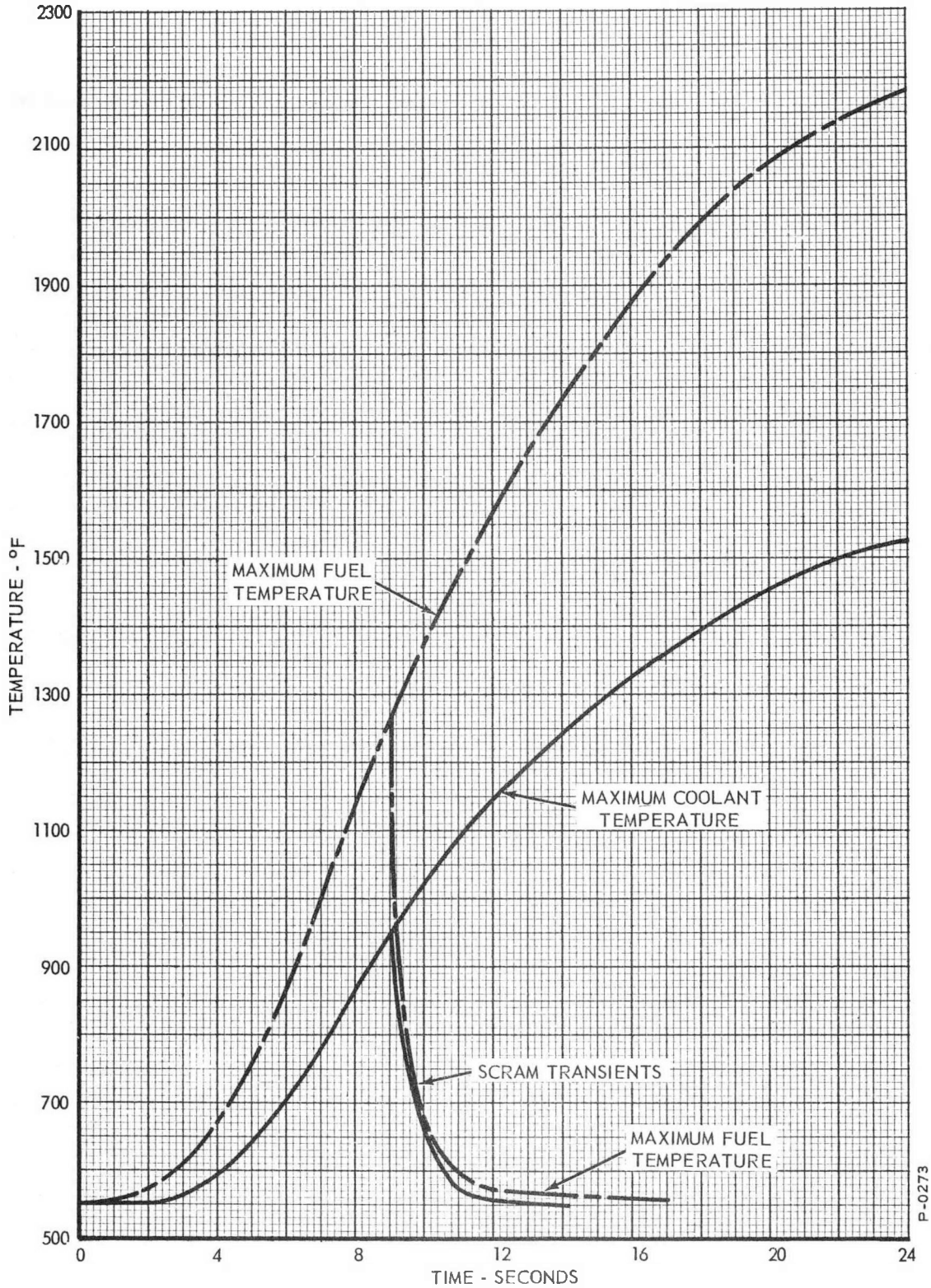

Figure 4.6 - Start-Up Transient Stopped by Scram at 390 Megawatts

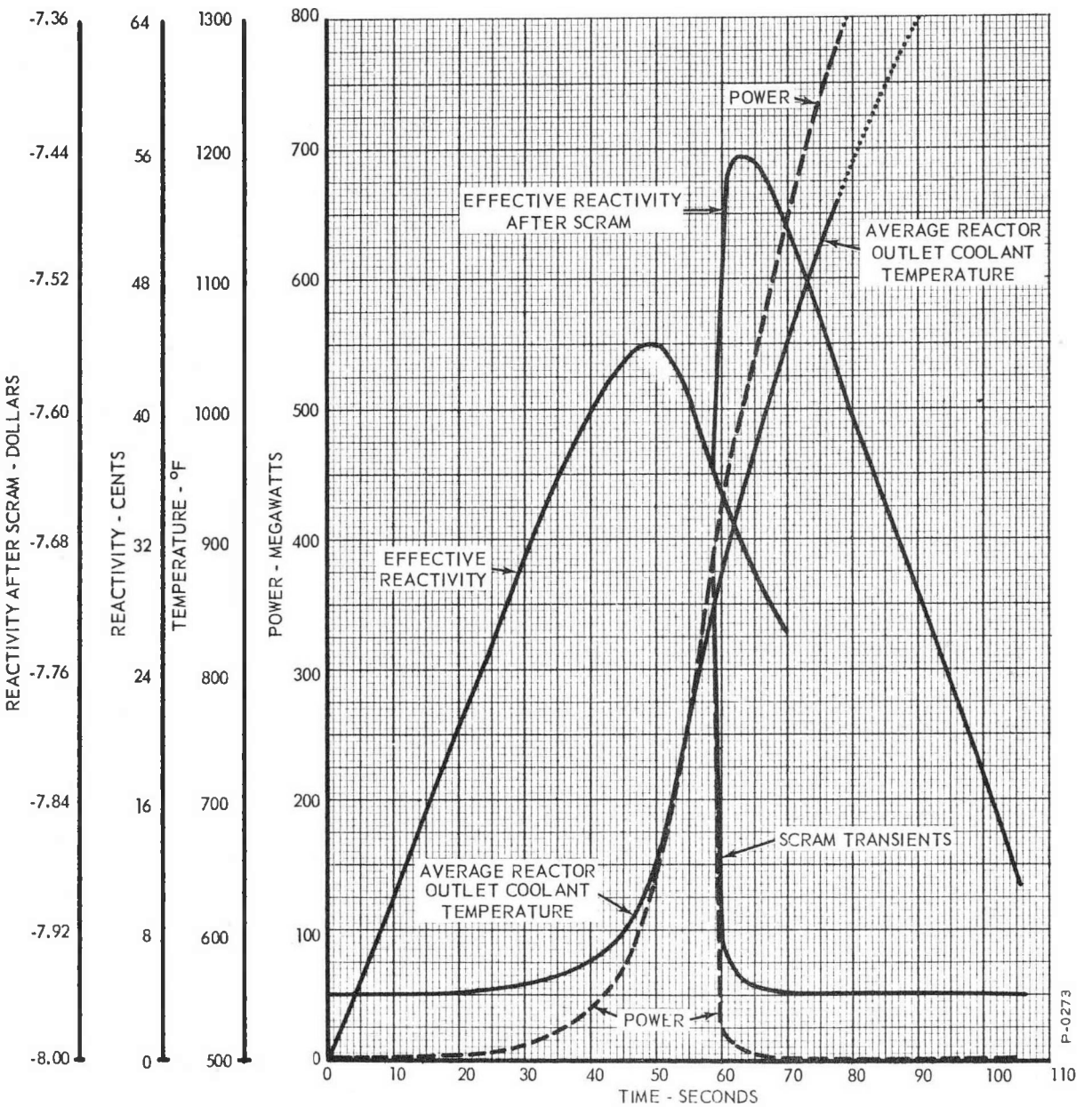

Figure 4.7 - Transient from Three Megawatts Stopped by a Scram at 390 Megawatts

reactivity was used. Figure 4.8 shows the behavior of the maximum fuel and coolant temperatures under the same conditions.

4.3.2 Scram Actuated by The Rate Trip

Figure 4.9 shows the effect, on power and on average outlet coolant temperature, of a scram actuated by the rate trip. The rate trip was set at six megawatts per second. The curves corresponding to an uncontrolled transient are shown for comparison. Only the calculated temperature coefficient of reactivity was used. Figure 4.10 shows the behavior of the maximum fuel and coolant temperatures under the same conditions.

4.4 FLOW DISTURBANCES

A computer run was made to examine the effect of a scram during a complete primary flow failure. Another run was made to study the effect of a scram during steady full power operation; such as might be tripped by a feedwater flow disturbance before any temperature changes could reach the core. The data obtained from these runs are presented below.

4.4.1 Scram During A Complete Primary Flow Failure

Figure 4.11 shows the effect, on power and on average reactor outlet temperature, of a scram during a complete primary flow failure. The scram was tripped 0.7 seconds after the start of a flow failure, by a negative rate trip set at minus ten megawatts per second. Again, the curves corresponding to the uncontrolled transient are shown for comparison. Only the calculated temperature coefficient of reactivity was used. Figure 4.12 shows the behavior of the maximum fuel and coolant temperatures under the same conditions.

4.4.2 Scram During Steady Operation at Full Power

Figure 4.13 shows the effect of a scram during steady operation at full power. This run was made to study the behavior of the reactor power and temperatures, in the event a scram is triggered by a flow disturbance in the secondary loop or in feedwater flow. Only the calculated value of the temperature coefficient was used. The curves in Figure 4.13 can be applied to the case of the failure of one primary pump, by overlaying the scram transients on the curves of Figure 2.5; making allowance for the delay in the actuation of the trip.

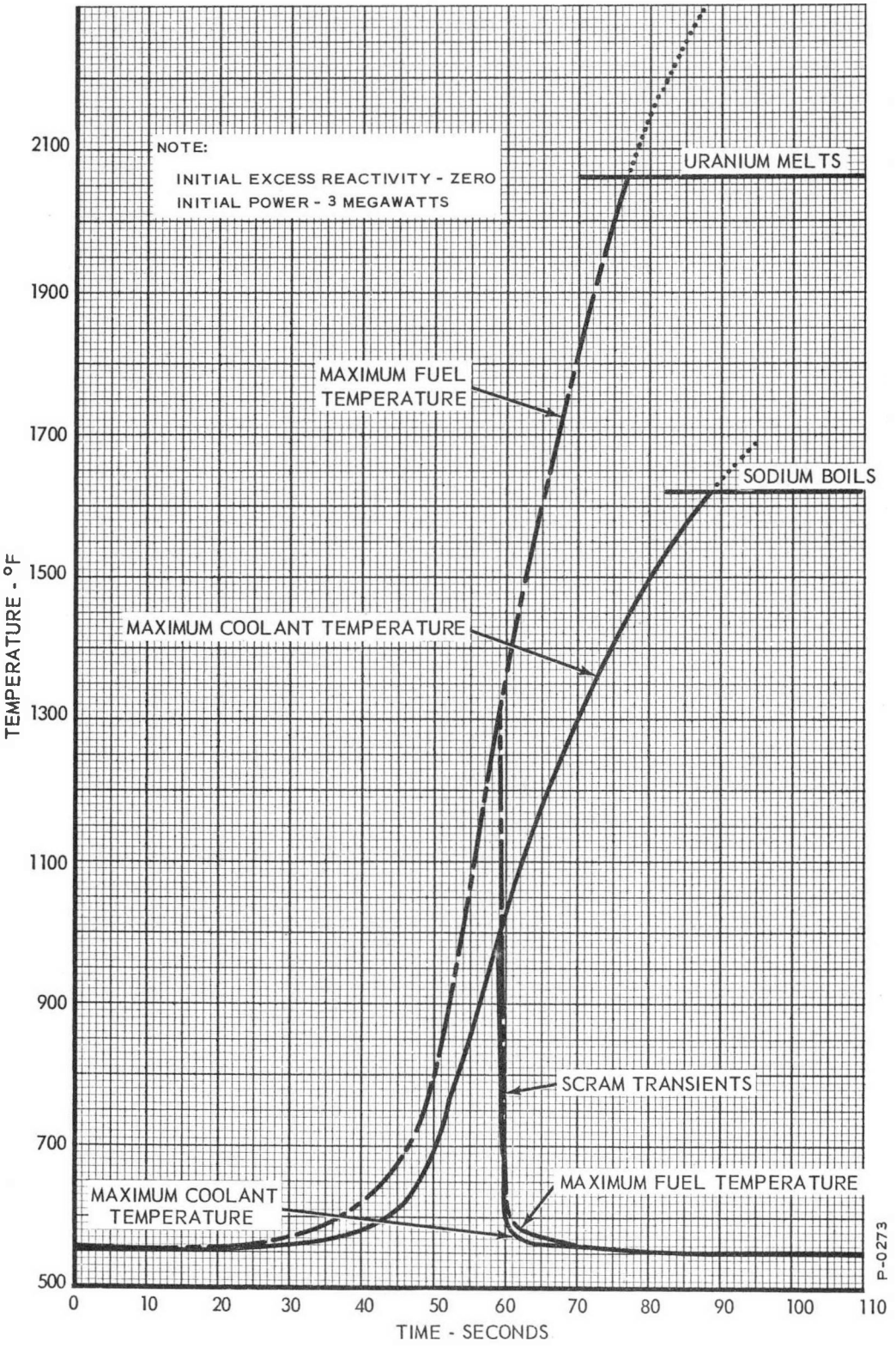

Figure 4.8 - Transient from Three Megawatts Stopped by a Scram at 390 Megawatts

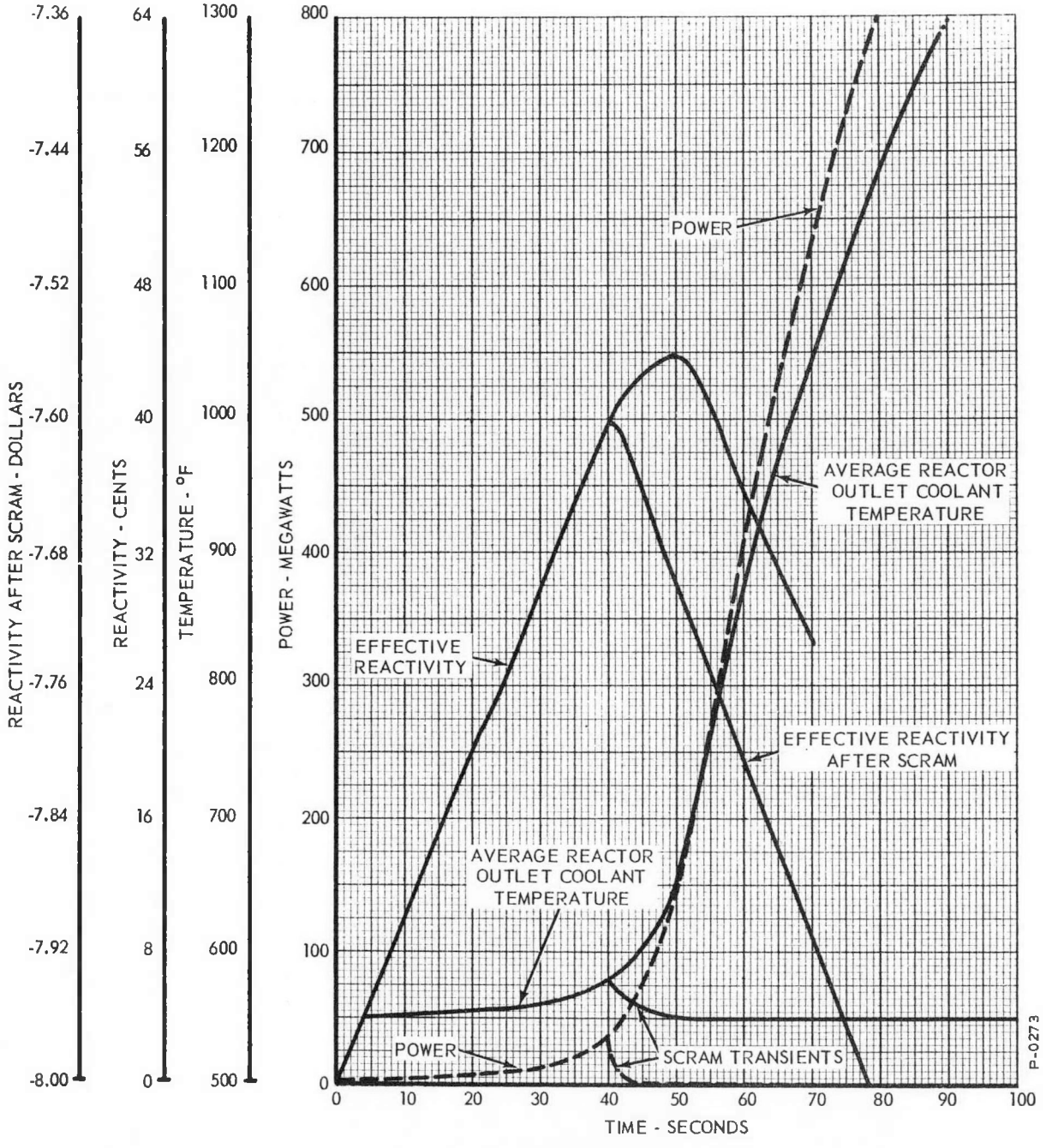

Figure 4 9 - Transient from Three Megawatts Stopped by a Scram at Six Megawatts Per Second

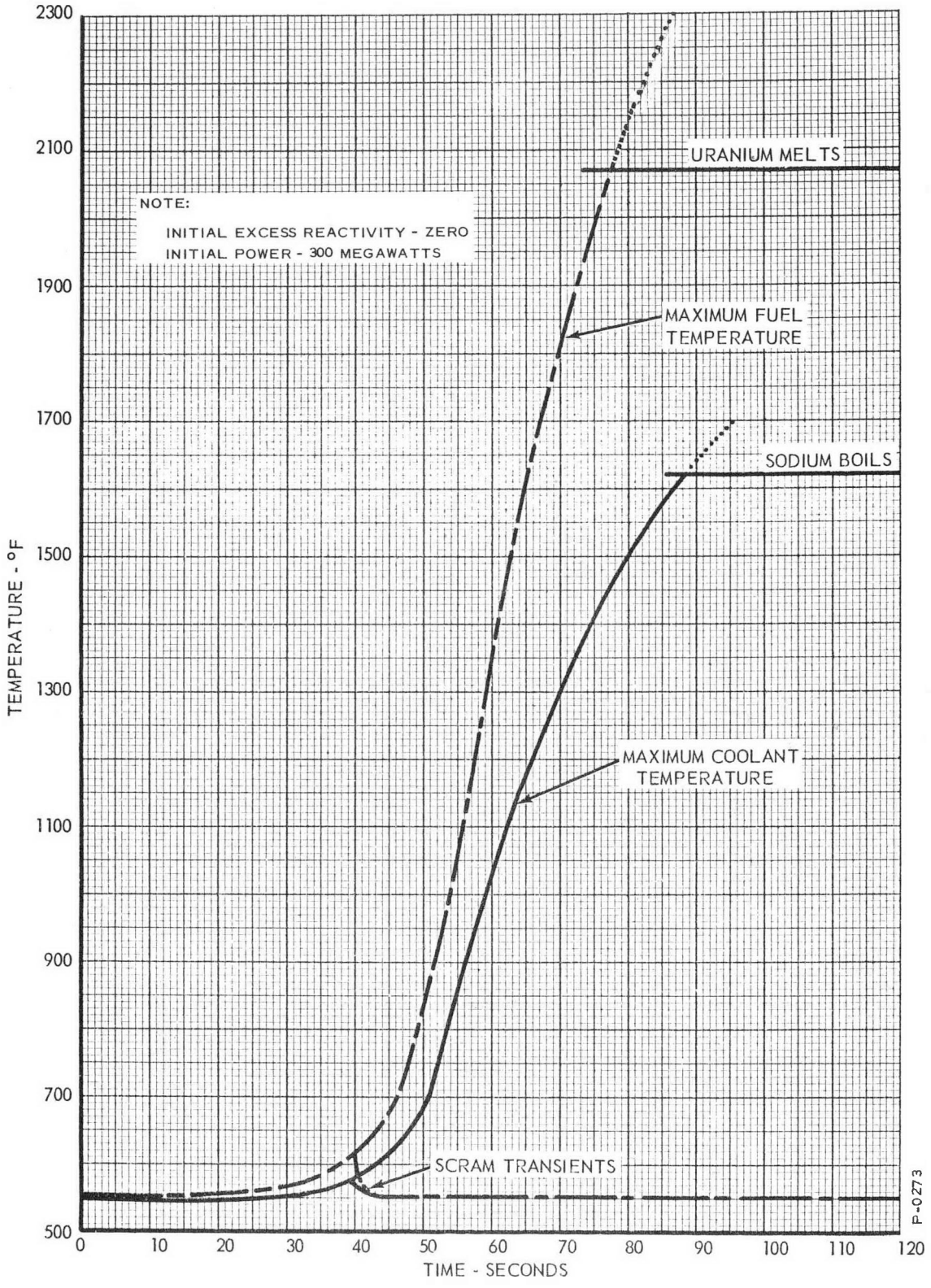

Figure 4.10 - Transient from Three Megawatts Stopped by a Scram at Six Megawatts Per Second

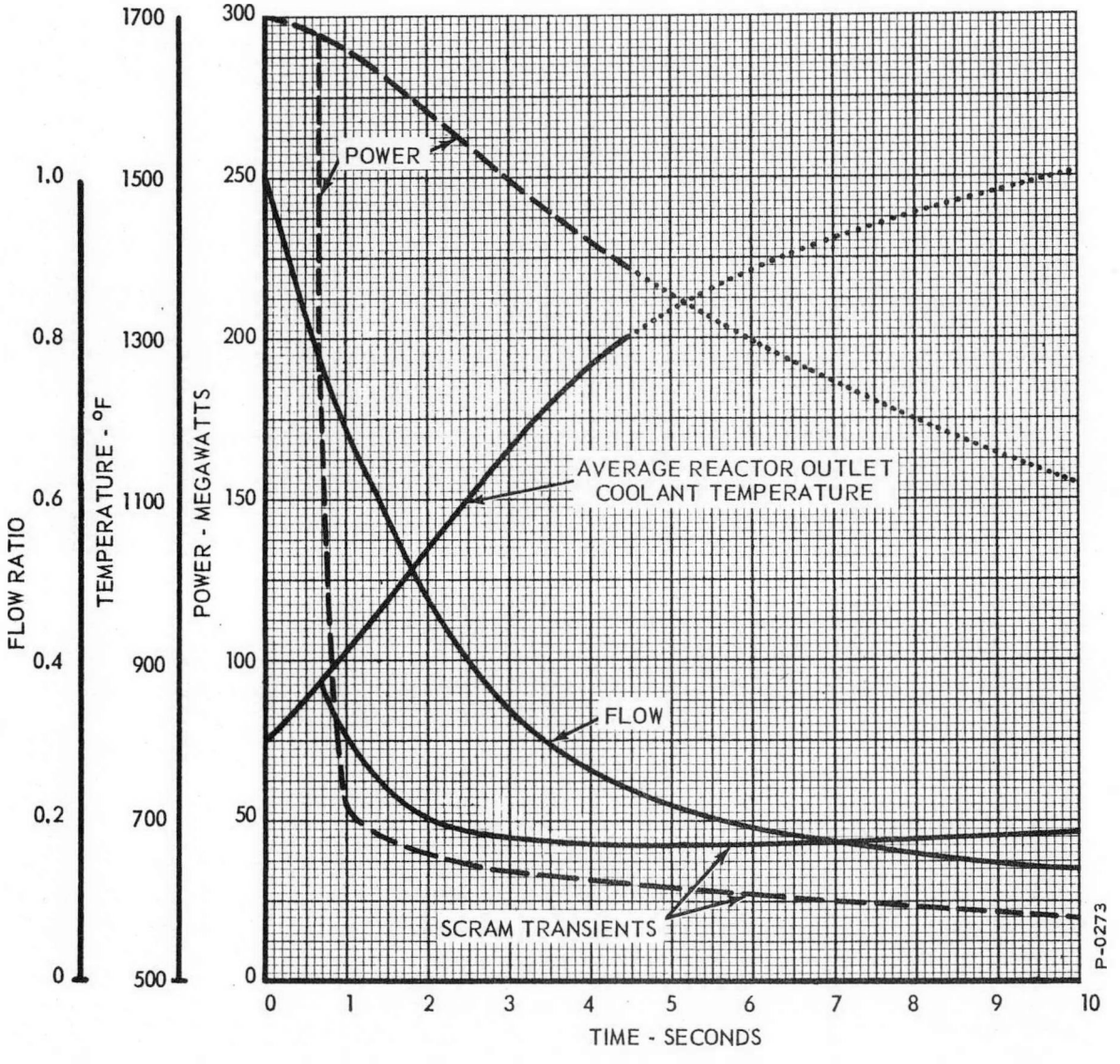

Figure 4.11 - Complete Primary Flow Failure: Scram at Minus 10 Megawatts Per Second - Power and Reactor Outlet Coolant Temperature

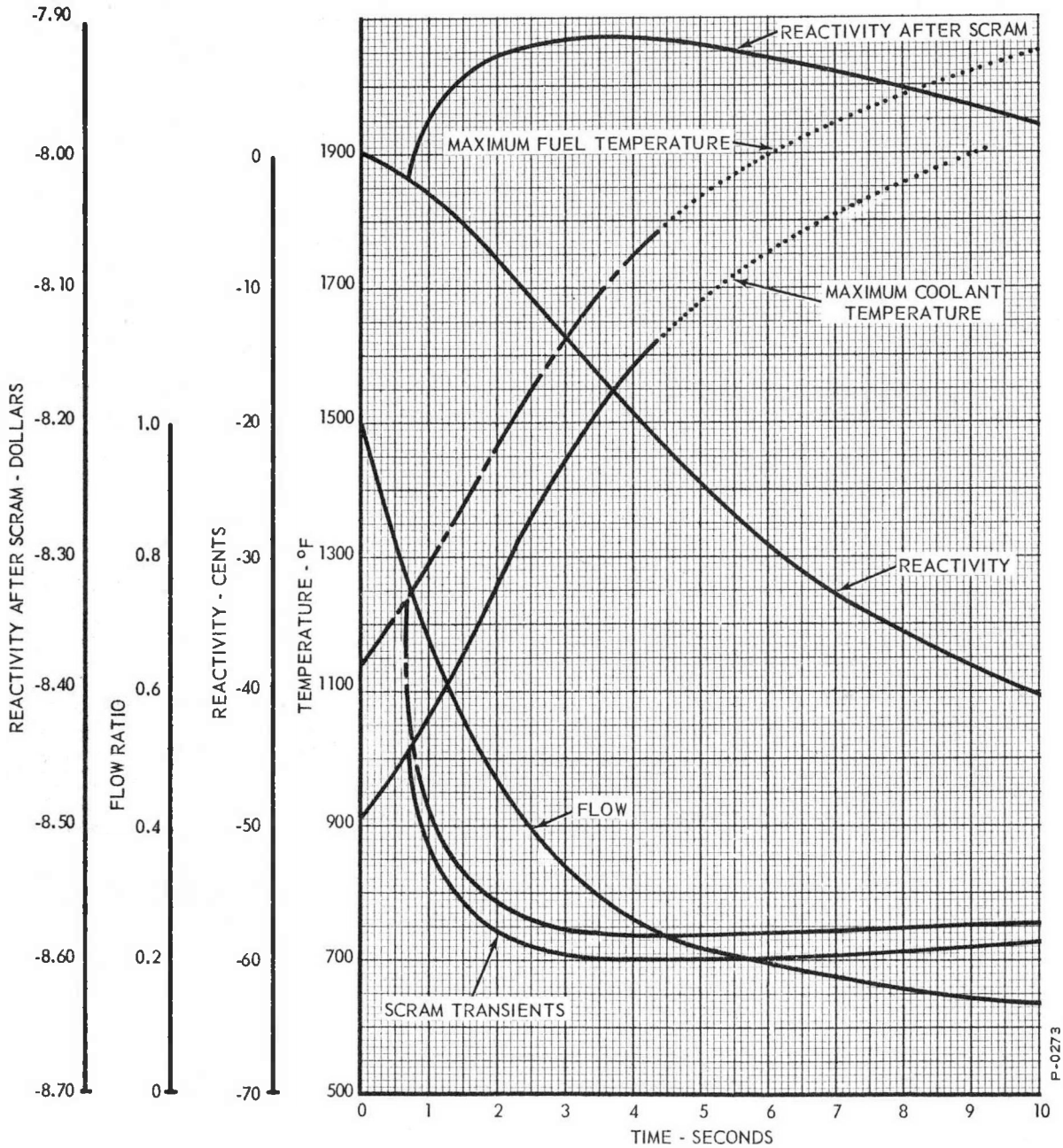

Figure 4.12 - Maximum Hot-Channel Temperatures and Effective Reactivity

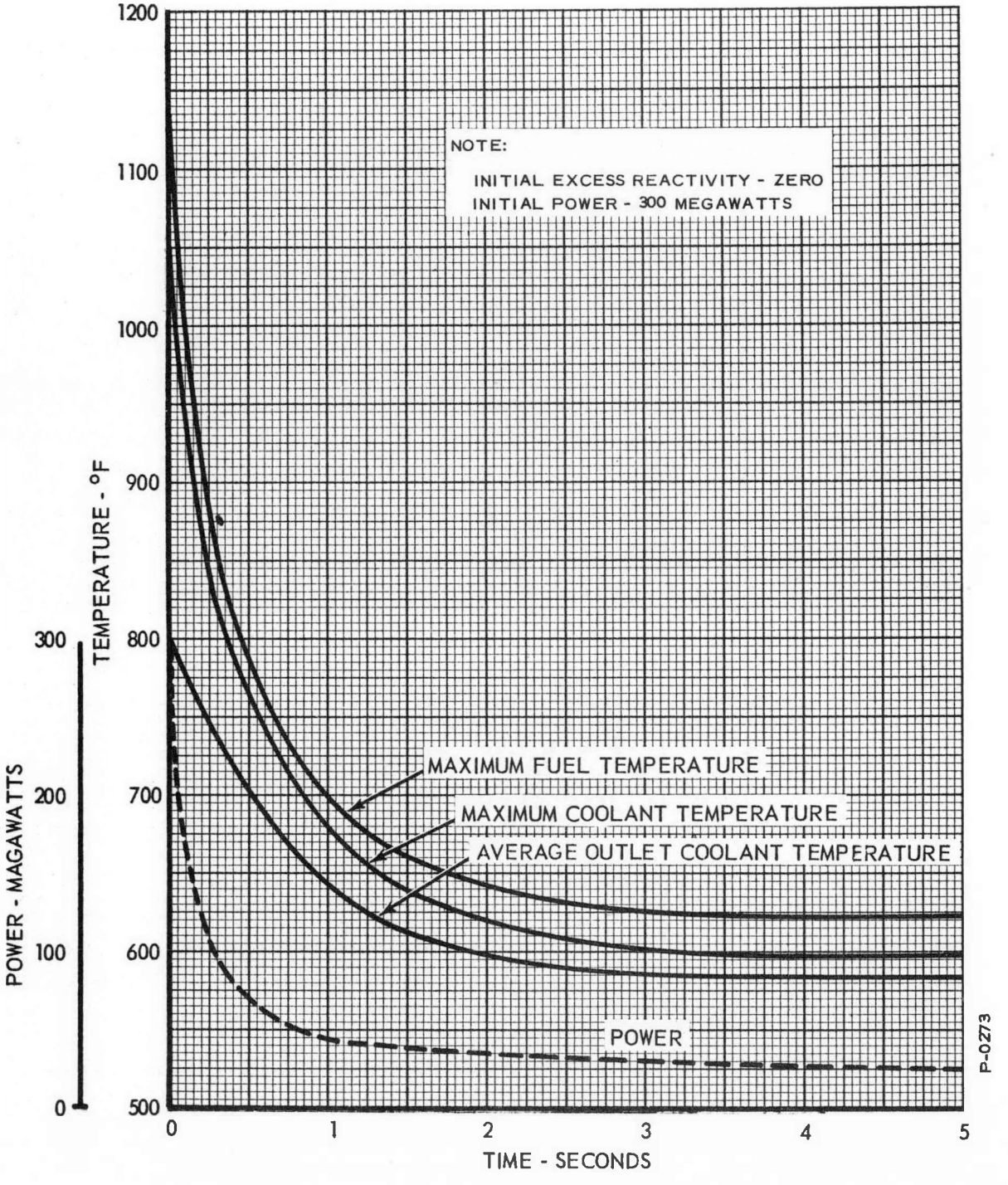

Figure 4.13 - Scram from Full Power: Tripped by Interlock

For convenient comparison, the corresponding results from the previous study are shown in Figure C11, of Appendix C of this report.

SECTION 5

SOME EFFECTS OF REGULATING ROD-DESIGN CHANGE

5.0 GENERAL

After the analysis, discussed in the foregoing pages of this report, was well underway, APDA changed the design of the regulating system. The two regulating rods now introduce reactivity at different rates. The fast rod can introduce reactivity at the maximum rate of one cent per second, while the slow rod can only introduce reactivity at the maximum rate of one cent per minute. This section presents a short discussion of some of the results of this design change. The computer curves presented here were obtained using temperature coefficients of reactivity resulting from the critical experiments. These coefficients are listed in Appendix A.

5.1 EXCURSION FROM FULL POWER

Figure 5.1 shows the behavior of the maximum fuel and coolant temperature during an excursion from 300 megawatts. Both rods were assumed to be inserting positive reactivity at their maximum rates. Initially, the reactor temperature was assumed to have compensated for 23 cents worth of reactivity in the fast rod, and 11.8 cents in the slow rod. Figure 5.2 shows the behavior of the power and average reactor outlet coolant temperature during the same excursion. Figure 5.3 shows the growth-factor and rate signals accompanying the excursion.

It is seen that the rate signal is never large enough to operate the scram trip set at six megawatts per second, so the power trip must be relied upon to scram the reactor. However, the setback will operate. It must be pointed out that the severity of the transient depends strongly on the initial conditions. If more reactivity worth had been available in the fast rod the excursion would have been faster. Of course the converse is true; if the compensated reactivity is mostly taken from the fast rod, the excursion will be very slow.

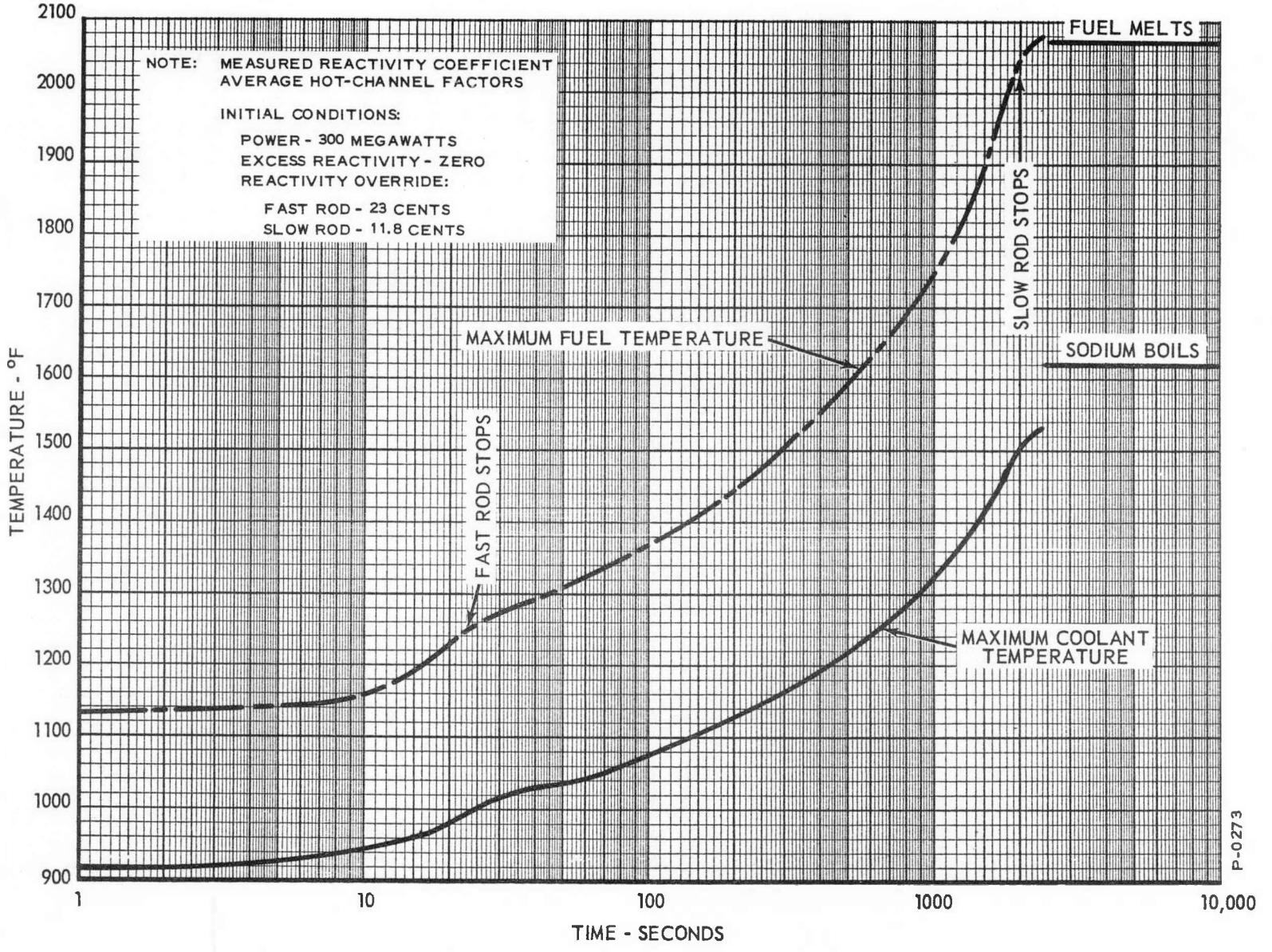

Figure 5.1 - Excursion from Full Power: Fast Rod, One Cent Per Second. Slow Rod, One Cent Per Minute

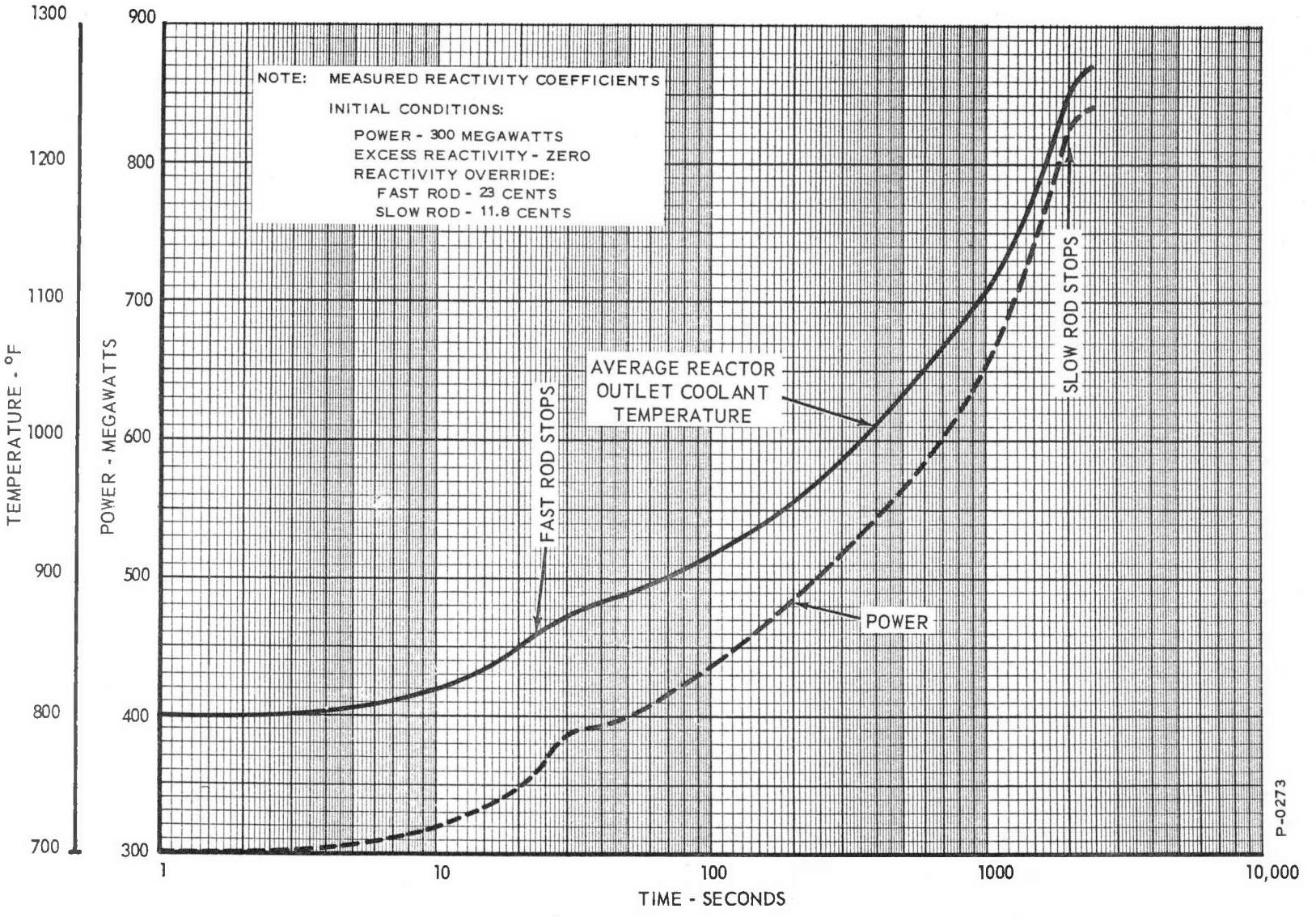

Figure 5.2 - Excursion from Full Power: Fast Rod, One Cent Per Second. Slow Rod, One Cent Per Minute

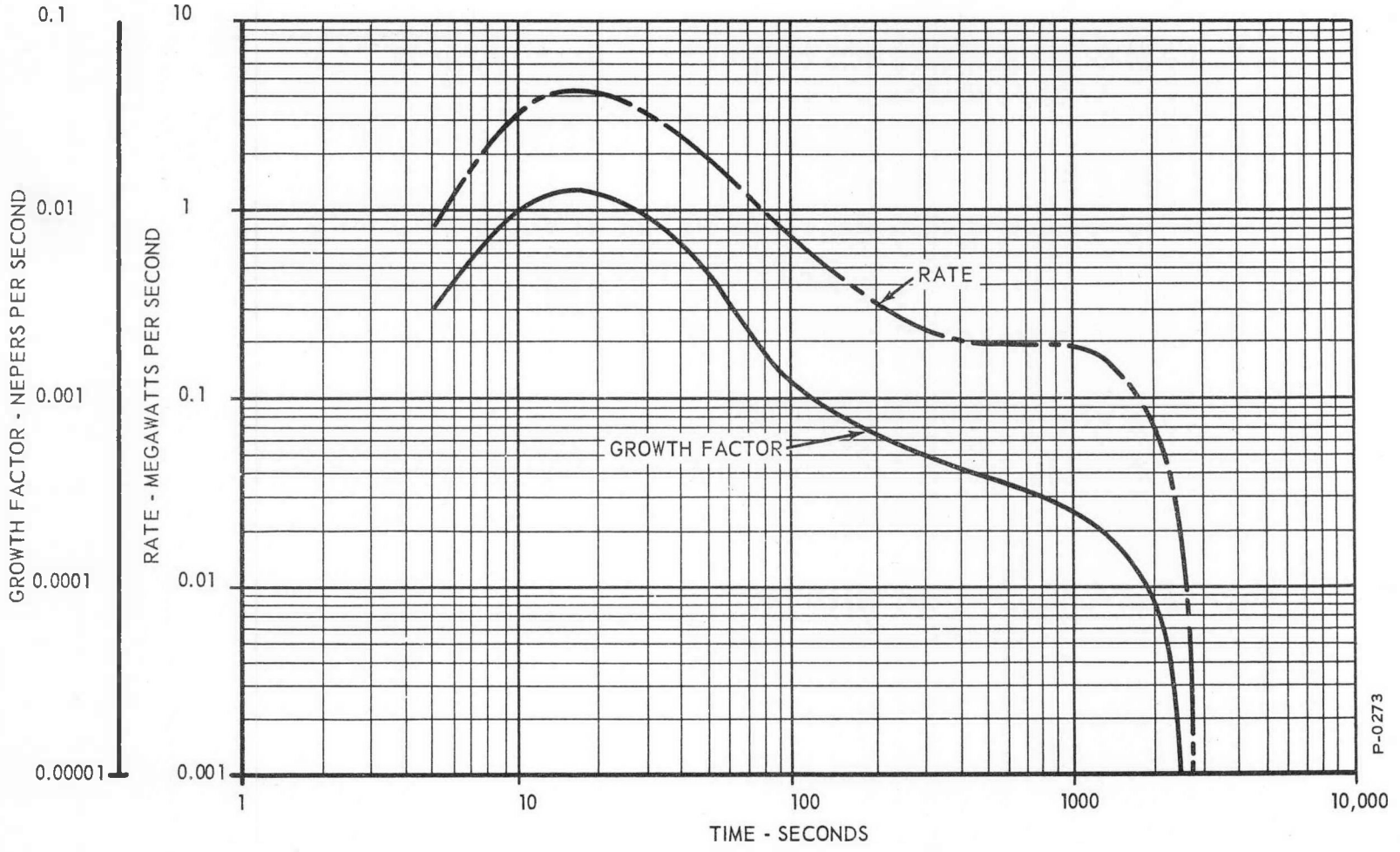

Figure 5.3 - Excursion from Full Power: Fast Rod by One Cent Per Second. Slow Rod, One Cent Per Minute

5.3 START-UP TRANSIENT

Figure 5.4 shows the behavior of the maximum fuel and coolant temperatures during a start-up transient. Here the excursion has been going on for 145 seconds before the three-megawatt power level was reached. The fast rod stopped at 46 seconds, while the slow rod continued to insert reactivity. The excess reactivity, at three megawatts, is 48.42 cents. Figure 5.5 shows the behavior of the power, and the average reactor outlet coolant temperature during the same excursion. Figure 5.6 shows the growth-factor and rate signals accompanying the transient.

It is seen that growth-factor just reaches the scram level at one second. At this time some temperature effects are influencing the signal, so it is expected that it will be larger in the sub-power region; especially when the fast rod is running. The rate signal is never large enough to operate any trips. The power scram, set at 390 megawatts, gives adequate protection.

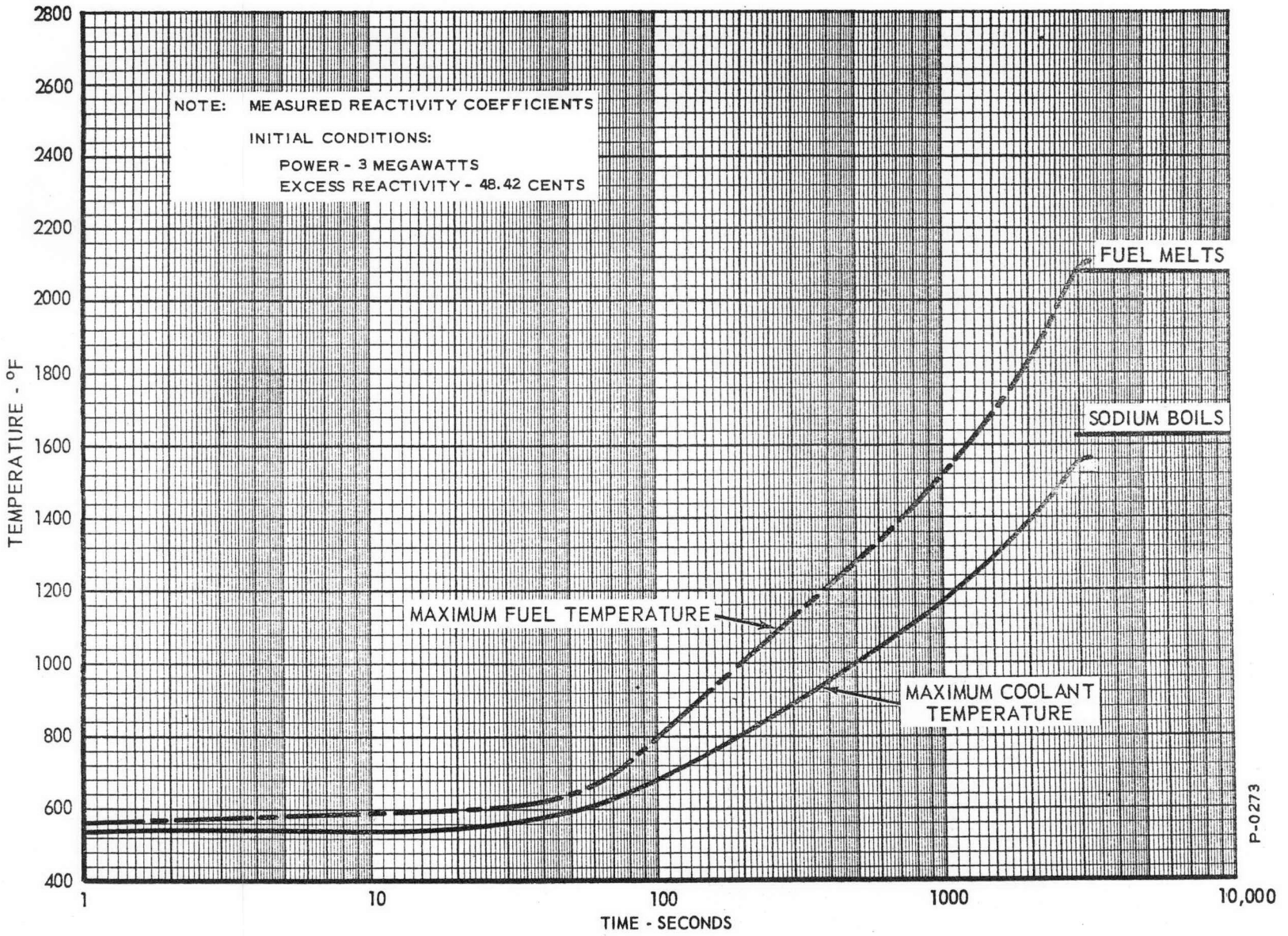

Figure 5.4 - Start-Up Transient. Fast Rod Stopped in Sub-Power Region. Slow Rod, One Cent Per Minute

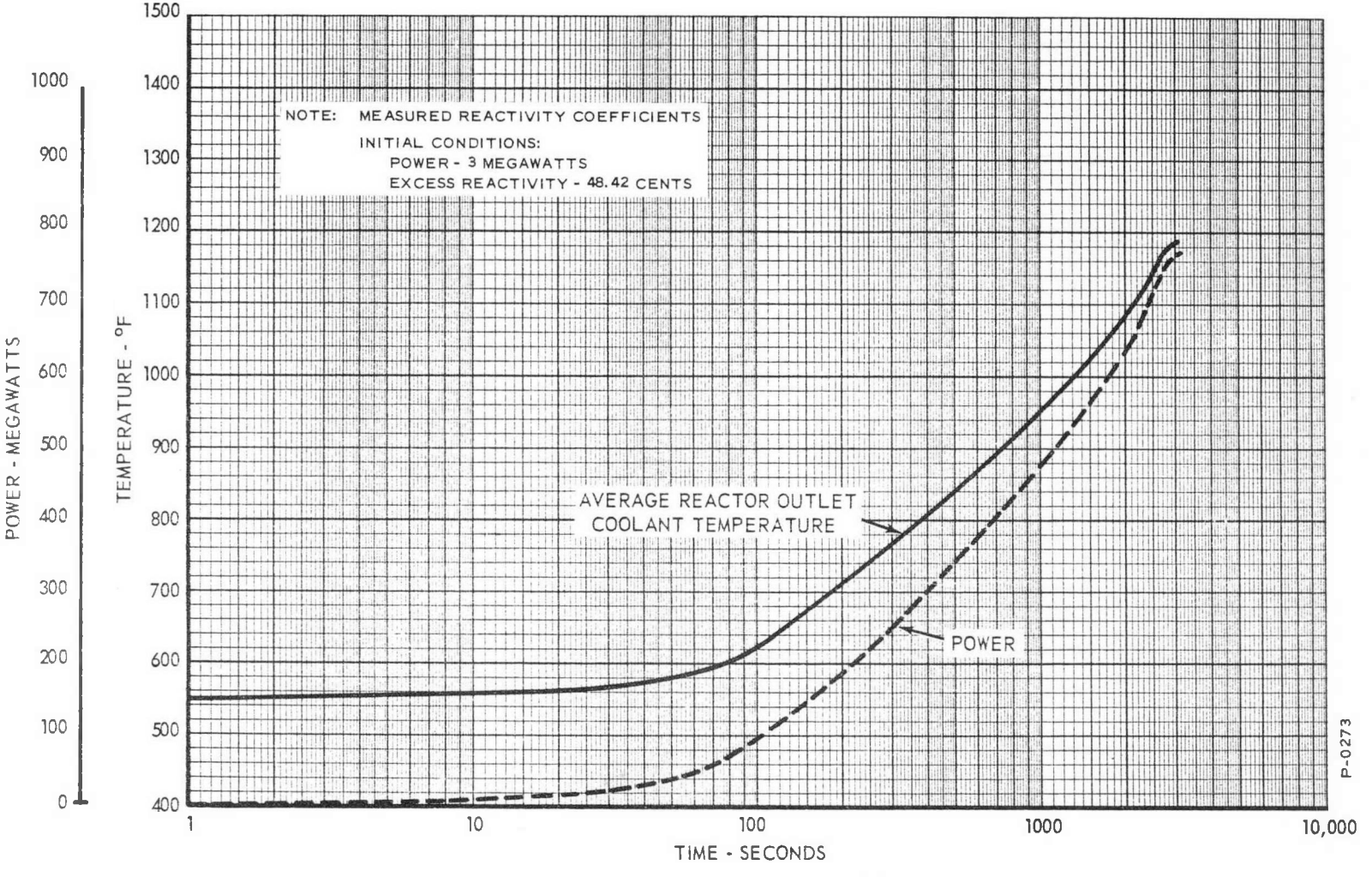

Figure 5.5 - Start-Up Transient Fast Rod Stopped in Sub-Power Region - Slow Rod, One Cent Per Minute

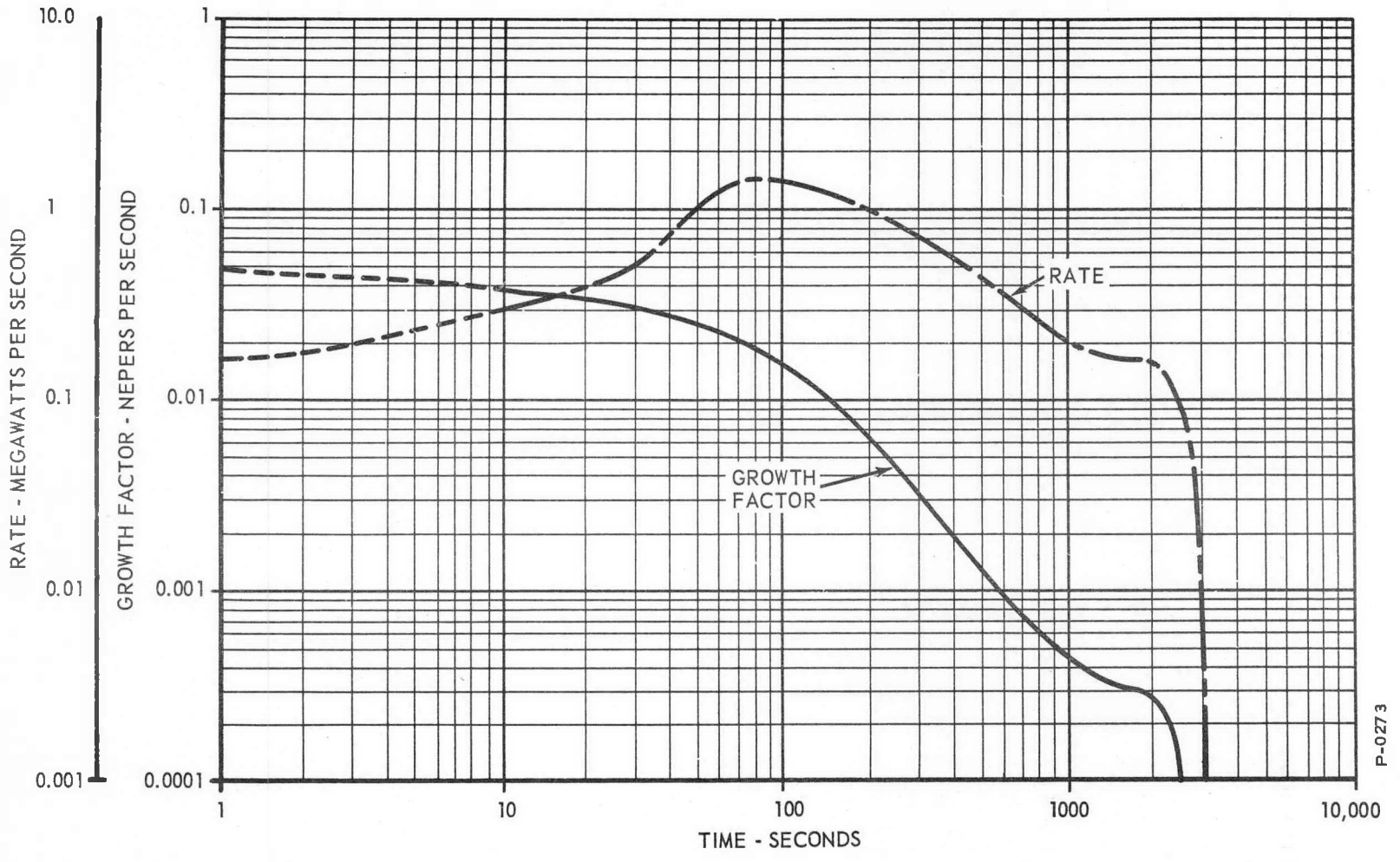

Figure 5.6 - Start-Up Transient. Fast Rod Stopped in Sub-Power Region. Slow Rod, One Cent Per Minute

APPENDIX A

SYMBOLS AND CONSTANTS

A.1 INTRODUCTION

This appendix contains a list of symbols which were used in the analog computer study of the Enrico Fermi Atomic Power Plant. The symbols are defined, together with their units, in Section A.2. The constant parameters and the specific values used for this study are tabulated in Section A.3. The values, for the most part, are based upon data in the APDA Report No. 115 - Enrico Fermi Fast Breeder Reactor Plant, November 1, 1956. Those which were not included, or those that differ from those given in that report, were supplied by the APDA staff.

SECTION A.2

DEFINITIONS OF SYMBOLS AND UNITS

C_{bf}	= The specific heat of the blanket fuel elements.	$\frac{BTU}{lb - {}^{o}F}$
C_c	= The specific heat of the coolant.	$\frac{BTU}{lb - {}^{o}F}$
C_{cf}	= The specific heat of the core fuel.	$\frac{BTU}{lb - {}^{o}F}$
g	= Acceleration due to gravity.	(ft/sec/ sec).
H_b	= The heat transfer coefficient for the blanket assembly.	(BTU/^{o}F - sec)
H_c	= The heat transfer coefficient for the core assembly.	(BTU/^{o}F - sec)
K	= Thermal conductivity of sodium.	(BTU/hr-ft-^{o}F)
ℓ^*	= The mean lifetime of prompt neutrons	(sec)
M_{bc}	= The weight of the blanket coolant contained in the blanket assembly heat transfer space.	(lbs)
M_{bf}	= The weight of the blanket fuel elements	(lbs)
M_{bip}	= The weight of the coolant contained within the blanket inlet plenum.	(lbs)
M_{cc}	= The weight of the core coolant contained in the active region of the core assembly.	(lbs)
M_{cf}	= The weight of the core fuel elements	(lbs)
M_{cip}	= The weight of the coolant contained in the core inlet plenum	(lbs)

M_{pip}	= The weight of coolant contained in a pump inlet plenum.	(lbs)
M_{rop}	= The weight of the coolant contained in the reactor outlet plenum above the hold down plate.	(lbs)
M_{xc}	= The weight of the coolant contained in the active portion of the cold side of the heat exchanger.	(lbs)
M_{xh}	= The weight of coolant contained in the active portion of the hot side of the heat exchanger	(lbs)
P	= The total power produced in the reactor (proportional to the neutron flux density)	(Mw)
P_o	= Initial power level	(Mw)
P_f	= Power produced in the reactor due to fission product decay heat.	(Mw)
q	= The total power produced in the reactor	(Mw)
q_b	= The power produced in the blanket assembly.	(Mw)
q_c	= The power produced in the core assembly	(Mw)
t	= Time	(sec)
$\bar{T}_{bc}$	= The average temperature of the blanket coolant.	(^oF)
T_{bci}	= The temperature of the coolant entering the inlet to the blanket	(^oF)
T_{bco}	= The temperature of the coolant leaving the outlet of the blanket section.	(^oF)

$\overline{T}_{bf}$ = The average temperature of the blanket fuel elements (^{o}F)

$\overline{T}_{bip}$ = The average temperature of the coolant in the blanket inlet plenum. (^{o}F)

t_{bipi} = The transport time of coolant thru the feed pipe to the blanket inlet plenum inlet. (sec)

$\overline{T}_{cc}$ = The average temperature of the core coolant. (^{o}F)

T_{cci} = The temperature of the coolant entering the inlet to the core. (^{o}F)

T_{cco} = The temperature of the coolant leaving the outlet of the core. (^{o}F)

$\overline{T}_{cf}$ = The average temperature of the core fuel elements. (^{o}F)

$\overline{T}_{cip}$ = The average temperature of the coolant in the core inlet plenum. (^{o}F)

T_{cm} = The maximum temperature of the coolant in the hottest channel at the outer surface of the fuel cladding (^{o}F)

$\overline{T}_{\ell p}$ = The average temperature of the lower plate of the reactor assembly. (^{o}F)

T_{m} = The maximum temperature of the hottest part of the hottest fuel element in the reactor. (^{o}F)

T_{pip} = The temperature of the coolant in the pump inlet plenum. (^{o}F)

t_{pori} = Transport delay time between the pump outlet and the inlet to the reactor (sec)

T_{ri} = The temperature of the coolant at the Y joint which delivers coolant to both the reactor core and blanket inlet plenums from the pump. (^{o}F)

t_{rici} = The transport time of the coolant from the reactor inlet to the core inlet. (sec)

T_{ro} = The outlet temperature of the coolant leaving reactor assembly. (^{o}F)

$\overline{T}_{rop}$ = The average temperature of the coolant contained in the reactor outlet plenum. (^{o}F)

t_{rxi} = The transport time of coolant from the reactor to the heat exchanger inlet. (sec)

W = The rate of weight flow of coolant thru the reactor as a whole. (lb/sec)

W_b = The rate of weight flow of coolant thru the blanket. (lb/sec)

$(W_b)_o$ = The nominal rate of weight flow of coolant thru the blanket assembly. (lb/sec)

W_c = The rate of weight flow of coolant thru the core. (lb/sec)

$(W_c)_o$ = The nominal rate of weight flow of coolant thru the core assembly. (lb/sec)

W_o = Nominal rate of weight flow of coolant thru the reactor as a whole. (lb/sec)

Z_r = The displacement of the regulating rod. (in.)

Z_{rc} = The commanded displacement of the regulating rod. (in.)

Z_s = The displacement of the safety rods. (in.)

α = The fraction of the total beat that is produced in the core.

β = The fraction of neutrons that are delayed.

β_l = The fraction of neutrons that are delayed which are associated with ith group of delayed neutron precursors.

γ = The fraction of the total heat that is produced in the blanket.

δ_c = The weight density of the coolant. (lb/ft^3)

δ_k = The effective change in the neutron multiplication factor

δ_r = The total effective change in reactivity. (dollars)

Δr_r = The reactivity increment due to a change in position of the regulating rod. (dollars)

Δr_s = The reactivity increment due to a change in position of the safety rods. (dollars)

Δr_t = The total thermal reactivity increment due to a change in the temperature balance in the reactor. (dollars)

λ_i = The inverse of the mean lifetime of the ith delayed neutron precursor. (sec^{-1})

ρ_{bc} = The change in the effective neutron multiplication factor due to a change in the average temperature of the blanket coolant. ($\delta k/k\ ^oF$)

ρ_{bf} = The change in effective neutron multiplication factor due to a change in the average temperature of blanket fuel. ($\delta k/k\,^{o}F$)

$\rho_{\ell p}$ = The effective change in the neutron multiplication factor due to thermal expansion of the lower plate of the reactor. ($\delta k/k\,^{o}F$)

ρ_{cc} = The change in the effective neutron multiplication factor due to a change in the average temperature of the core coolant. ($\delta k/k\,^{o}F$)

ρ_{cf} = The change in the effective neutron multiplication factor due to a change in the average temperature of the core fuel. ($\delta k/k\,^{o}F$)

ρ_{E} = The effective change in the neutron multiplication factor due to thermal expansion of the core center line. $\delta k/k\,^{o}F$

ρ_{up} = The effective change in the neutron multiplication factor due to thermal expansion of the upper plate of the reactor. ($\delta k/k\,^{o}F$)

τ = The period of the reactor. (sec/neper)

$\tau_{\ell p}$ = Thermal time constant of the average temperature of the lower structural plate. (sec.)

τ_{up} = Thermal time constant of the average temperature of the upper structural plate. (sec.)

SECTION A 3

CONSTANT PARAMETERS

A.3.1 NEUTRON KINETICS PARAMETERS

β_1	= 0.00023	λ_1	= 0.0127 sec^{-1}
β_2	= 0.00134	λ_2	= 0.0318 sec^{-1}
β_3	= 0.00125	λ_3	= 0.1155 sec^{-1}
β_4	= 0.00275	λ_4	= 0.3150 sec^{-1}
β_5	= 0.00104	λ_5	= 1.386 sec^{-1}
β_6	= 0.00026	λ_6	= 3.850 sec^{-1}

$$\beta = 0.00687 = \sum_{i=1}^{6} \beta_1$$

$$\ell^* = 1.8 \times 10^{-7} \text{ sec.}$$

A.3.2 CORE PARAMETERS

α	= 0.91667
q_c	= 260712 BTU/sec.
H_c	= 1834.56 BTU/sec-^oF
C_c	= 0.308 BTU/lb^oF
$(W_c)_o$	= 3386.1 lb/sec.
$M_{cf}C_{cf}$	= 187.642 BTU/^oF
$M_{cc}C_c$	= 84.357 BTU/^oF

A.3.3 BLANKET PARAMETERS

γ	0.08333
q_b	23701 BTU/sec.
H_b	819.91 BTU/sec-^oF

157 121

$(W_b)_o$ 307.78 lb/sec.

$M_{bf}C_{bf}$ 552.37 BTU/°F

$M_{bc}C_c$ 125.58 BTU/°F

A.3.4 CALCULATED REACTIVITY COEFFICIENTS

ρ_{cf} $-1.72 \times 10^{-6} \frac{\Delta k}{k} / {}^{o}F$

ρ_{bf} $-0.444 \times 10^{-6} \frac{\Delta k}{k} / {}^{o}F$

ρ_{cc} $-3.94 \times 10^{-6} \frac{\Delta k}{k} / {}^{o}F$

ρ_{bc} $-1.83 \times 10^{-6} \frac{\Delta k}{k} / {}^{o}F$

ρ_{E} $-0.5 \times 10^{-6} \frac{\Delta k}{k} / {}^{o}F$

A.3.5 MEASURED REACTIVITY COEFFICIENTS

ρ_{cf} $-4.16 \times 10^{-6} \frac{\Delta k}{k} / {}^{o}F$

ρ_{bf} $-0.44 \times 10^{-6} \frac{\Delta k}{k} / {}^{o}F$

ρ_{bc} $-1.55 \times 10^{-6} \frac{\Delta k}{k} / {}^{o}F$

ρ_{cc} $-2.61 \times 10^{-6} \frac{\Delta k}{k} / {}^{o}F$

ρ_{E} $-5.55 \times 10^{-6} \frac{\Delta k}{k} / {}^{o}F$

A.3.6 STEADY STATE TEMPERATURES AT 300 MEGAWATTS

$T_{ro} = T_{cco} = T_{bco} = 800^{o}F$

$T_{cci} = T_{bci} = 550^{o}F$

$\overline{T}_{bc} = \overline{T}_{cc} = 675^{o}F$

$\overline{T}_{bf} = 703.9^{o}F$

$\overline{T}_{cf} = 817.1^{o}F$

A.3.7 MISCELLANEOUS

$(W)_o$ 3693.9 lb/sec.

$M_{rop}(W)_o$ 16.6 sec

1 BTU/sec. 1054.8 watts

$\frac{\partial T_{cm}}{\partial \bar{T}_{cc}} = 2.88$

$L\left(\frac{\partial T_{cm}(L)}{\partial L}\right)$ 0.26389

$K\left(\frac{\partial T_m}{\partial q}\right)_L$ 2.2449

g 32.2 ft/sec/sec

M_{bip} 1593.5 lb

M_{cip} 8701.1 lb

M_{pip} 7002.8 lb

M_{rop} 75894 lb

M_{xc} 4613.2 lb

M_{xh} 6629.7 lb

$(W_{xh})_o$ 1231.2 lb/sec

t_{bipi} 2.64 sec

t_{pori} 4.73 sec

t_{rxi} 14.45 sec

157 123

Physical Properties of Sodium

T	δ_c	C_c	K
207°F	57.87 lb/ft^3	0.33 BTU/lb°F	49.6 BTU/hr ft°F
400°F	56.37 lb/ft^3	0.32 BTU/lb°F	46.6 BTU/hr ft°F
600°F	54.73 lb/ft^3	0.3106 BTU/lb°F	43.5 BTU/hr ft°F
675°F	54.12 lb/ft^3	0.308 BTU/lb°F	42.35 BTU/hr ft°F
800°F	53.11 lb/ft^3	0.304 BTU/lb°F	40.4 BTU/hr ft°F

APPENDIX B

EQUATIONS AND COMPUTER CIRCUITS

B.1 INTRODUCTION

The equations and computer circuits used for this study are, for the most part, the same as those used in the previous study. The reader is referred to Appendix B of Bendix Report 1052. The equations and computer circuits that were used in both reports are listed in Section B.2, below. In the succeeding sections, of this Appendix, the equations and circuits particular to this study are discussed in detail.

B.2 EQUATIONS AND CIRCUITS USED IN BOTH STUDIES

The details of the separate computations used in both this study and the previous one are to be found in the references listed below. All references are to sections in Appendix B of Bendix Report 1052, - Analysis of the Power-Limiting System for the Enrico Fermi Atomic Power Plant.

1. Neutron kinetics, Section 1.
2. Core and blanket temperatures, Section 2.
3. Upper plenum temperature, Section 3.
4. Growth factor, Section 8.
5. Fission product power, Section 13.

B.3 NEW EQUATIONS AND COMPUTER CIRCUITS

Some of the equations and circuits used in this study differ from those used previously. These will be discussed in detail below.

B.3.1 Hot Channel Temperatures

The equations used to calculate the temperatures expected in the hottest channel are

$$T_{cm} = T_{cci} + \frac{D}{2C} (T_{cco} - T_{cci}),$$

and

$$T_m = T_{cm} = \left(\frac{W}{W_o}\right) \frac{E}{D} (T_{cm} - T_{cci}) + \frac{B}{A} (\bar{T}_{cf} - \bar{T}_{cc}),$$

where

$$\frac{D}{2C} = 1.44, \quad \frac{E}{D} = 0.264, \text{ and } \frac{B}{A} = 2.245.$$

The quantities A, B, C, D, and E were derived from the expected distribution of temperatures in the hottest channel. The curves from which the above quantities were derived are given in the report, APDA-124, Enrico Fermi Atomic Power Plant, January 1959.. The curves shown in Figure B.1 are copied from a figure given in that report, on page 44, and show the expected temperature distributions along the axis of the hottest channel. The coolant temperature curves were approximated by straight lines for purposes of estimating the quantities A, B, C, D, and E. These quantities are also shown in the figure. The assumptions made in the formulation of the above equations are: the total change of the coolant temperature in the hottest channel is proportional to the total change of the temperature in an average channel, the fuel temperature rise above the adjacent coolant in the hottest channel is proportional to the average fuel temperature rise above the adjacent coolant in and average channel, and the location of the maximum fuel temperature moves to the outlet end of the fuel pin as the coolant flow becomes zero. The analog computer circuit that was used to represent the equations is shown in Figure B.2.

B.3.2 Thermal Reactivity

The equation used to calculate the thermal reactivity is,

$$\Delta r_t = \frac{1}{\beta} (\rho_{cf} \Delta\bar{T}_{cf} + \rho_{cc} \Delta\bar{T}_{cc} + \rho_{bf} \Delta\bar{T}_{bf} + \rho_{bc} \Delta\bar{T}_{bc} + \rho_E \Delta T_E),$$

where,

$$\Delta\dot{T}_E = \Delta\bar{T}_{cc} - \Delta T_E.$$

ΔT_E is a ficticious temperature which causes the expansion of the core radius at its mid-section. ρ_E is the corresponding temperature coefficient of reactivity. The computer circuit used to represent the above equation is shown in Figure B.3. The regulating-rod reactivity

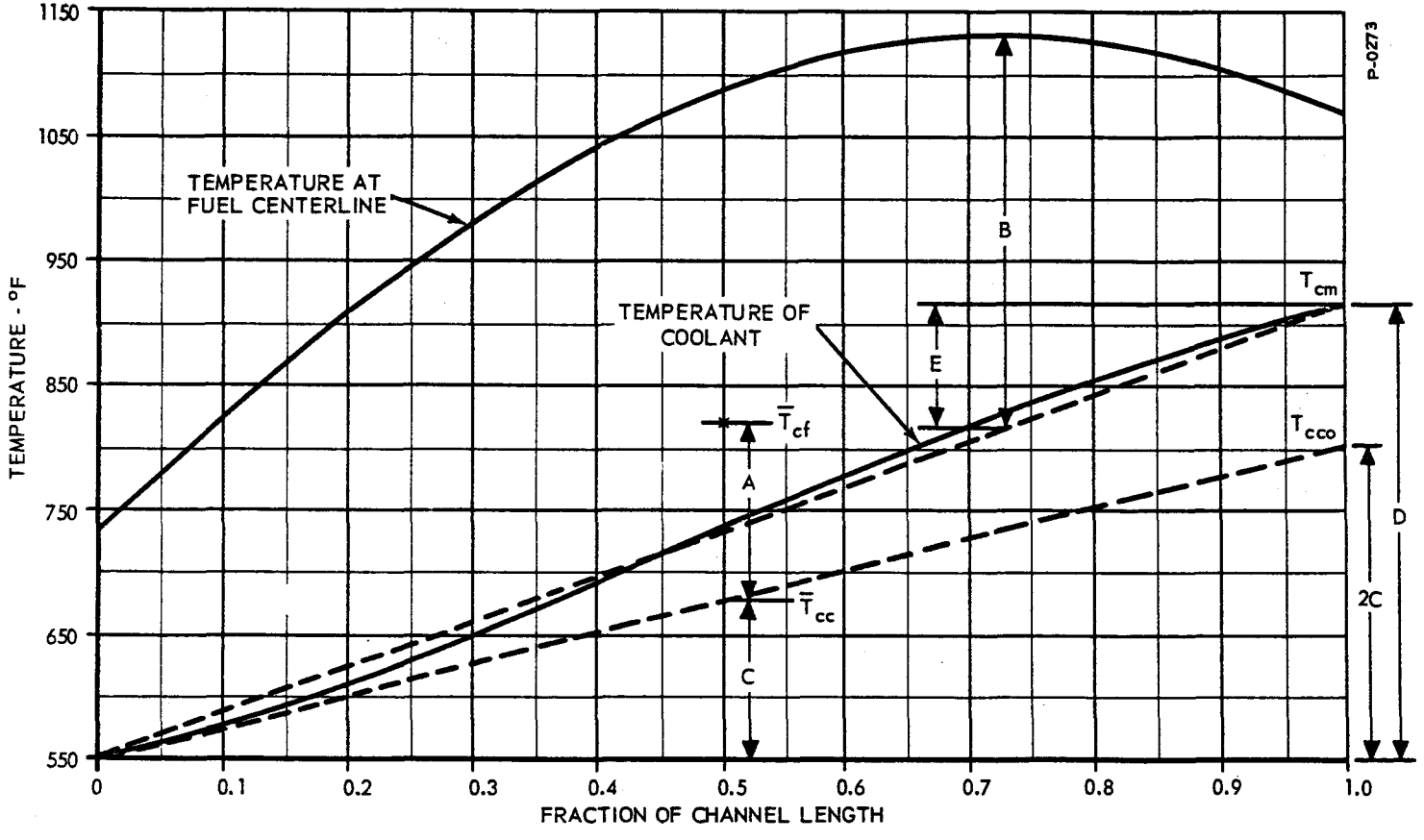

* TAKEN FROM: APDA-124, ENRICO FERMI ATOMIC POWER PLANT, JAN. 1959, P. 44

Figure B.1 - Temperatures in the Hottest Core Channel

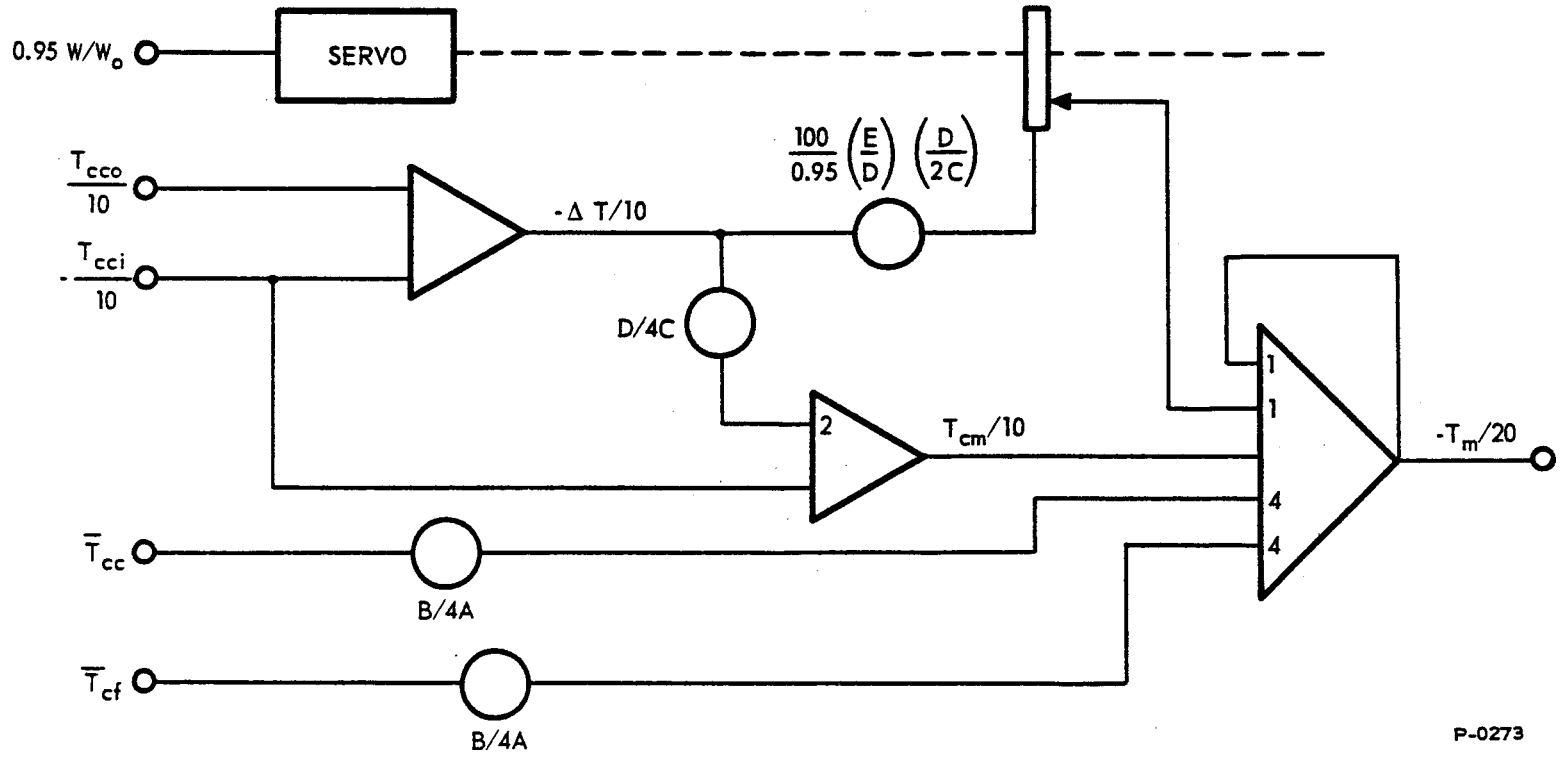

Figure B.2 - The Circuit for Simulating the Hot Channel Temperature

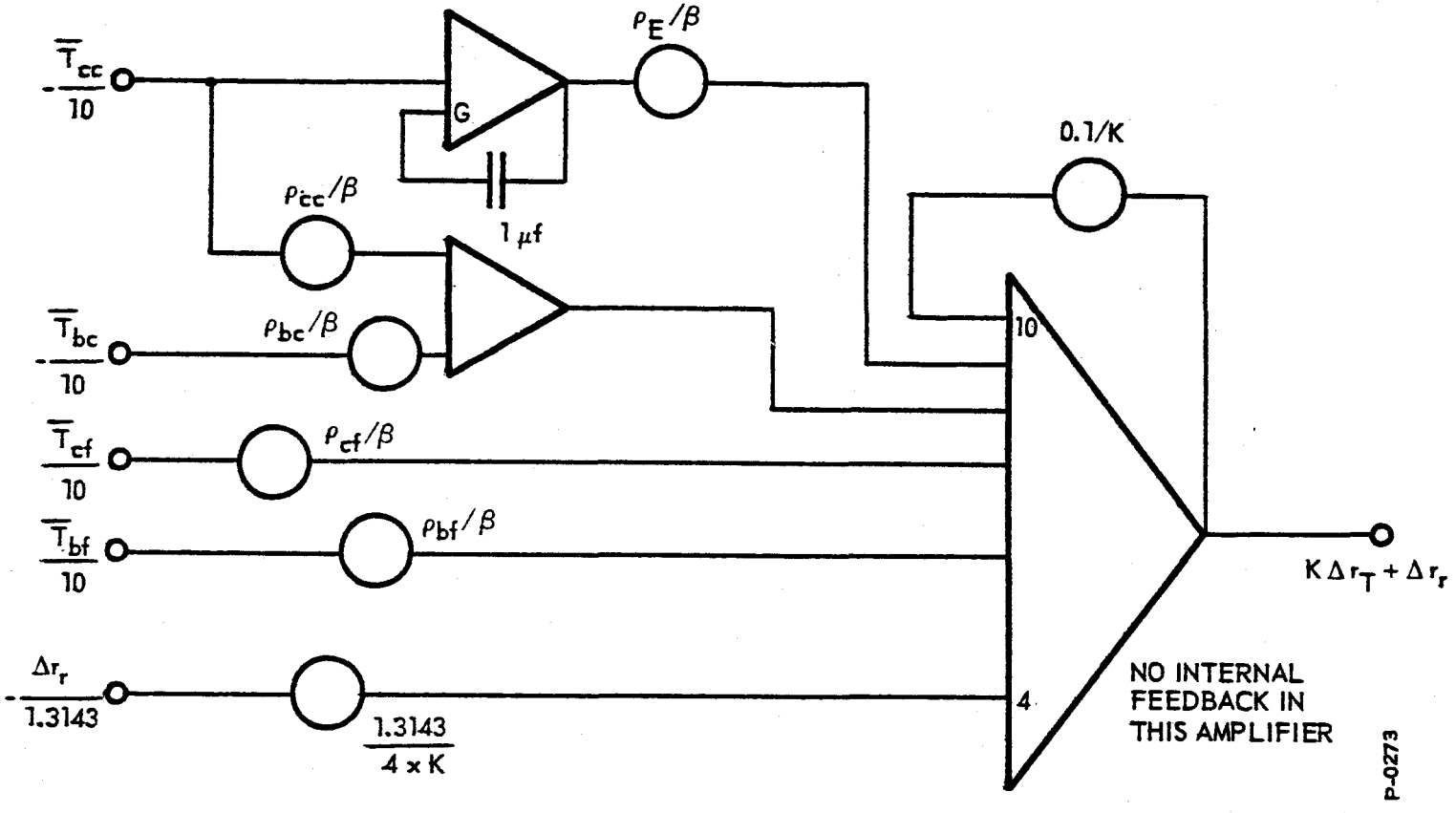

Figure B.3 - The Circuit Diagram of the Thermal Reactivity Simulator

is included as part of the output of the circuit. The three values of the temperature coefficient of reactivity were obtained by choosing K to be: 0.5, 1.0, and 1.5.

B.3.3 Control Rod Worth

The equations describing the reactivity worth of the safety and regulating rods are:

$$\Delta r_r = F(Z_r),$$

$$Z_r = \int_0^t \dot{Z}_r \, dt,$$

where

$$\dot{Z}_r = -0.15 \text{ in/sec}, \; t > t_s, \text{ or manual control},$$

$$= +0.15 \text{ in/sec on manual control},$$

$$= 0 \text{ otherwise},$$

and

$$\Delta r_s = \frac{8}{0.3}(t_s - t) + \frac{8}{0.3}(t_s - t - 0.3).$$

The circuit used to represent these equations is shown in Figure B.4.

The relay which operates from the 26-volt computer-control voltage provides a memory, so that the circuit will remain in a tripped condition once it is tripped. The time required for the safety rods to traverse the upper axial blanket is not simulated because its effect is not important in the situations studies.

B.3.4 Delays in Inlet Pipes and Plenums

The configuration of time delays in the core and blanket inlet plenums and inlet pipes are assumed to be those of an average primary loop. The values used are shown in Table B.1.

Table B.1

TIME DELAYS

Location	Inlet Plenum Mixing	Inlet Piping
core	2.57 sec	3.59 sec
blanket	7.59 sec	6.33 sec

The circuit used to simulate these delays is shown in Figure B.5. The circuit includes two first-order Pade' approximate for the time delays, and two first-order time lags for the mixing delays. The Pade' approximates have a bandwidth limitation determined by the frequency at which the phase shift is 55 degrees. In the case of non-periodic inputs, the bandwidth is defined by the frequency of the fundamental Fourier component of the input function.

B.3.5 Inlet Coolant Temperature Equations

The inlet coolant temperature changes resulting from a secondary coolant flow failure and from feedwater-flow changes were supplied by APDA in graphical form. These graphs were obtained during simulator studies of the secondary coolant loops, and steam portions of the plant, by the Holley Carburetor Company.

The equations representing the temperature at a time t after the flow change are:

1. Feedwater-flow increase to 150 percent,

$$T_{ri} = \int_0^t \left[0.86\,(\lambda - 18) - 0.86\,(\lambda - 49)\right] \left[\exp - \frac{(t-\lambda)}{19.8}\right] d\lambda.$$

2. Feedwater-flow decrease to 10 percent,

$$T_{ri} = \int_0^t \left\{\left[7.63\,(\lambda - 24) - 7.63\,(\lambda - 47.6) + 0.49\,(\lambda - 47.6)\right] x \exp\left[0.09184\,(t - \lambda)\right]\right\} d\lambda.$$

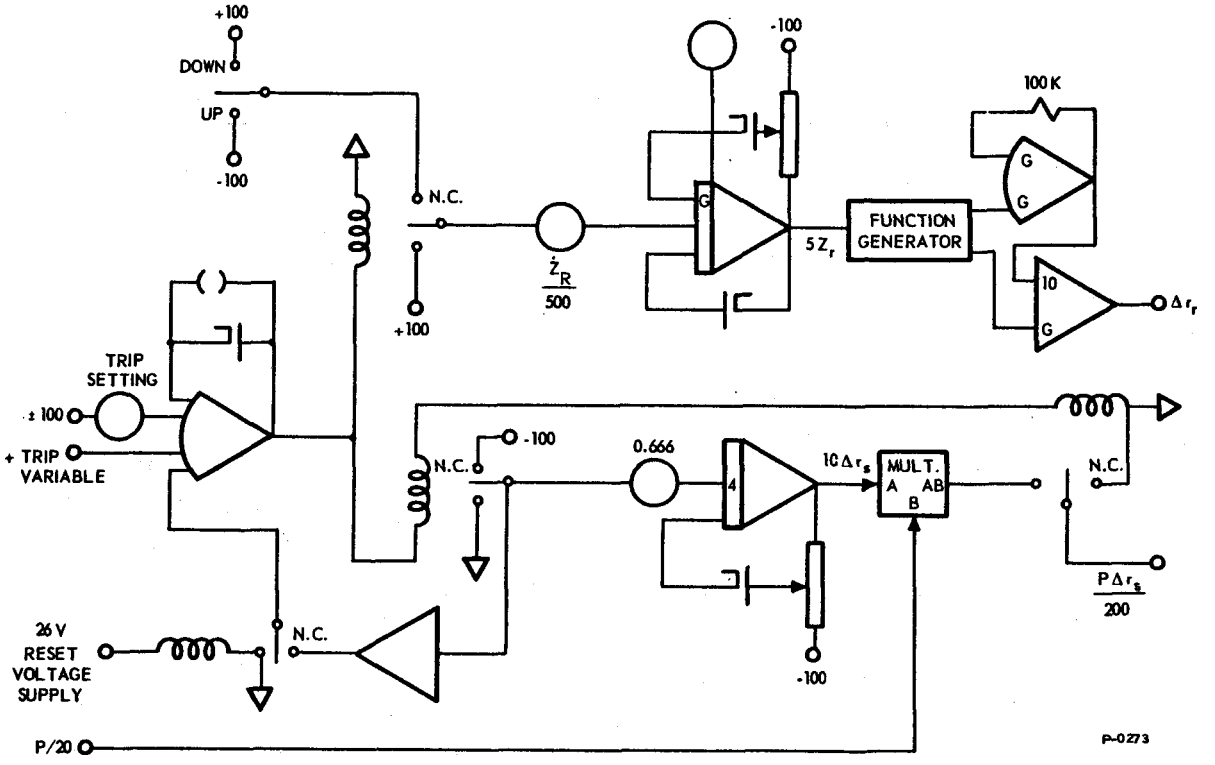

Figure B.4 - The Circuit Diagram of the Regulating Rod Simulator

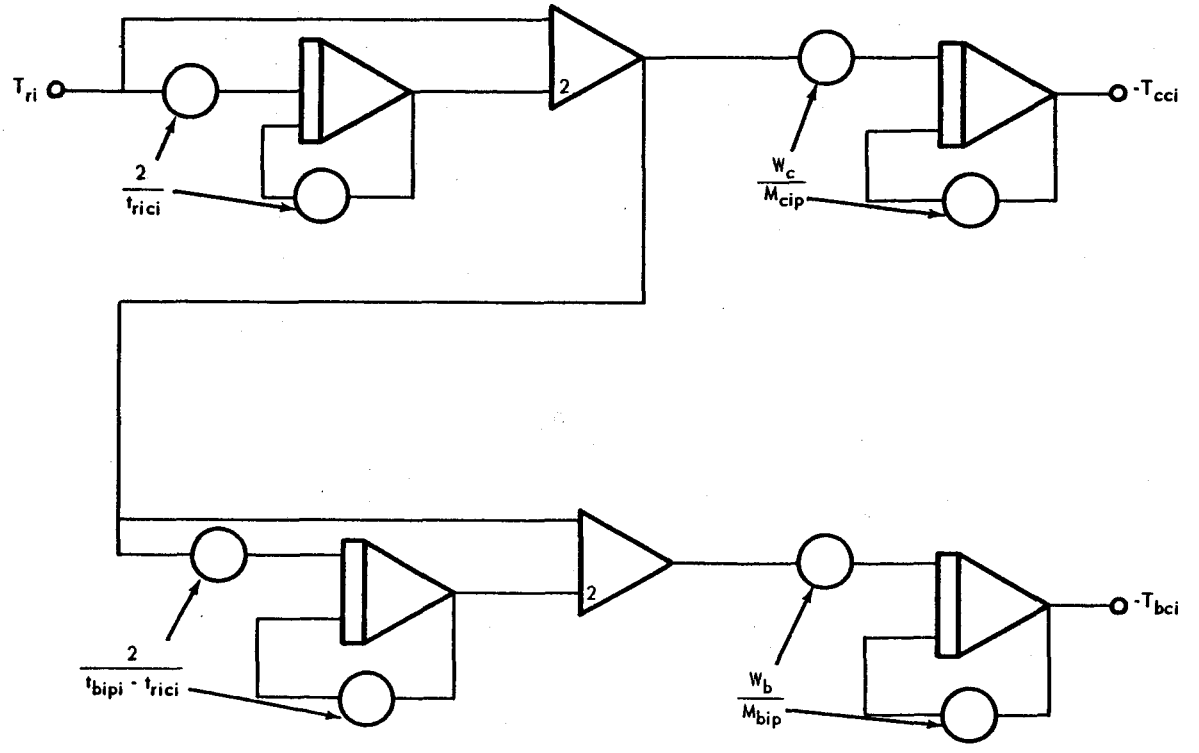

Figure B.5 - Delay Simulator

157 132

3. Secondary-flow decrease to 15 percent,

$$T_{ri} = \int_0^t \left\{ \left[13.1\lambda - 13.1\,(\lambda - 17) + 0.94\,(\lambda - 17) - 0.94\,(\lambda - 58) \right.\right.$$

$$\left. + 3.74\,(\lambda - 58) - 3.74\,(\lambda - 75) + 0.87\,(\lambda - 75) \right]$$

$$\left. \exp\left[\frac{-(t - \lambda)}{9.4755} \right] \right\} d\lambda.$$

The above equations are of the form

$$T_{ri} = \int_0^t F(\lambda)\ G\ (t - \lambda)\ d\lambda,$$

which is the response of a network whose impulse response is G(t) when forced by an input function F(t). Figure B.6 shows how T_{ri} is approximated, by a series of straight lines. The straight lines represent the function F(t). G(t) is chosen to be,

$$G(t) = e^{-\frac{t}{\tau}}.$$

The slopes and break points of F(t) and the time constant of G(t) were determined empirically so as to adequately fit the desired curve. All of the constants thus determined are included in the above equations.

The computer circuit used to represent these equations is shown in Figure B.7. The switches were manually operated in the proper sequence with the help of a stop watch.

B.4 STATISTICAL HOT CHANNEL FACTORS

The maximum fuel and coolant temperatures that have been calculated during this study were based on the curves given in APDA-124, Enrico Fermi Atomic Power Plant, January 1959, p. 44. Since the computer runs were finished, the authors have been made aware of a different method of calculating a temperature in a fuel pin, account must be taken of: the coolant temperature rise above the inlet temperature, the temperature difference across the coolant film boundary layer, the temperature difference across the oxide layer, the temperature difference across the clad, and the temperature

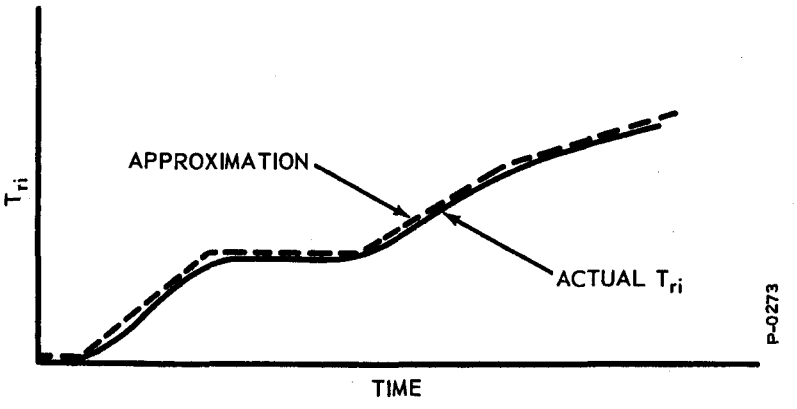

Figure B.6 - Approximation of T_{ri}

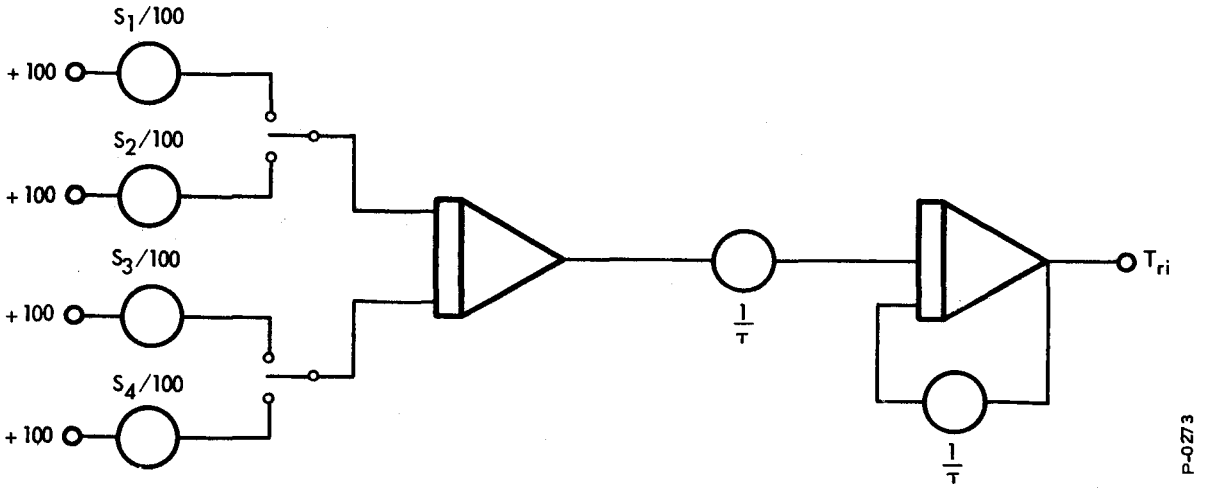

Figure B.7 - Reactor Inlet Coolant Temperature Simulator

difference from the fuel centerline to the clad. It is possible to choose mean values for all these quantities and calculate the temperature at a point on the fuel pin centerline. In this way the average hot-channel factors are calculated. However, the above quantities are subject to uncertainties, which in turn affect the end result. To take these uncertainties into account, one can use a statistical approach to calculate a value which corresponds to a three standard deviation upper limit for the temperature at the fuel pin centerline. When this method is used, a range of values for each of the temperature differences is assigned. In assigning the range of values one assumes that they are distributed about a most probable value in a normal manner. The application of this method to the calculation of the maximum fuel temperature implies a confidence limit of 99.87 percent. Under these circumstances there is a probability of only 1.3 in 1000 that the temperature of any fuel pin will exceed this specified maximum temperature. This calculation is shown in APDA-124, Enrico Fermi Atomic Power Plant, January, 1959, p. 48.

The maximum fuel temperature curves presented in this report are based on calculations done where the variation in temperature rises were not taken into account. Under steady-state conditions, this fuel temperature is given by,

$$T_m = T_{cci} + \frac{584}{300} P, \qquad \text{(B.4.1)}$$

where T_{cci} is the core inlet coolant temperature and P is the power in megawatts. It is seen that, when T_{cci} is 550°F and P is 300 megawatts, T_m is 1134°F; the value assigned a 50 percent confidence in APDA-124. Now, if the statistical approach is used, APDA-124 (p. 49) gives the value 1235°F for T_m (3σ), with a 99.9 percent confidence of not being exceeded. Therefore, we can write

$$T_m (3\sigma) = T_{cci} + \frac{685P}{300}, \qquad \text{(B.4.2)}$$

which reduces to 1235°F for T_{cci} equal to 550°F and P equal to 300 megawatts. Equations B.4.1 and B.4.2 can be combined to yield.

$$T_m (3\sigma) = T_{cci} + 1.173 (T_m - T_{cci}). \qquad \text{(B.4.3)}$$

This last equation can be used to estimate T_m (3σ) from the curves for T_m given in this report.

Under steady-state conditions we can write,

$$T_{cm} = T_{cci} + \frac{365}{300} P \qquad \text{(B.4.4)}$$

for the maximum coolant temperature. Equation B.4.4 yields a value of 915°F for T_{cm} when T_{cci} is 550°F and P is 300 megawatts. APDA-124 (p. 53) gives a value of 985°F to T_{cm} (3σ) with 99.9 percent confidence of not being exceeded. Therefore we can write,

$$T_{cm}(3\sigma) = T_{cci} + \frac{435}{300} P \qquad \text{(B.4.5)}$$

which yields 985°F for T_{cm} (3σ) under full-power conditions. Equations B.4.4 and B.4.5 can be combined to give,

$$T_{cm}(3\sigma) = T_{cci} + 1.192\,(T_{cm} - T_{cci}) \qquad \text{(B.4.6)}$$

This last equation can be used to estimate T_{cm} (3σ) from the curves for T_{cm} given in this report.

Equations B.4.1 thru B.4.6 are strictly valid only for small variations of coolant inlet temperature and reactor power from 550°F and 300 megawatts respectively, but they can be used to make estimates.

APPENDIX C

REFERENCE DATA FROM BENDIX REPORT 1052

C.0 GENERAL

In some cases it may be desirable to compare the results of the calculations given in this report with those whose results were shown in Bendix Report 1052. It may happen that the reader is not familiar with the results presented in that report, nor have ready access to it. Therefore, in this Appendix, some of the curves originally given in Bendix Report 1052 are reproduced for the convenience of the reader, in comparing the effect of the change the temperature coefficient of reactivity, shut-down temperature, and in the coolant flow dynamics. So that a good comparison can be made, the Table of Constant Parameters given in the last report is also reproduced here.

C.1 TABLE OF CONSTANT PARAMETERS FROM BENDIX REPORT 1052

α	0.9067	λ_5	1.51 sec^{-1}
γ	0.0933	λ_6	5.78 sec^{-1}
β_1	0.00023	ρ_{cf}	$-1.72 \times 10^{-6} \frac{\delta k}{k} / ^oF$
β_2	0.00142	ρ_{cc}	$-3.94 \times 10^{-6} \frac{\delta k}{k} / ^oF$
β_3	0.00140	ρ_{bf}	$-0.444 \times 10^{-6} \frac{\delta k}{k} / ^oF$
β_4	0.00303	ρ_{bc}	$-1.83 \times 10^{-6} \frac{\delta k}{k} / ^oF$
β_5	0.00117	ρ_{up}	$-1.77 \times 10^{-6} \frac{\delta k}{k} / ^oF$
β_6	0.00016	$\rho_{\ell p}$	$-1.77 \times 10^{-6} \frac{\delta k}{k} / ^oF$
β	0.00741	C_c	0.308 BTU/lb-^oF
λ_1	0.0128 sec^{-1}	g	32.2 ft/sec/sec
λ_2	0.0322 sec^{-1}	H_c	1665 BTU/sec-^oF
λ_3	0.119 sec^{-1}	H_b	237.5 BTU/sec-^oF
λ_4	0.322 sec^{-1}	t_{pori}	4.73 sec
ℓ^*	1.8×10^{-7} sec	$\tau_{\ell p}$	1 sec

157 137

M_{bip}	1593.5 lb	τ_{up}	60 sec
M_{cip}	8701.1 lb	H_x	2056.6 BTU/sec-^oF
M_{pip}	7002.8 lb		
M_{rop}	75894 lb		
M_{xc}	4613.2 lb		
M_{xh}	6629.7 lb		
$M_{bc}C_c$	97.4 BTU/^oF		
$M_{bf}C_{bf}$	341.2 BTU/^oF		
$M_{cc}C_c$	85.2 BTU/^oF		
$M_{cf}C_{cf}$	177 BTU/^oF		
$(W)_o$	3693.7 lb/sec		
$(W_b)_o$	344.7 lb/sec		
$(W_c)_o$	3349 lb/sec		
$(W_{xc})_o$	1224.1 lb/sec		
$(W_{xh})_o$	1231.2 lb/sec		
T_{bipi}	2.64 sec		

C.2 TRANSIENTS DURING FULL-POWER OPERATION

In this section we present curves, copied from the previous report, for the transients dueing full-power operation that were studied there.

C.2.1 Positive Reactivity Insertion

Figure C1 is a copy of the curves for the transient, from full power, caused by introducing reactivity at the rate of one cent per second.

C.2.2 Complete Primary Flow Failure

Figure C2 is a copy of the curves presented in the previous report for the effect of a complete primary flow failure. In that computation the flow was assumed to decay in such a manner that

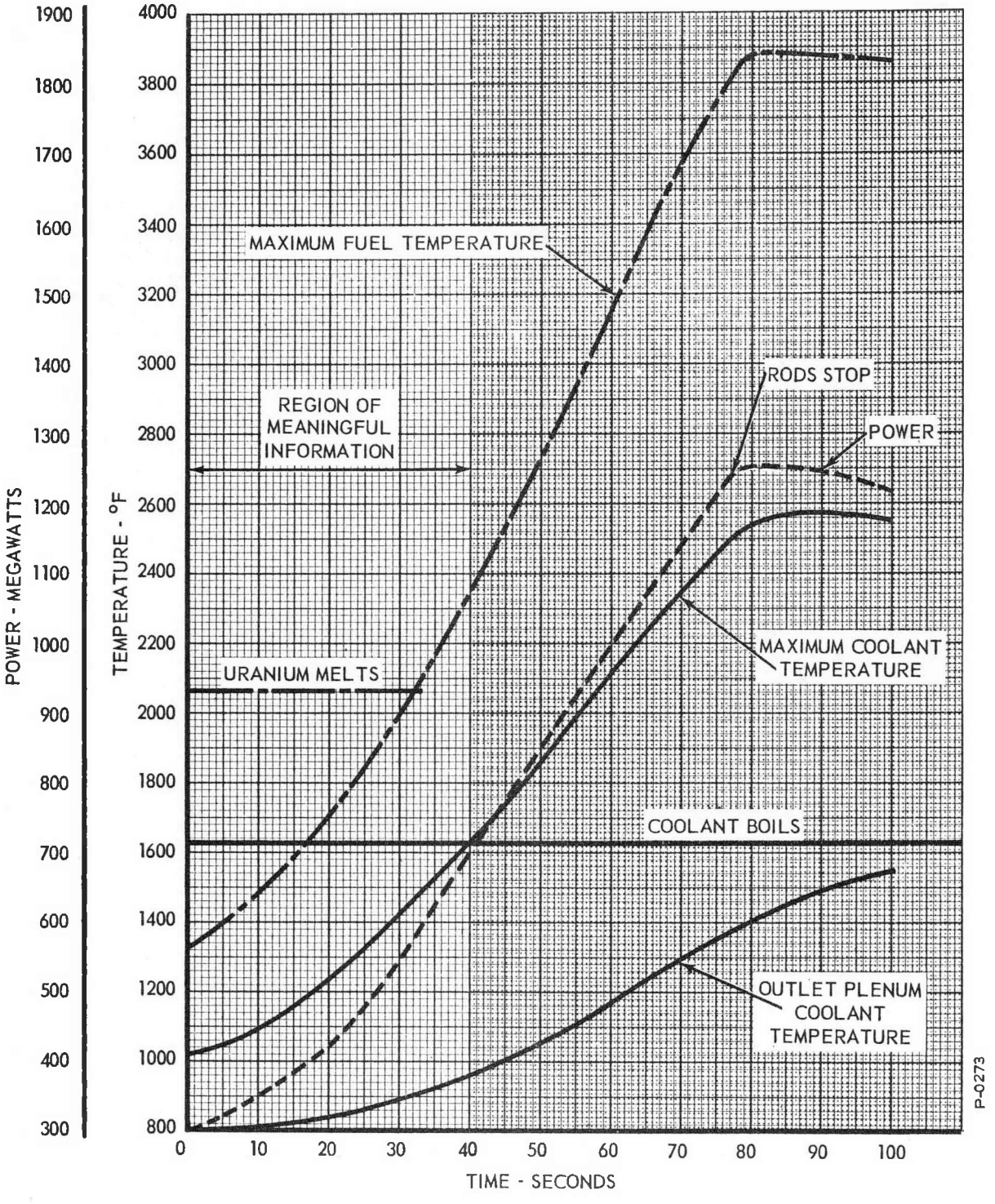

Figure C.1 - Excursion from Full Power: Power and Reactor Temperature

157 139

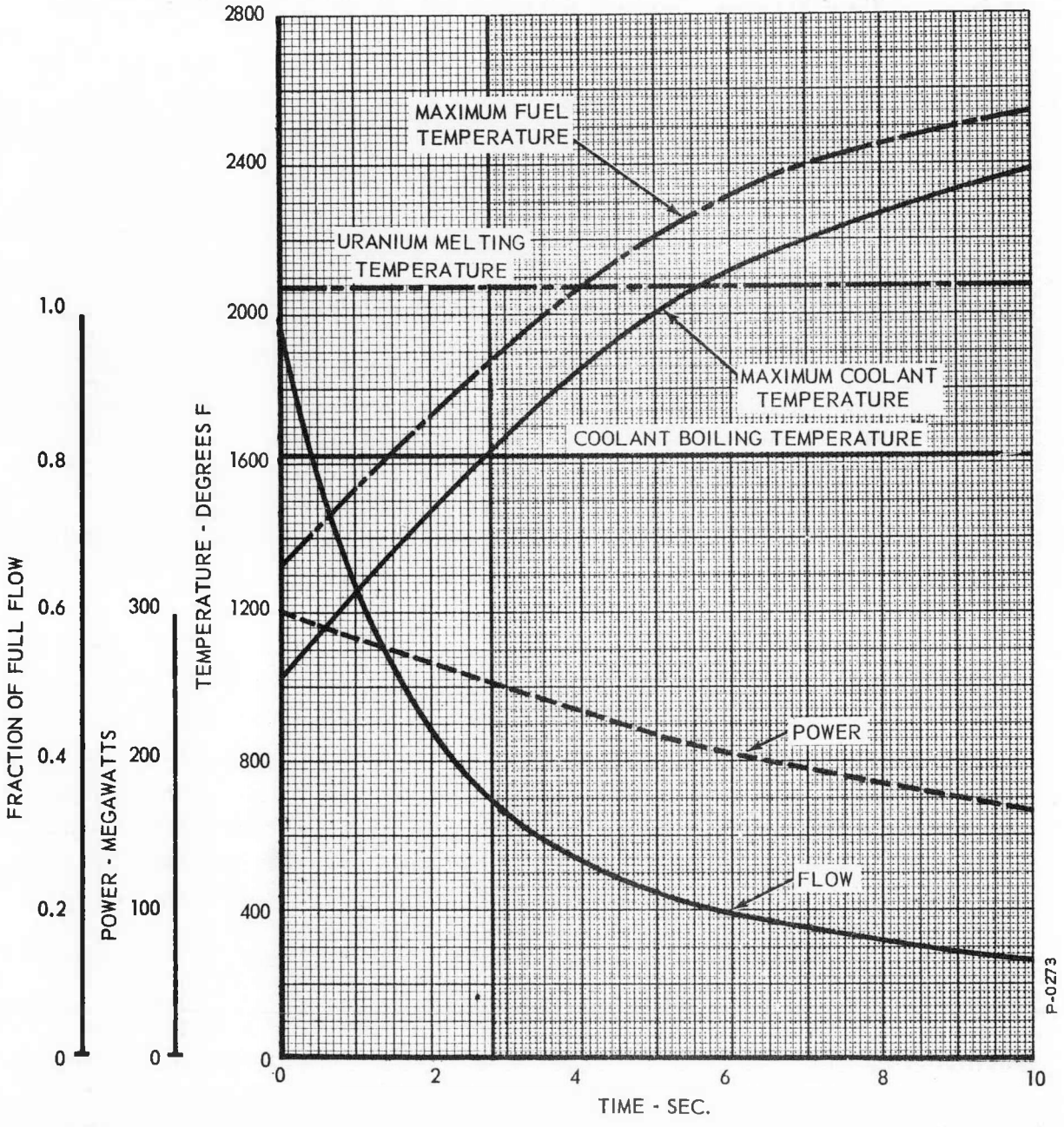

Figure C.2 - Complete Primary Flow Failure: Power, Flow, and Reactor Temperature

the flow at any time, W(t) was given by

$$\frac{W(t)}{W_o} = 0.7 \exp\left[\frac{-t}{1.5}\right] + 0.26 \exp\left[\frac{-t}{10}\right] + 0.04,$$ where W_o is the flow at normal operating conditions, and t is the time in seconds. The above equation differs from the one used in the present study. The fission product power was assumed to be given by the same equation as that used in this study. (See Section 2.1.2).

C.2.3 Reactor Coolant Inlet Temperature Changes

C.2.3.1 Loss of One Primary Coolant Pump

Figure C.3 is a copy of the curves from the previous report for the transient caused by the failure of one primary coolant pump. In that calculation, the flow through the operative loops was assumed to increase by 40 percent when the one pump failed. The temperature of the outlet of the primary of the intermediate heat exchanger, when the secondary flow was held constant, was assumed to be given by

$$T_{po} = T_{pi} + \frac{(T_{si} - T_{pi}) \left\{1 - \exp\left[-\frac{H}{C}\frac{(W_s - W_p)}{W_s \quad W_p}\right]\right\}}{1 - \frac{W_p}{W_s}\exp\left[-\frac{H}{C}\frac{(W_s - W_p)}{W_s \quad W_p}\right]}$$

Here T_{pi} is the primary inlet temperature, T_{si} is the secondary inlet temperature, W_p and W_s are the weight flow rates of the primary and secondary coolants respectively, H is the heat transfer coefficient, and C is the specific heat of the two coolants when they are the same fluid. This expression is derived in Appendix C of the previous report. Using this expression, and an estimate of the time constant of the heat exchanger, it is found that the temperature of the fluid leaving the primary of the heat exchanger increases a total of 54°F with a five-second time constant. The reactor inlet coolant temperature was programmed accordingly, and the data shown in Figure C3 resulted. It is seen that there is about a five-second delay after the pump fails before the inlet coolant temperature begins to change because of the transport lag in the pipes.

157 141

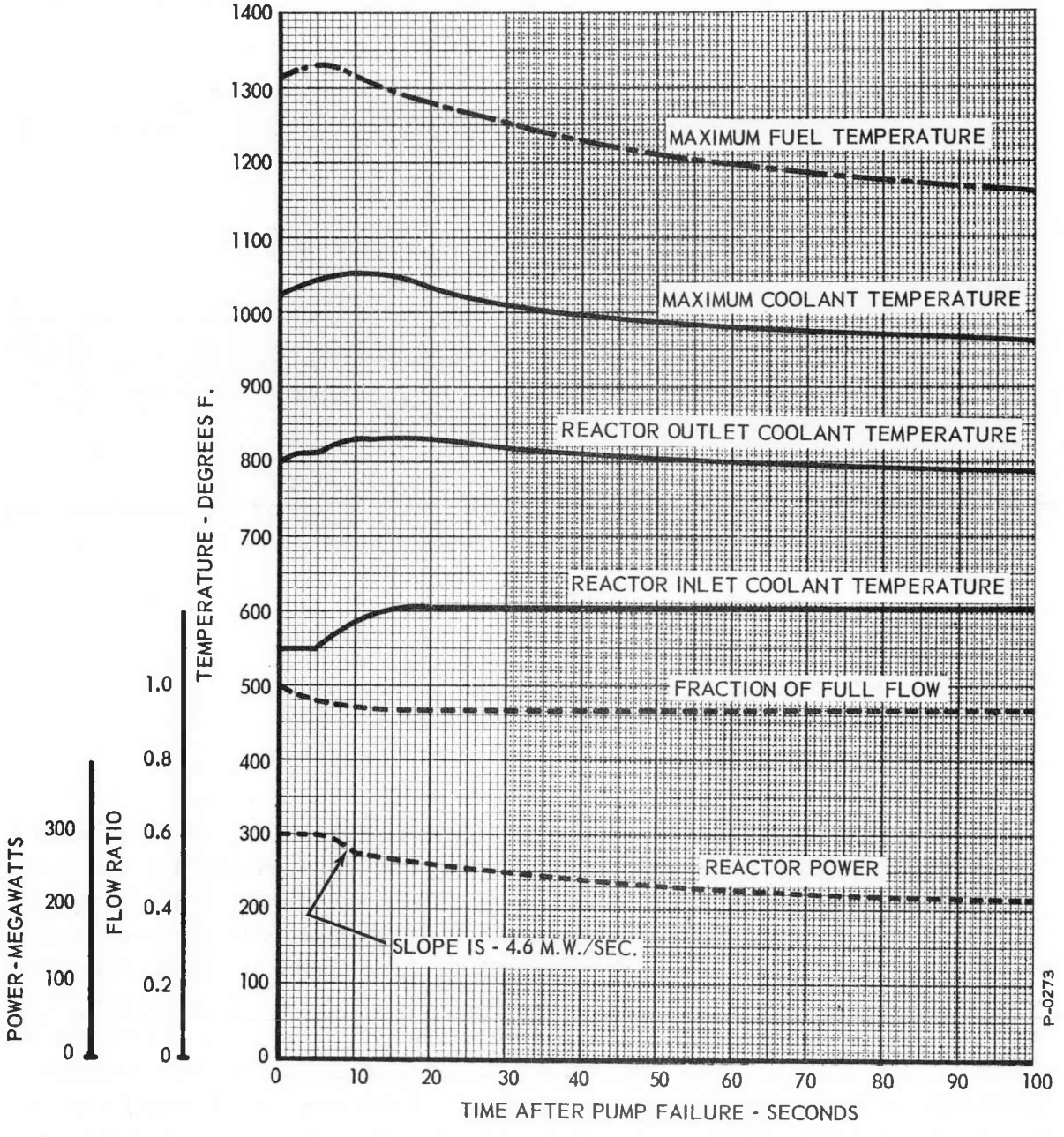

Figure C.3 - Failure of One Primary Pump: Power and Reactor Temperature

C.2.3.2 Loss of All Secondary Pumps

Figure C.4 is a copy of the curves from the previous study for the transient caused by the failure of all secondary coolant pumps. The curves are not good for times longer than 30 seconds, as the effect of the recirculation of the coolant has not been included. The reactor inlet coolant temperature is assumed to rise toward that of the reactor outlet coolant with an appropriate time constant.

C.2.3.3 Loss of One Secondary Pump

Figure C.5 is a copy of the figure in the previous report presenting the curves for the transient caused by the failure of one secondary pump. A reactor inlet coolant temperature increase of $83^{o}F$ on a time constant determined by the mixing that takes place between the heat exchanger and the core was assumed.

C.2.3.4 Changes in Feedwater Flow

In the previous report only the case where one feedwater pump was considered. This loss was assumed to affect only one loop, and the computer run shown in Figure C5, with a longer time constant was assumed to apply.

C.3 START-UP TRANSIENT

In this section we present data, copied from the previous report, for the start-up transient investigated there. Although a start-up transient, with four percent flow, was investigated previously, no corresponding study was made in this report so we only present the data for the start-up transient with full coolant flow. The conditions under which the run was made are the same as those described in Section 2.2.1 of this report, and so will not be repeated here. It is to be noted that a change in shut-down temperature has been made since Bendix Report 1052 was written. In that report, a value of 600 degrees F was used, while now a value of 550 degrees F is used. Figure C6 is a copy of the curves from the previous study for the start-up transient.

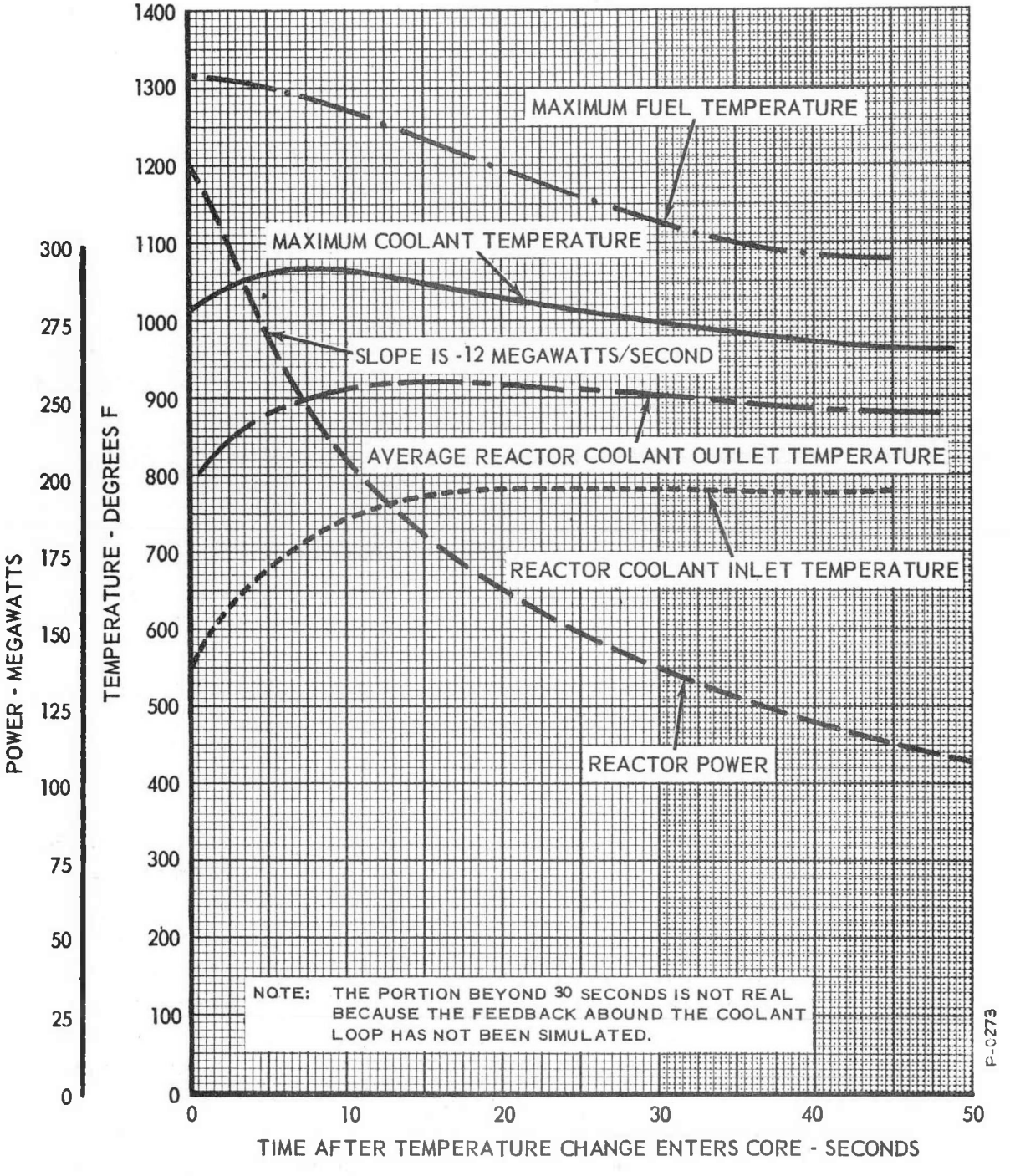

Figure C.4 - Complete Secondary Flow Failure: Power and Reactor Temperatures

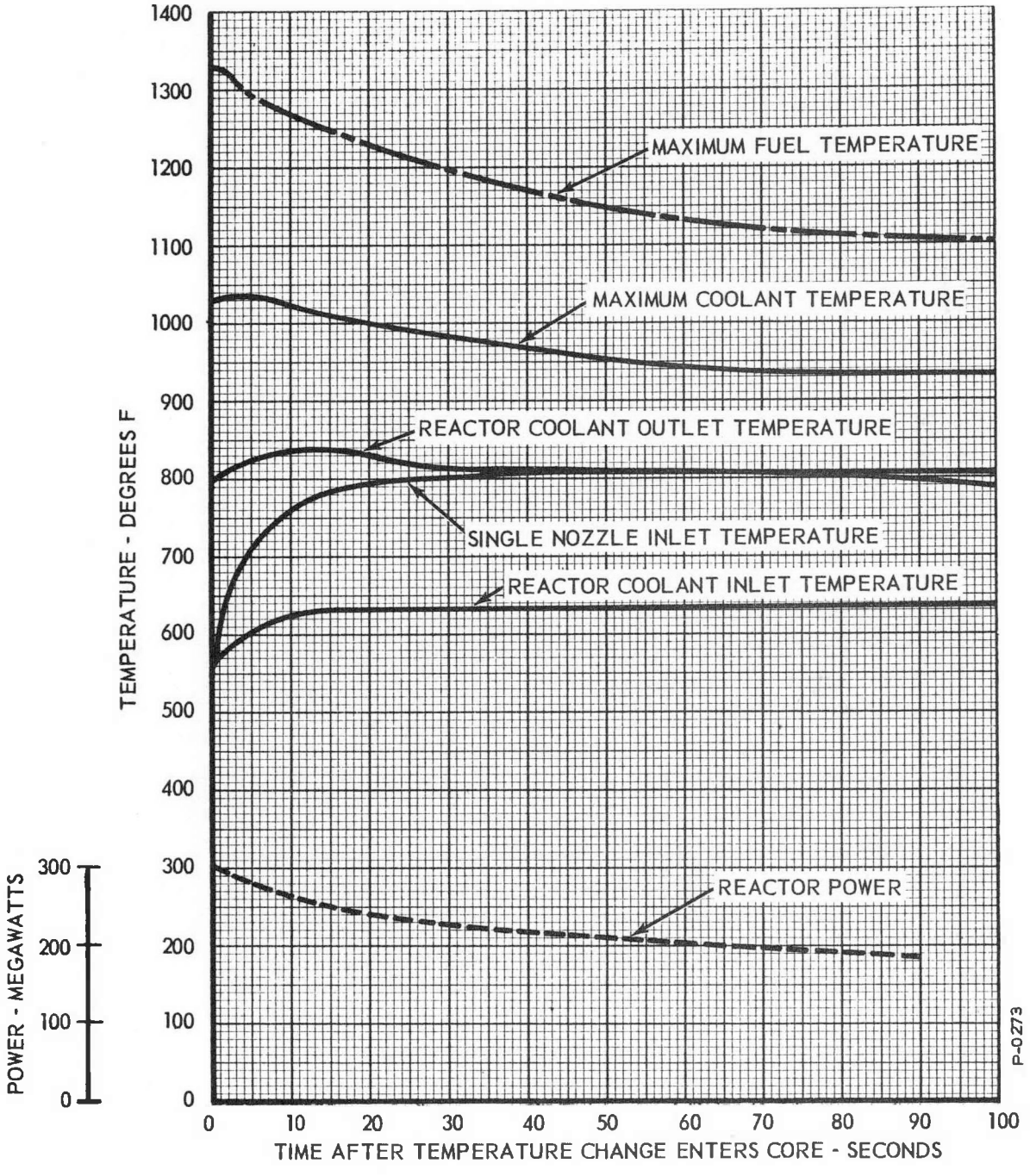

Figure C.5 - Failure of One Secondary Pump: Power and Reactor Temperatures

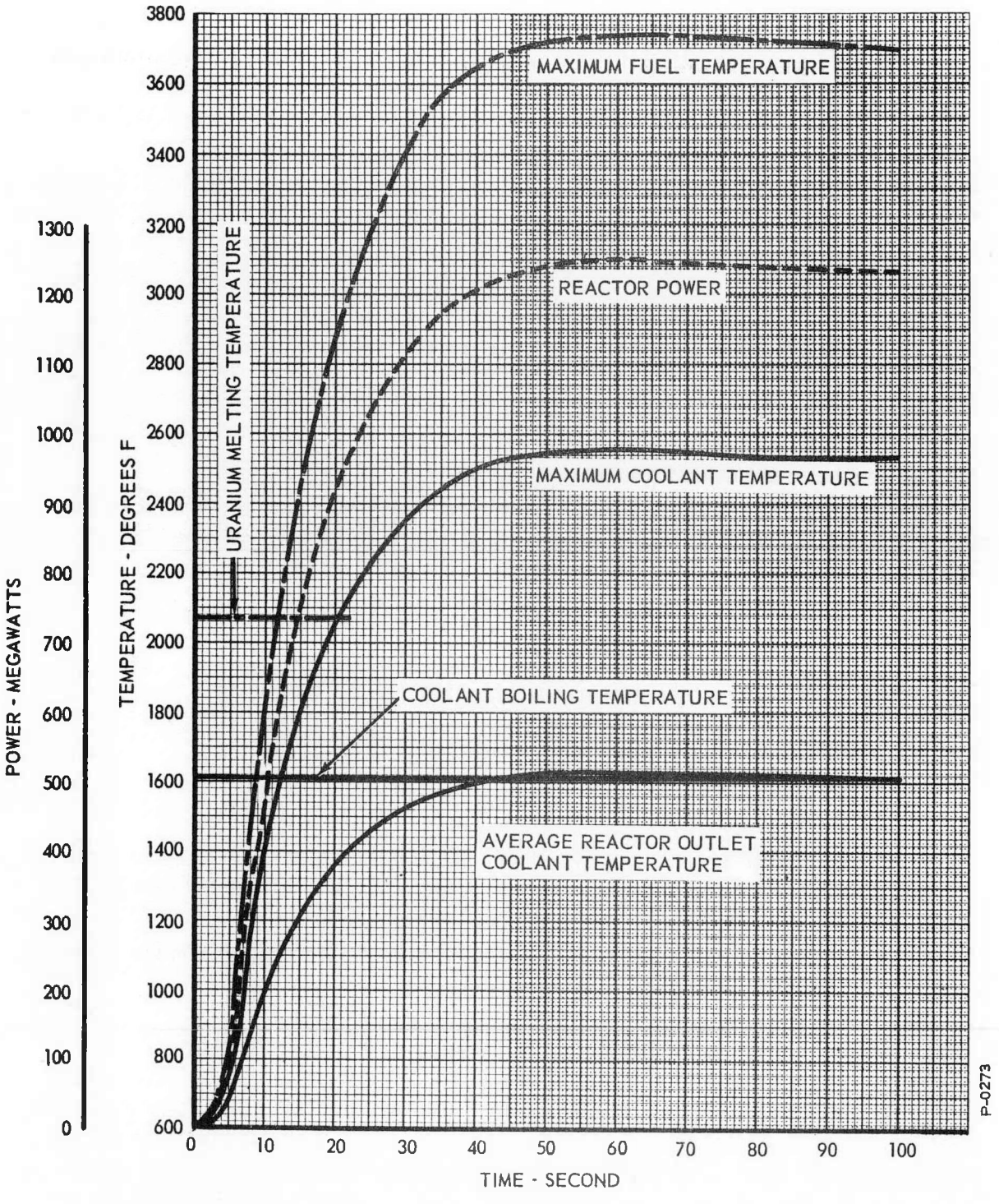

Figure C.6 - Start-Up Excursion Power and Reactor Temperature

C.4 THE EFFECT OF SETBACK ACTION

Figure C7 is a copy of the data from the previous report for the effect of setback action. The figure shows the effect of a power trip set at 120 percent of full power (360 megawatts). The initial transient was produced by inserting positive reactivity at the rate of one cent per second, starting from full power. When a power level of 360 megawatts was reached, the regulating rods were reversed at their maximum rate. When the power had decreased to some value below 360 megawatts, determined by the hysteresis of the trigger circuit used, the rods were stopped. It is to be noted that the simulation is not valid for times greater than 30 seconds, as the effect of the recirculation of the coolant is not included.

C.5 SIGNALS GENERATED BY TRANSIENTS DURING FULL POWER

In this section we present data, copied from the previous report, for the signals generated by transients during full-power operation.

C.5.1 Complete Primary Flow Failure

Figure C.8 is a copy of the data for the power, rate, and growth-factor signals generated by the transient, from full power, caused by introducing reactivity at the rate of one cent per second.

C.5.2 Complete Primary Flow Failure

Figure C.9 is a copy of the data from the previous report, for the power, rate, and growth-factor signals generated by the loss of all the primary coolant pumps. Of course, the simulation is not valid after the coolant boils in the hottest channel, as indicated by the shaded portion of the figure.

C.6 SIGNALS GENERATED BY A START-UP TRANSIENT

Figure C10 is a copy of the data for the power, rate, and growth-factor signals generated by a start-up transient. The transient is simulated by assuming that the reactor power level passes one percent of full power with a growth factor corresponding to 70 cents worth of initial reactivity. Note that when this simulation was made, the shutdown temperature was assumed to be 600 degrees F.

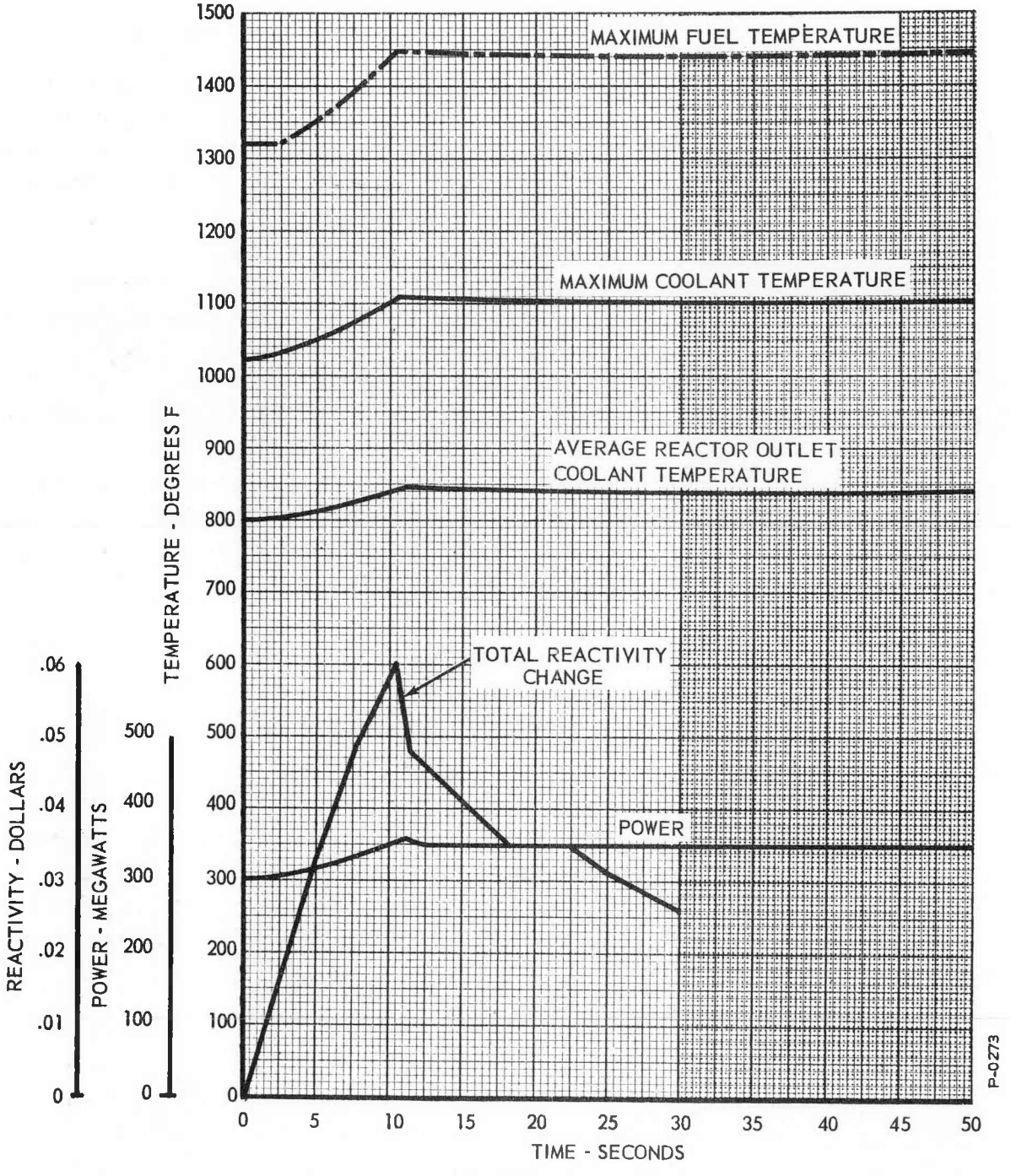

Figure C.7 - Setback Power and Reactor Temperature

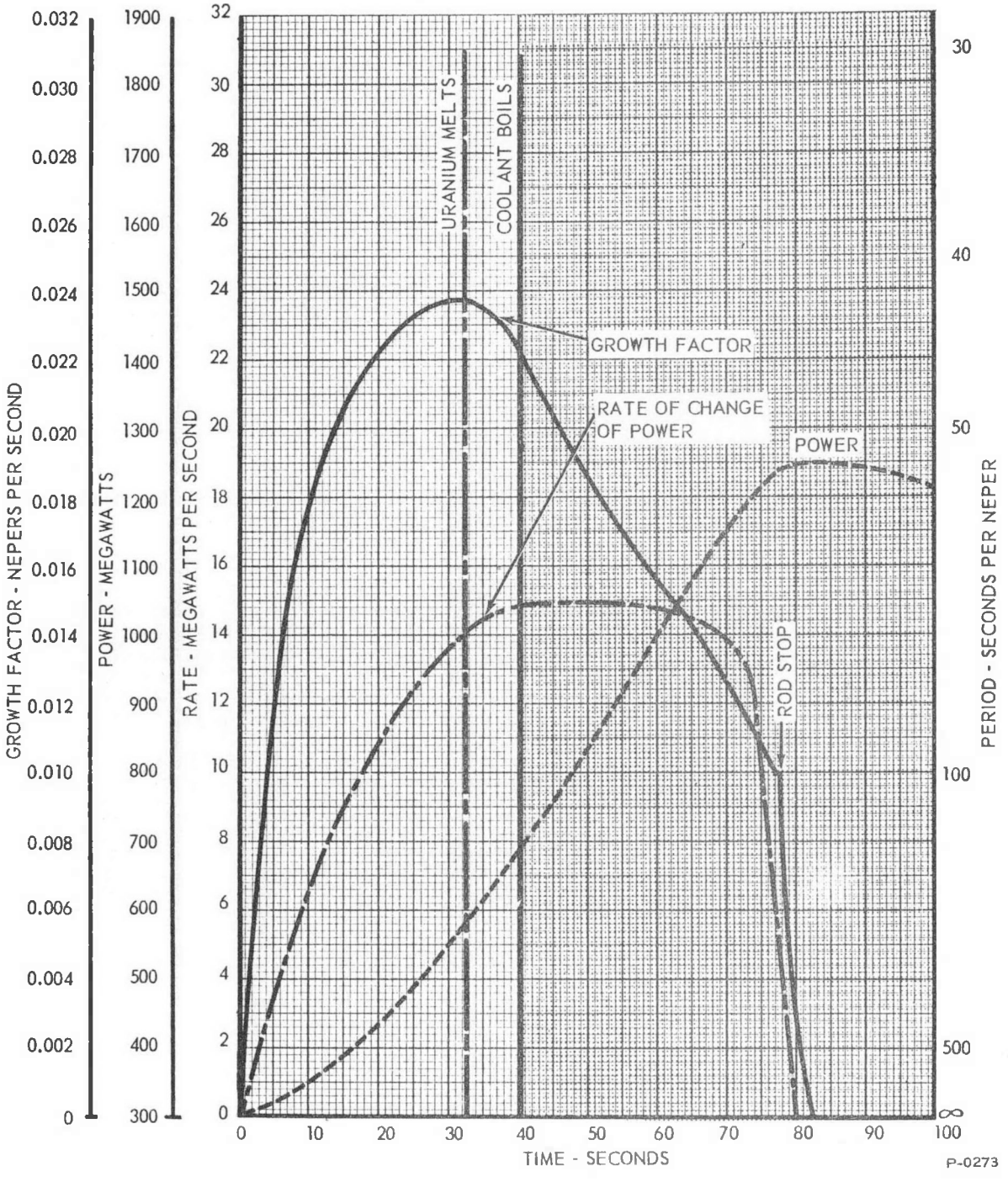

Figure C 8 - Excursion from Full Power - Power and Rate and Growth-Factor Signals

157 149

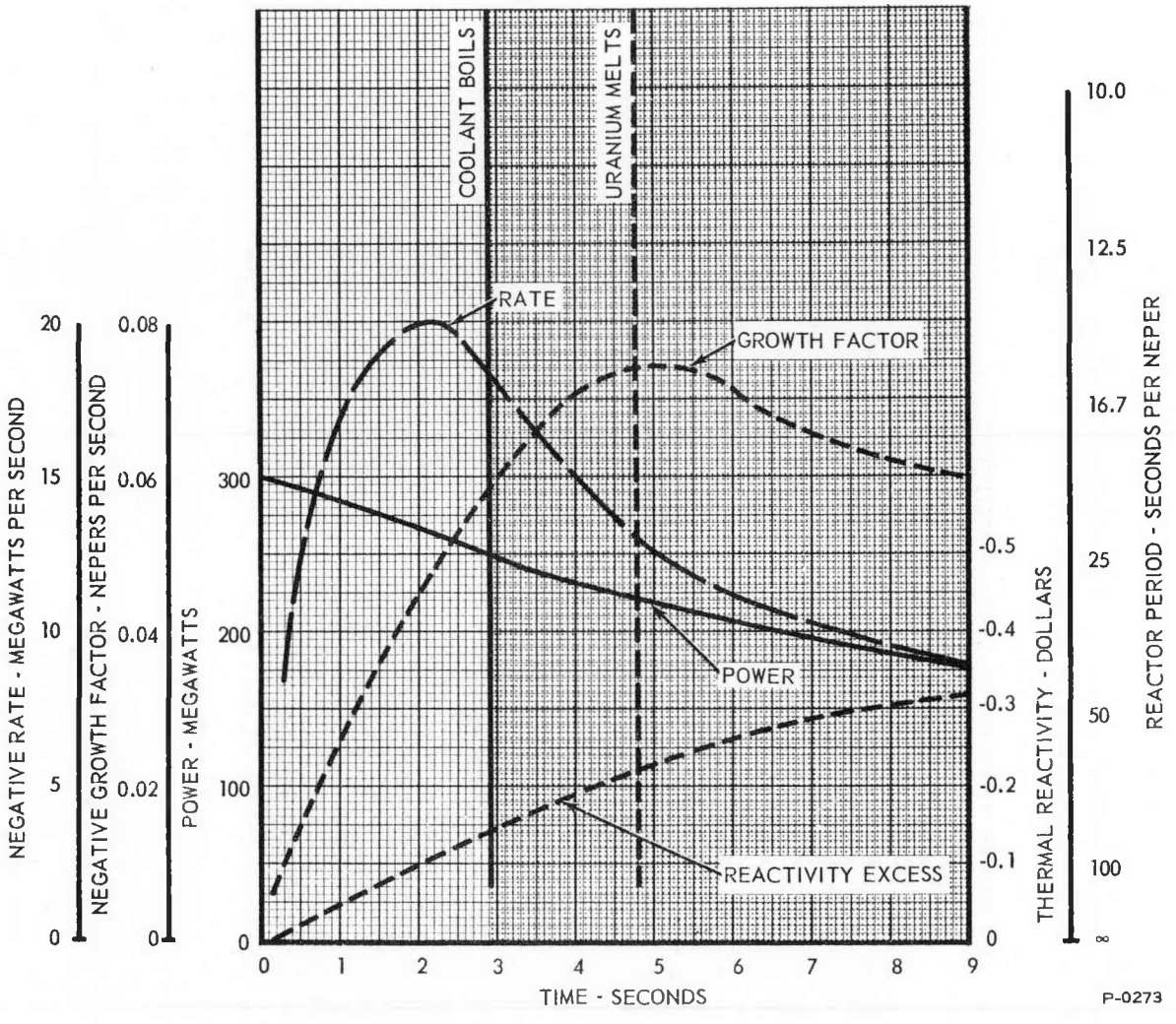

Figure C.9 - Complete Primary Flow: Power and Rate and Growth-Factor Signals

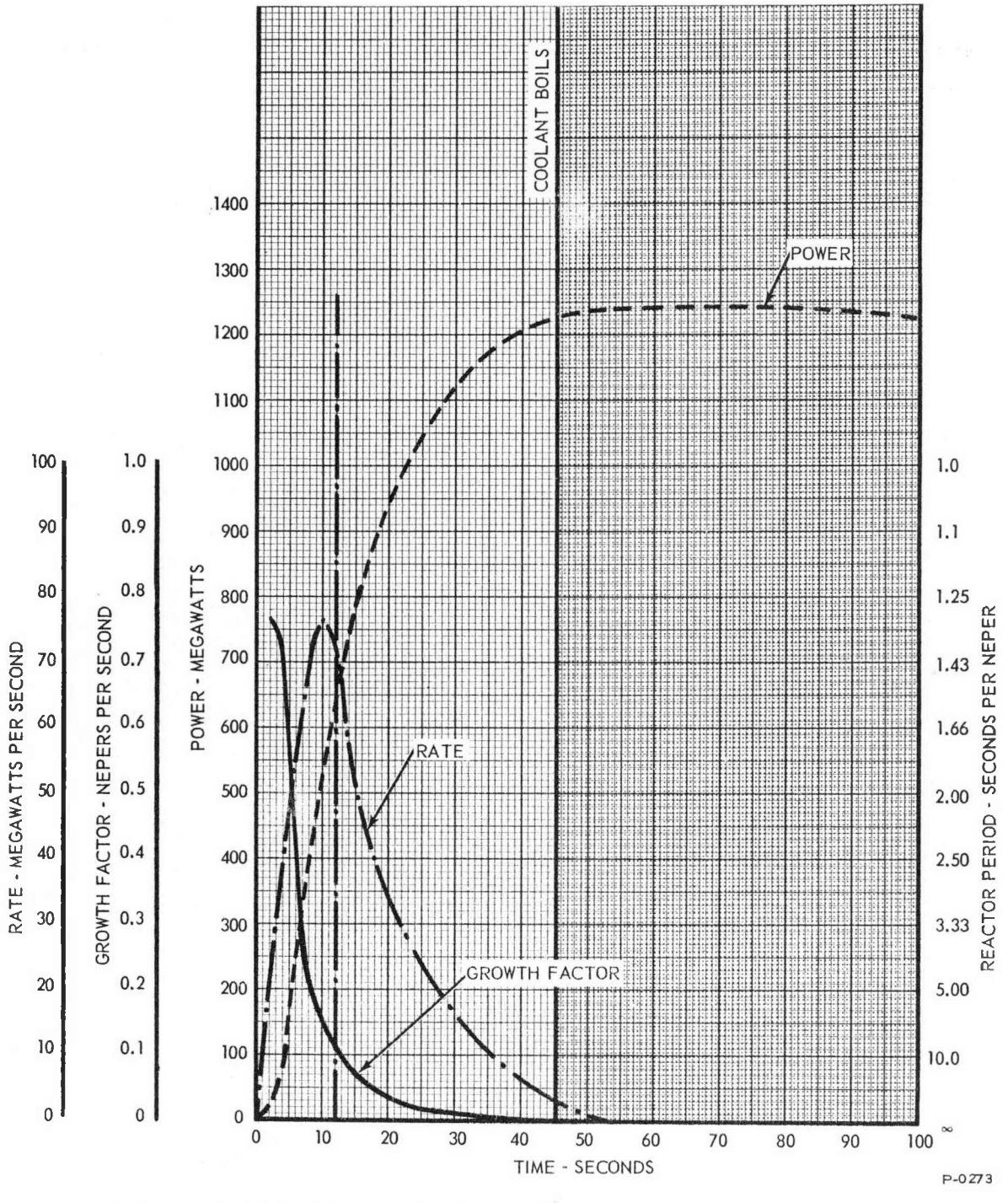

Figure C.10 - Start-Up Excursion: Power and Rate and Growth-Factor Signals

157 151

C.7 SCRAM FROM FULL POWER

Figure C.11 is a copy of the data in the previous report for a scram from full power. The figure shows the behavior of the power, and fuel and coolant temperatures after the scram.

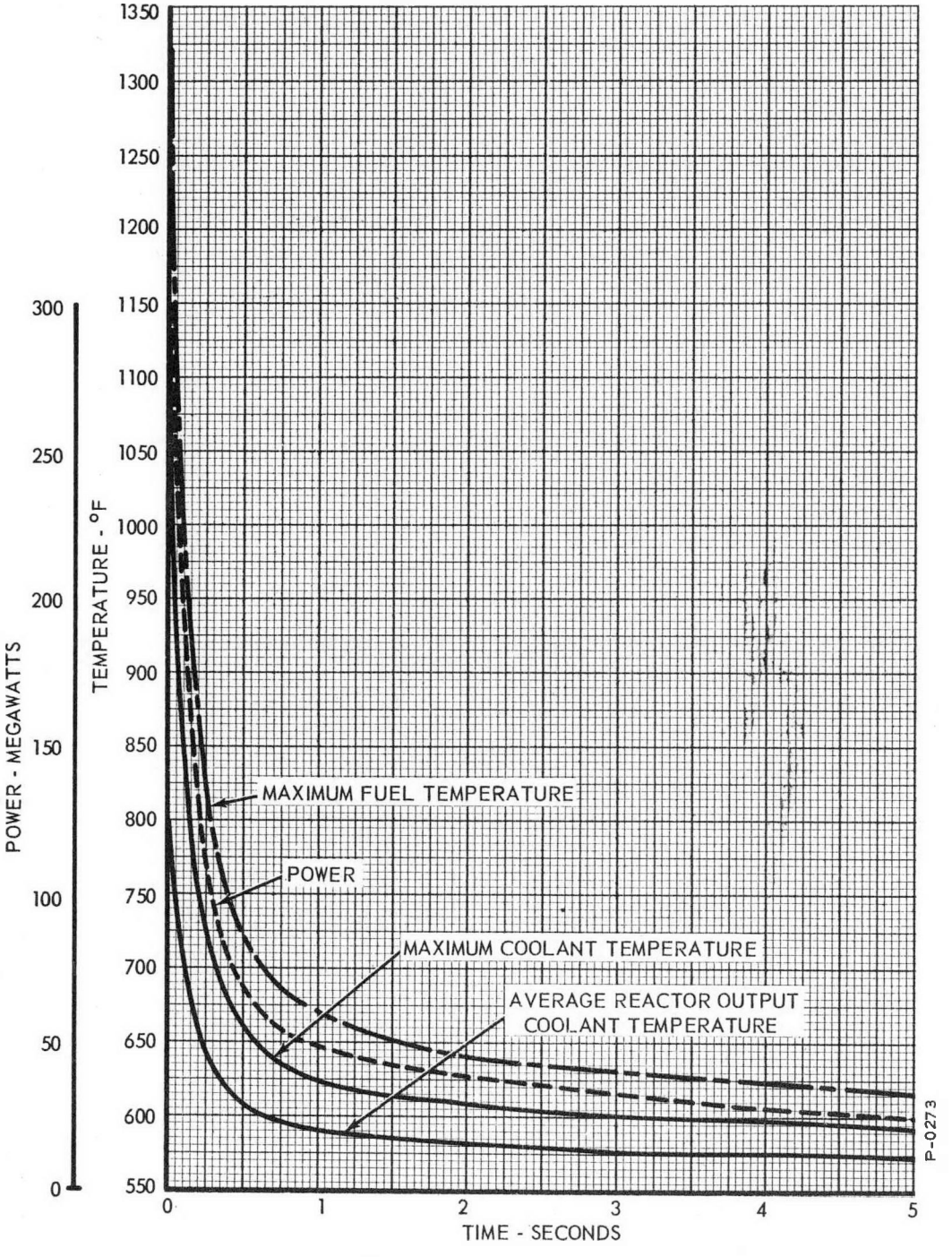

Figure C.11 - Scram from Full Power: Tripped by Interlock